BERICHTE
aus dem Fachbereich Geowissenschaften
der Universität Bremen

No. 171

Gerhardt, S.

LATE QUATERNARY WATER MASS VARIABILITY DERIVED FROM THE PTEROPOD PRESERVATION STATE IN SEDIMENTS OF THE WESTERN SOUTH ATLANTIC OCEAN AND THE CARIBBEAN SEA

Berichte, Fachbereich Geowissenschaften, Universität Bremen, No. 171,
109 pages, Bremen 2001

ISSN 0931-0800

The "Berichte aus dem Fachbereich Geowissenschaften" are produced at irregular intervals by the Department of Geosciences, Bremen University.

They serve for the publication of experimental works, Ph.D.-theses and scientific contributions made by members of the department.

Reports can be ordered from:

Gisela Boelen

Sonderforschungsbereich 261

Universität Bremen

Postfach 330 440

D 28334 BREMEN

Phone: (49) 421 218-4124

Fax: (49) 421 218-3116

e-mail: boelen@uni-bremen.de

Citation:

Gerhardt, S.

Late Quaternary water mass variability derived from the pteropod preservation state in sediments of the western South Atlantic Ocean and the Caribbean Sea.

Berichte, Fachbereich Geowissenschaften, Universität Bremen, No. 171, 109 pages, Bremen, 2001.

ISSN 0931-0800

Late Quaternary water mass variability derived from the pteropod preservation state in sediments of the western South Atlantic Ocean and the Caribbean Sea

Dissertation
zur Erlangung des Doktorgrades
der Naturwissenschaften

am Fachbereich Geowissenschaften
der Universität Bremen

vorgelegt von
Sabine Gerhardt
Bremen 2001

Tag des Kolloquiums: 14. Dezember 2000

Gutachter:
Prof. Dr. R. Henrich
Prof. Dr. H. Willems

Prüfer:
Prof. Dr. D. Fütterer
Prof. Dr. R.X. Fischer

Table of contents

Abstract

Evaluation of production, accumulation, and dissolution of calcium carbonate ($CaCO_3$) is of major interest for paleoceanographers since the carbonate system is intimately related to atmospheric CO_2. Pteropods are marine gastropods, which have adapted themselves to pelagic life and are widely distributed and abundant in all oceans. Shelled pteropods and heteropods are the principal pelagic producers of aragonite, a metastable polymorph of $CaCO_3$ that is more soluble in seawater than calcite. Aragonitic pteropod production is calculated to average about 10% (Fabry, 1990; Fabry and Deuser 1991, 1992) to 12% (Berner and Honjo, 1981) of the total carbonate production. However, pteropod oozes are predominantly found in shallow and intermediate water environments since aragonite dissolves at much shallower water depths than calcite. Alternating modes of preservation of pteropod shells are related to differences in the bottom-water saturation state with respect to aragonite.

In the present study, variations in the preservation state of pteropod tests are used to reconstruct late Quaternary changes in intermediate and deep water circulation in the South Atlantic Ocean and in the Caribbean Sea. Both areas are assumed to be good locations for studying glacial to interglacial changes in the relative contributions of southern-source intermediate waters and southward flowing North Atlantic Deep Water (NADW). Part I of this thesis provides an introduction into the central themes of this study; part II presents the results of this study, which are compiled in four manuscripts, and part III summarizes the results and main conclusions of the manuscripts and includes a future outlook.

Based on the observation that pteropod tests display changing modes of preservation (Almogi-Labin et al., 1986; Haddad and Droxler, 1996), two new proxies have been developed in the present study, i.e. the *Limacina* Dissolution Index (LDX) and the *Limacina* Fragmentation Index (LFX). These proxies are compared with other parameters including $CaCO_3$ and aragonite contents, particle counts, and water-derived $\delta^{13}C_{DIC}$ and $[CO_3^{2-}]$. The LDX has been applied on three species of the genus *Limacina*, i.e. *L. inflata*, *L. bulimoides*, and *L. lesueuri*, of which *L. inflata* appears to be the most reliable. In order to obtain both spatial and temporal information on aragonite preservation patterns, the LDX is applied on 310 surface sediment samples, on 87 last glacial maximum (LGM) samples from 38 gravity cores, and on short- and long-term records of six sediment cores.

Calibration of the LDX under modern hydrographic conditions (part II-1) reveals that preservation of pteropods is good within the surface water and the Upper NADW, whereas it is worse between these water masses, i.e. in the Antarctic Intermediate Water (AAIW) and the Upper Circumpolar Deep Water (UCDW). Therefore, preservation does not decrease regularly with water depth, but shows an S-shaped trend. Moreover, two aragonite lysoclines are

observed at about 750 and 2500 m water depth. Application of the LDX on western South Atlantic LGM sediments (part II-2) reveals a rather different water mass configuration for the glacial Atlantic. Non- or only slightly aragonite-corrosive Glacial North Atlantic Intermediate Water (GNAIW) occupied the intermediate water level at least as far south as 20°S, thereby replacing AAIW and UCDW. An upper aragonite lysocline is not observed and the deep lysocline was positioned about 500 m shallower than today. LDX and LFX records of late Quaternary sediment cores from the western South Atlantic suggest that changes in the influence of northern versus southern water masses occurred during much of the late Quaternary (with a studied time interval of 430 kyrs; part II-3). Poor aragonite preservation is mainly found during glacials and is most noticeable around Terminations I, II, and IV. In addition, a long-term aragonite dissolution trend can be observed, which may be diagenetically induced. It appears that large-scale variations in the Atlantic thermohaline circulation occurred even throughout the Holocene. This is based on the observation that good agreement is found between aragonite dissolution and the strength of the Iceland-Scotland Overflow Water (ISOW), which significantly contributes to NADW production (part II-4).

Part I *Introduction*

1. Motivation and main objectives

Present-day production of $CaCO_3$ in the world ocean is calculated to be about 5 billion tons per year. It is assumed that about 60% accumulates in sediments, whereas the remaining 40% is dissolved (Milliman, 1993). The carbonate system is intimately related to atmospheric CO_2 content and thus represents an important part of the global carbon cycle. Calculation of the global ocean carbonate budget includes carbonate production, accumulation, and dissolution, but published estimations of the carbonate budget vary widely as it is difficult to account for all input and output mechanisms of the system. On a longer time scale, for example during the late Quaternary, calculation of the carbonate budget should even take the glacial and interglacial end-members into account. Marine aragonitic detritus is an important component of the oceanic CO_2 system and dissolution of aragonite must therefore be taken into account when generating models of the oceanic CO_2 system. Previous studies suggest that aragonitic pteropod production averages about 10% (Fabry, 1990; Fabry and Deuser 1991, 1992) to 12% (Berner and Honjo, 1981) of the total $CaCO_3$ production. Aragonite, a metastable polymorph of $CaCO_3$, dissolves at shallower water depths than calcite as it is much more soluble in seawater (by an approximate factor of 1.5: Morse et al., 1980; Millero, 1996). Therefore, aragonite as well as magnesian calcite have proven to be useful in yielding information on $[CO_3^{2-}]$ variations at much shallower water depths than are possible based on calcite studies. For example, metastable $CaCO_3$ dissolution has been determined at intermediate water depths of the Caribbean and western North Atlantic in order to reconstruct variations in the flow of low $[CO_3^{2-}]$ Antarctic Intermediate Water (AAIW) (e.g. Droxler et al., 1991; Haddad and Droxler, 1996).

This thesis focuses on the preservation patterns of aragonite within surface sediments and last glacial maximum (LGM) sediments as well as in late Quaternary sediment cores. Initially, special emphasis was placed on the determination of spatial and temporal variations of pteropod assemblages in order to improve our knowledge of changing ecologic and environmental conditions through time. Changes in pteropod preservation had to be determined additionally to reveal changes in bottom-water corrosiveness towards aragonite. During the course of the present study, the main objectives changed from being rather ecological to focussing more on the preservational aspects, as it was observed that pteropods are highly susceptible to fragmentation, which causes uncertainties in the faunal analysis. Reliable reconstruction of ecologic and environmental conditions was therefore considered to be questionable. Instead, it was observed that pteropod tests display alternating modes of preservation, which could yield

important information on bottom-water corrosiveness against aragonite. The main objectives of this thesis, which led to the compilation of four manuscripts, can be summerized as follows:

(1) to study pteropod assemblages in long-term records of the late Quaternary (part II-3).
(2) to develop new methods to indicate the state of aragonite preservation in sediments, which led to the development of the *Limacina* Fragmentation Index = LFX and the *Limacina* Dissolution Index = LDX (part II-3). The LFX is the ratio of intact tests to fragments of *Limacina inflata*, whereas the LDX is characterized by six varying modes of preservation of *L. inflata*, *L. bulimoides*, and *L. lesueuri*.
(3) to examine the connection between preservation state and aragonite loss (part II-1).
(4) to test the LDX in surface sediments deposited under modern hydrographic conditions and to compare the index with other parameters (part II-1).
(5) to apply the LDX on another time slice (the LGM) and to compare the inferred water mass reconstruction with previous studies (part II-2).
(6) to apply the LDX on short- and long-term records of the late Quaternary and to interpret the results in terms of changes in water mass distribution and aragonite-corrosiveness (part II-3, 4).

2. Modern and past oceanography

2.1 Oceanic circulation and climate

During the past ten years, our view of the ocean's role in climate variability has changed substantially. In the past, it was assumed that changes in ocean circulation and deep-ocean carbon storage only played a passive role in altering the atmosphere's chemistry, as it was believed that ocean change was triggered by climate change itself and not vice versa. However, since the advance of the polar ice core records in the early 1990s (e.g. Barnola et al., 1991; Dansgaard et al., 1993; Grootes et al., 1993; Grootes and Stuiver, 1997), the ocean is no longer considered a passive component of climate change. From these records, it has become evident that the thermohaline circulation, which is primarily responsible source for northward ocean heat delivery, plays a key role in climate change. The evidence that changes in ocean circulation are crucial for climate variability has led to rapid progress in paleoceanography, aiming mainly at reconstructing ocean history and modelling future climate. Moreover, a large variety of methods and proxies has been developed for reconstructing ocean history (see reviews by Wefer et al., 1999; Lea, 1999). These methods are based on the fact that useful information is preserved in the sediments, for example in the form of micro- and nannofossil

assemblages, organic matter, and the elemental and isotopic composition of shells and other sediment components. In particular, a large research effort has been directed towards determining the distribution pattern of $\delta^{13}C$ of dissolved inorganic carbon in the water column (GEOSECS data: e.g. Kroopnick, 1985), as it was observed that $\delta^{13}C$ values differ significantly between different water masses due to the varying influences of photosynthesis and respiration. Since the $\delta^{13}C$ water mass signal is also imprinted in benthic foraminifera tests, it is possible to infer the distribution of water masses by determing the $\delta^{13}C$ values of benthic foraminifera from different water depths and different latitudes. The $\delta^{13}C$ proxy has considerably improved our knowledge about glacial to interglacial changes in deep and intermediate water production and flow (e.g. Curry and Lohmann, 1982; Curry et al., 1988; Duplessy et al., 1988; Raymo et al., 1990; deMenocal et al., 1992; Sarnthein et al., 1994; Bickert and Wefer, 1996; Curry, 1996; Venz et al., 1999; Oppo and Horowitz, 2000). Nevertheless, progress in our understanding of ocean history, which should contribute to models predicting future climate, requires the continuous improvement, combination, and development of new and existing proxies.

2.2 Modern oceanic circulation

Broecker et al. (1985) and Gordon (1986) were the first to generalize the modern ocean thermohaline circulation into the "global conveyor belt" model. This model is highly simplified (e.g. Schlitzer, 1996) as it does not take all source areas, water masses, and flow paths into account, but it does describe the close connection between the oceans. Briefly, the conveyor belt model can be summerized as follows. The Gulf Stream delivers warm and saline surface waters from the Caribbean Sea northward into the northern North Atlantic, where it cools and becomes more saline due to evaporation. There, the denser water sinks to form North Atlantic Deep Water (NADW). The NADW flows southward through the North and South Atlantic, and moves eastward south of Africa to enter the Indian Ocean (where some of the deep water circulates) via the Antarctic Circumpolar Current (ACC). In the Weddell Sea, a part of the NADW reaches the surface again. When the deep water arrives in the Pacific Ocean it rises, flows to the north and back into the Indian Ocean through the Indonesian Seas, ultimately feeding the Agulhas Current (AGC). The AGC transports this warm surface water westward south of Africa to enter the South Atlantic once again. This closes the conveyor belt, as the water is transported northwestward by the Benguela Oceanic Current (BOC) and the South Equatorial Current (SEC) into the equatorial region, where it crosses the equator, enters the Caribbean and joins the Gulf Stream again (see Fig. 2a).

The average residence time of water masses in the deep ocean is ≈1000 yrs. The deep water "ages" on its way from the North Atlantic to the North Pacific, resulting in a strong asymmetry between these oceans, which can be observed in the distribution patterns of its constituents, i.e. oxygen-rich, nutrient- and CO_2-poor North Atlantic surface water becomes strongly oxygen-depleted, but nutrient- and CO_2-enriched on arriving in the North Pacific as deep water. The oxygen-depletion is caused by two factors: (1) almost no contact with the atmosphere for a long time; and (2) oxidation of organic matter within the sediment and at the sediment-water interface. With the oxidation of organic matter, nutrient salts and CO_2 are released into the water, resulting in an enhanced carbonate-corrosiveness. The "aging" of NADW is recorded in the nutrient distribution and hence in the $\delta^{13}C$ records (Fig. 1). Highest $\delta^{13}C$ values are found in the North Atlantic (>1.0‰), while lowest values (<0.4‰) are observed in the northern Indian Ocean and the North Pacific. Interestingly, only the Atlantic shows a distinct layer of low $\delta^{13}C$ values at intermediate depths, indicating the presence of AAIW and Upper Circumpolar Deep Water (UCDW; Fig.1).

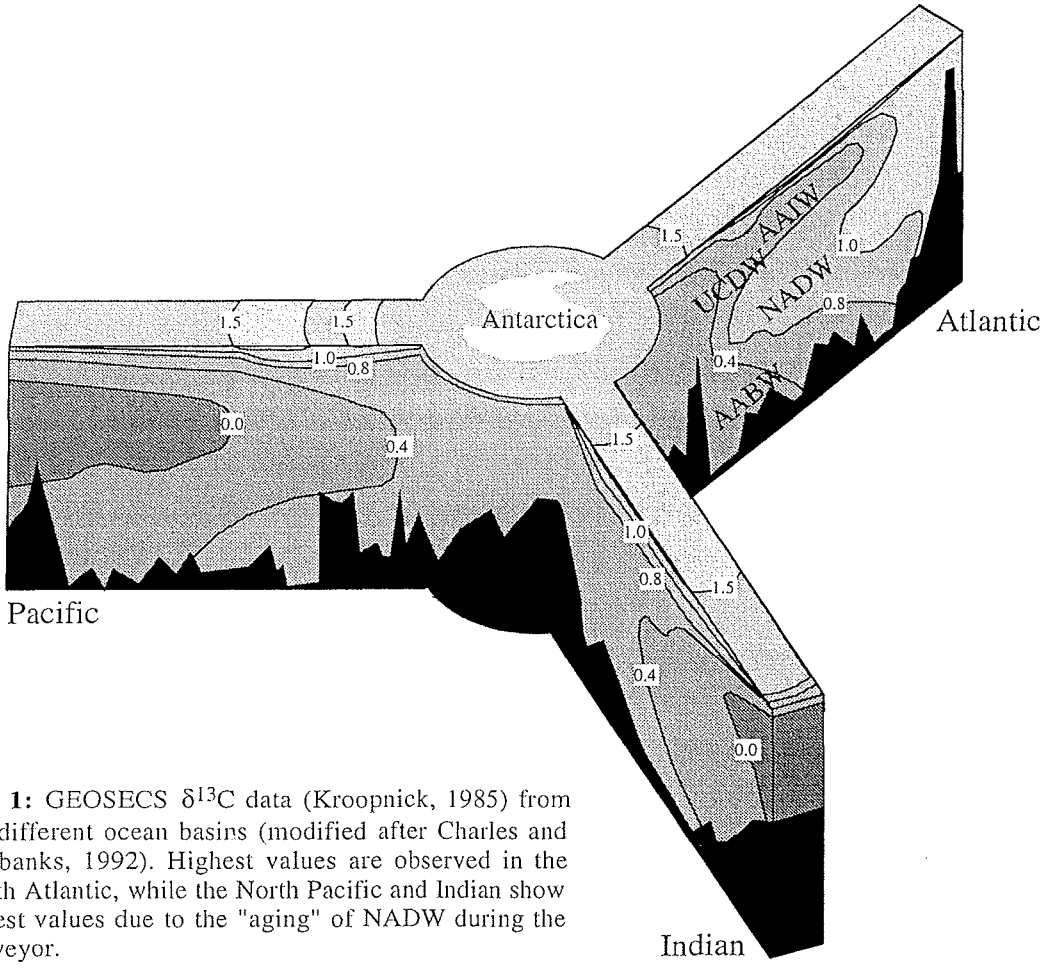

Fig. 1: GEOSECS $\delta^{13}C$ data (Kroopnick, 1985) from the different ocean basins (modified after Charles and Fairbanks, 1992). Highest values are observed in the North Atlantic, while the North Pacific and Indian show lowest values due to the "aging" of NADW during the conveyor.

2.3 Modern South Atlantic and Caribbean circulation

As described in the last chapters, the thermohaline circulation in the South Atlantic Ocean and in the Caribbean Sea plays a key role in northward heat transport, causing the relatively mild climate in the North Atlantic region (including Europe) in modern times. The South Atlantic receives waters from the North Atlantic, from the Indian Ocean by the Agulhas Current, from the Pacific through the Drake Passage, and from the Weddell Sea via the Antarctic Circumpolar Current (e.g. Reid, 1989). Circulation takes place in three water layers, occupied by surface, intermediate, and deep water masses.

Circulation in the upper layer is mainly driven by the winds in the major atmospheric cells. It depends, amongst other factors, on the rotation of the Earth and the shape of the ocean basins (Chester, 1990). In the South Atlantic, the surface circulation is dominated by the anticlockwise subtropical gyre (e.g. Peterson and Stramma, 1991; Fig. 2a).

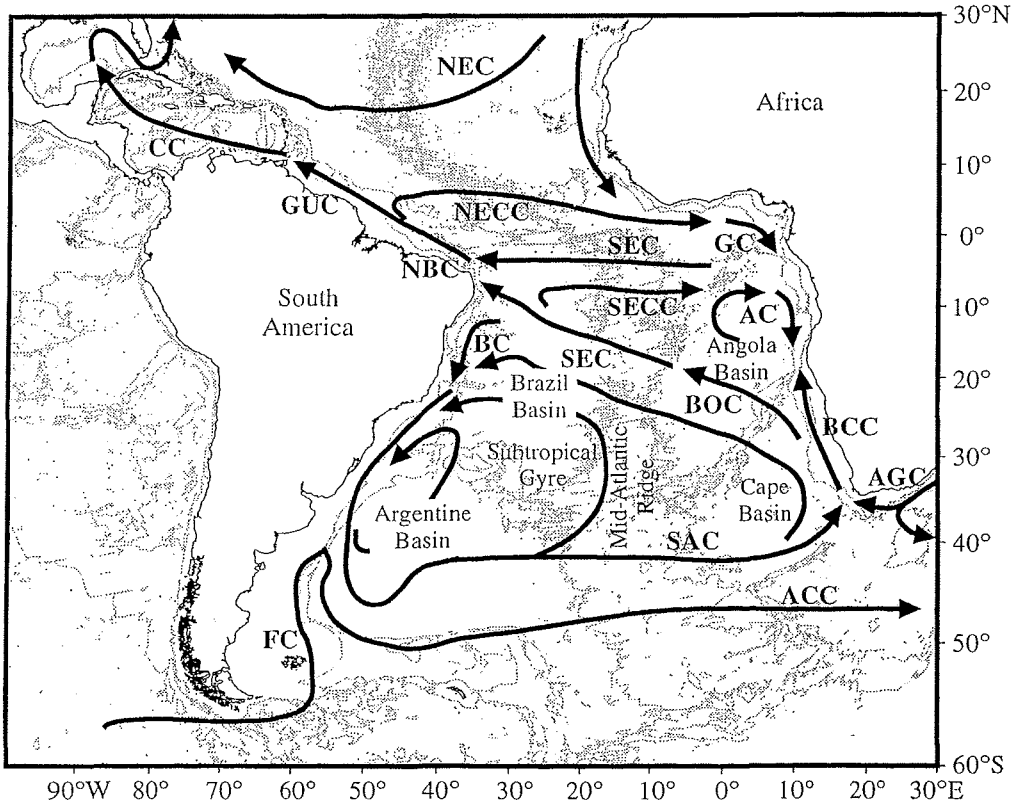

Fig. 2a: Recent South Atlantic and Caribbean surface water circulation. AC: Angola Current; ACC: Antarctic Circumpolar Current; AGC: Agulhas Current; BC: Brazil Current; BCC: Benguela Coastal Current; BOC: Benguela Oceanic Current; CC: Caribbean Current; FC: Falkland Current; GC: Guinea Current; GUC: Guyana Current; NBC: North Brazil Current; NEC: North Equatorial Current; NECC: North Equatorial Counter Current; SAC: South Atlantic Current; SEC: South Equatorial Current; SECC: South Equatorial Counter Current (modified after Peterson and Stramma, 1991; eastern Atlantic from Volbers et al., subm.).

The BOC, which represents the eastern boundary current of the subtropical gyre, joins the SEC at 30°S, transporting water northwestward across the South Atlantic. At 10°S, the SEC reaches the Brazilian coast and divides into the northward flowing North Brazil Current (NBC) and the southward flowing Brazil Current (BC). The NBC enters the Caribbean Sea through various passages, flows through the Caribbean and the Gulf of Mexico to join the Gulf Stream in the North Atlantic. Parts of the SEC and the NBC are retroflected around 5°S and 5°N, respectively, to form the South and North Equatorial Counter Currents (SECC, NECC) (Peterson and Stramma, 1991). The strength of the SEC is known to vary significantly between the different seasons resulting from changes in the strength of the southern trade winds (Peterson and Stramma, 1991).

Whereas the surface currents are wind-driven and flow mainly horizontally with relatively high velocities, the intermediate and deep ocean circulation is thermohaline-driven, moving horizontally as well as vertically with relatively low velocities (Chester, 1990). The mid-depth circulation in the South Atlantic is characterized by the northward flowing AAIW and UCDW (see Figs. 1, 2b). Likely sources of the South Atlantic AAIW are surface waters from the Drake Passage and from the Falkland Current (FC; Talley, 1996). The UCDW (as well as the LCDW) is a product of NADW, returning from the Pacific via the ACC through the Drake Passage into the Atlantic (Reid, 1989). Additional intermediate water possibly comes from the Indian Ocean via the AC (Fig. 2b; Talley, 1996). The AAIW can be traced in the South Atlantic due to its salinity minimum and oxygen maximum. The latter indicates the relatively recent contact with the atmosphere (Talley, 1996). In the South Atlantic, the UCDW can be differentiated from the AAIW by its silica maximum (Talley, 1996). As illustrated in Fig. 2b, the AAIW spreads out northward as a narrow, western boundary current, crosses the equator (a part of it flows eastward into the equatorial region) and flows into the Caribbean and Gulf of Mexico through various passages. Moreover, AAIW flows northwards out of the Caribbean as a less well-defined, western boundary current. The northern boundary of AAIW has been observed along ≈25°N (see Fig. 2b) where the AAIW signal is eliminated by mixing with overlying saline waters and with NADW (Talley, 1996). The UCDW likewise spreads out northward on similar circulation paths as the AAIW, but its silica maximum can even be traced farther north (Talley, 1996). In addition, highly saline and nutrient-poor Mediterranean Overflow Water (MOW) contributes to a small extent to the Caribbean Sea intermediate waters. MOW flows west and southwest from the Strait of Gibraltar at depths between 800 and 1500 m (Kaese and Zenk, 1987), and enters the Caribbean Sea between 10° and 20°N.

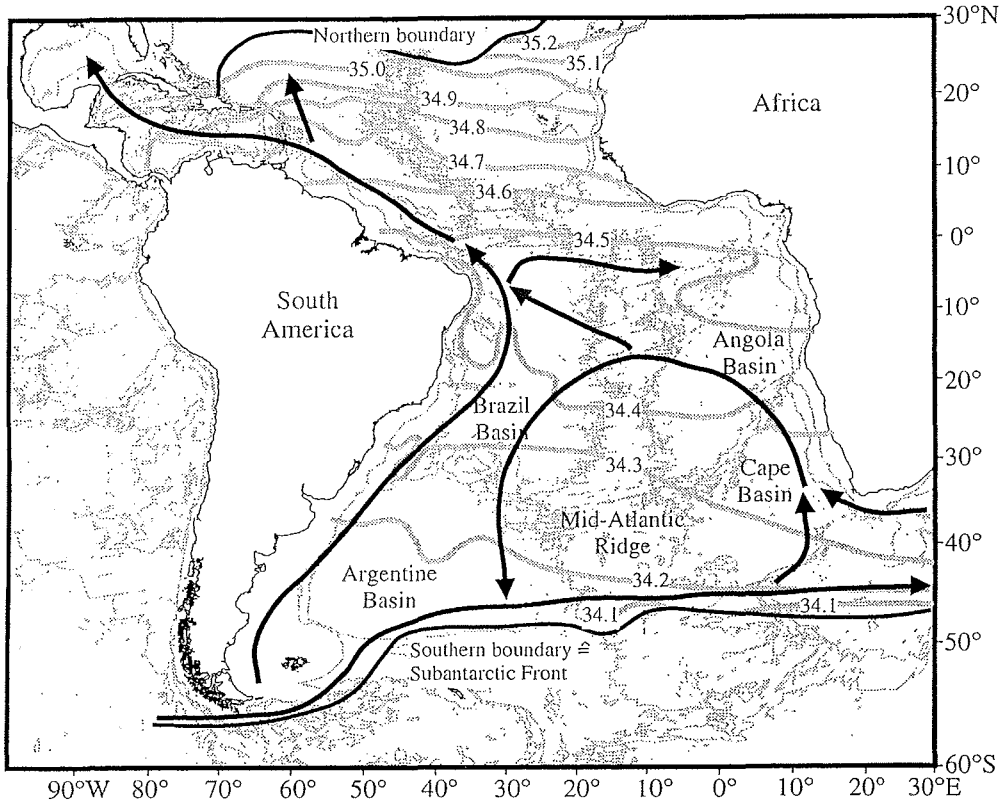

Fig. 2b: Recent South Atlantic and Caribbean Antarctic Intermediate Water (AAIW) distribution paths. Grey lines mark salinities at the AAIW salinity minimum (modified after Talley, 1996). Black arrows mark AAIW flow directions (inferred from the salinity distribution after Talley, 1996 and modified after Gordon, 1986 and Gordon et al., 1992).

The South Atlantic deep water circulation is characterized by the broad core of southward flowing NADW and northward flowing Lower Circumpolar Deep Water (LCDW) and Weddell Sea Deep Water (WSDW). The latter two are mostly unified and hence termed Antarctic Bottom Water (AABW). As already mentioned, the NADW is of key importance for the global thermohaline circulation as it transports the cold water out of the North Atlantic, through the South Atlantic into the Indian Ocean (Fig. 2c). The contributions to NADW come from various sources in the northern North Atlantic, including the Labrador Sea and the Denmark Strait (Reid, 1996). NADW is mostly distinguished into an upper and lower part (i.e. UNADW, LNADW). On its way towards the south, the warm and saline NADW penetrates into the lower-saline CDW, thereby splitting it into a lower and an upper branch (Reid, 1996; see also Fig. 1). Within the Caribbean Sea, UNADW appears to contribute the most to the water mass configuration. Kawase and Sarmiento (1986) and deMenocal et al. (1992) calculated that Atlantic intermediate waters adjacent to the Caribbean Sea (at 1800 m) contain approximately 85% UNADW, 10% AAIW/UCDW, and a small portion of MOW (≈5%). A near vertical

[CO_3^{2-}] profile near the Nicaragua Rise suggests that there is mixing between AAIW/UCDW and UNADW within the Caribbean Basin (Droxler et al., 1991; Haddad and Droxler, 1996). The mixing between AAIW/UCDW and UNADW may be largely responsible for the poor preservation of carbonate observed in the Caribbean today (Haddad and Droxler, 1996).

The salinity-poor and nutrient-rich AABW originates from the ACC (as NADW returns to the Atlantic through the Drake Passage) and the Weddell Sea (e.g. Reid, 1989). Northward spreading of AABW is limited by the Mid-Atlantic and the Walvis Ridges, resulting in a quite different deep ocean circulation pattern (see Fig. 2c) than is known from surface and intermediate waters. In the western South Atlantic, AABW flows northward into the Brazil Basin through the Vema Channel, whereas in the eastern Atlantic the northward flow is stopped by the Walvis Ridge. However, small portions of AABW pass through the Romanche and Chain Fracture Zones and the Walvis Passage (Shannon and Chapman, 1991; Mercier et al., 1994). AABW does not enter the Caribbean as the Caribbean sill depth lies between 1600 and 1800 m (see Haddad and Droxler, 1996 and references therein).

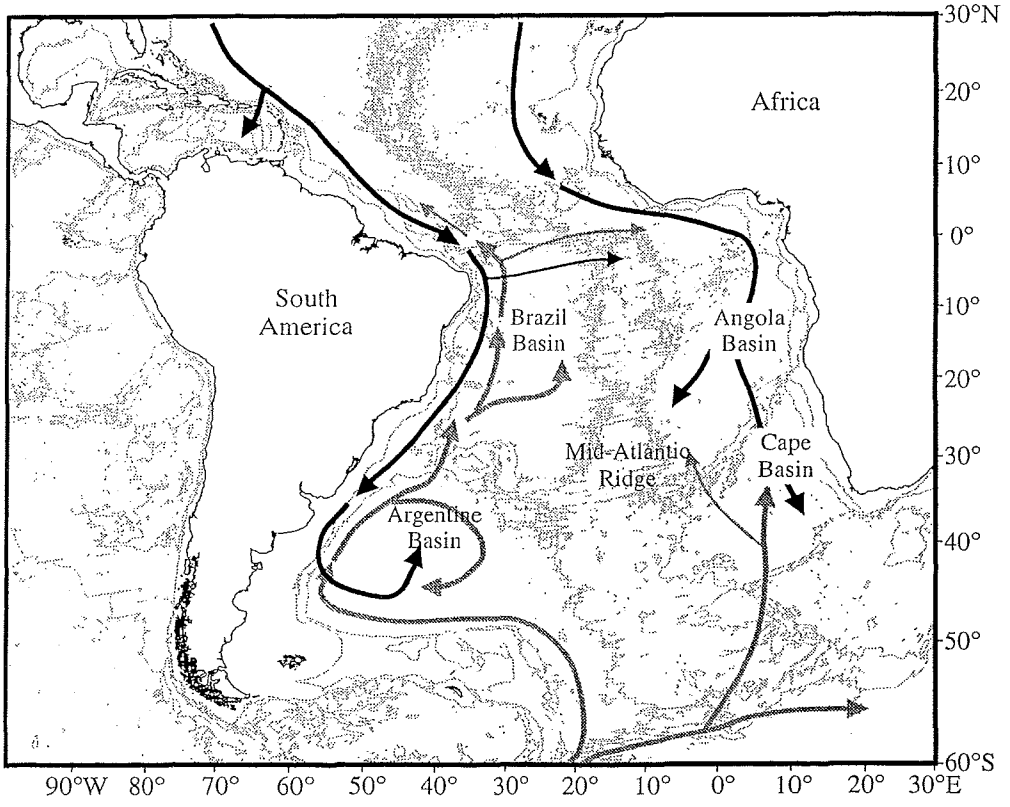

Fig. 2c: Recent South Atlantic and Caribbean deep water distribution paths. Grey arrows mark the main and subordinate flow directions of Antarctic Bottom Water; black arrows indicate the main and subordinate flow directions of North Atlantic Deep Water (modified after Wüst, 1935 and Reid, 1994, 1996).

2.4 Water mass properties

Water masses can be distinguished by the differences in their physical and chemical properties. For instance, differences in temperature, salinity, and oxygen are widely used for tracing the flow paths of water masses (e.g. Reid, 1989, 1996). Oxygen and carbon dioxide are the two most important gases for oceanic biogeochemical cycles. Moreover, the seawater carbon dioxide content has a major influence on carbonate preservation since it is extremely chemically reactive. Carbon dioxide is released during the oxidative destruction of organic matter, which lowers the pH and results in an increased carbonate-corrosiveness (Chester, 1990). Over 99% of the dissolved CO_2 is present in the form of CO_3^{2-} and HCO_3^- ions (at the pH range normally found in seawater) and the total carbon dioxide (ΣCO_2) content may be simply defined as the sum of the concentrations (c) of these carbonate species:

$$\Sigma CO_2 = c_{HCO_3} + c_{CO_3} \quad (1)$$

$[CO_3^{2-}]$ profiles (such as in Fig. 3) are used to describe the connection between calcium carbonate dissolution and water chemistry, as there is a roughly inverse relationship between $[CO_3^{2-}]$ and pCO_2 (Broecker et al., 1999). For instance, Droxler et al. (1991) examined the influence of the overlying water chemistry on the preservation of metastable carbonate minerals (i.e. aragonite and magnesian calcite) in the Bahamas and Nicaragua Rise regions. More recently, the connection between calcium carbonate dissolution and overlying water $[CO_3^{2-}]$ has been illustrated in gridded global maps by Archer (1996). By extrapolating the GEOSECS and other data sets to a global domain, he revealed regional variations in the shape of the calcite lysocline (and hence in carbonate preservation). On the basis of the GEOSECS data, it was concluded that the aragonite lysocline horizon lies where the CO_3^{2-} versus depth curve passes through the aragonite saturation horizon, which is given by the following equation:

$$(CO_3^{2-})_{aragcrit}\,(\mu M/kg) = 120\exp\{0.15(Z - 4)\} \quad (2)$$

where Z is the water depth in km (Broecker and Takahashi, 1978).

By using the above equation and the GEOSECS carbonate ion data, the topography of the critical carbonate ion horizons and hence of the calcite and aragonite lysoclines have been inferred by Broecker and Takahashi (1978). However, examination of the modes of aragonite preservation in the sediment reveals that the depths of the sedimentary and hydrographic lysoclines may differ because the position of the GEOSECS stations and the sediment cores vary significantly. Consequently, physical and chemical conditions, including current velocity

and CO_2 content, differ significantly. Moreover, the GEOSECS data were determined in the last decades whereas the studied surface sediments may be hundreds to thousands of years old, depending on the sedimentation rate. The water-derived aragonite saturation states (GEOSECS data; Bainbridge, 1981) and the observed bottom-water corrosiveness against aragonite (see part II-1) may differ strongly as can be seen in an example from the western equatorial Atlantic Ocean (Fig. 3). AAIW and UCDW appear to be aragonite-corrosive, which is recorded in the LDX (see methods section and part II-1 for a detailed description about the LDX) even though the $[CO_3^{2-}]$ profile indicates that the waters are supersaturated (though close to saturation) with respect to aragonite. The differences between water-derived GEOSECS saturation state and sediment-derived preservation state suggest that it would be more accurate to determine the aragonite saturation state directly at the sediment-water interface.

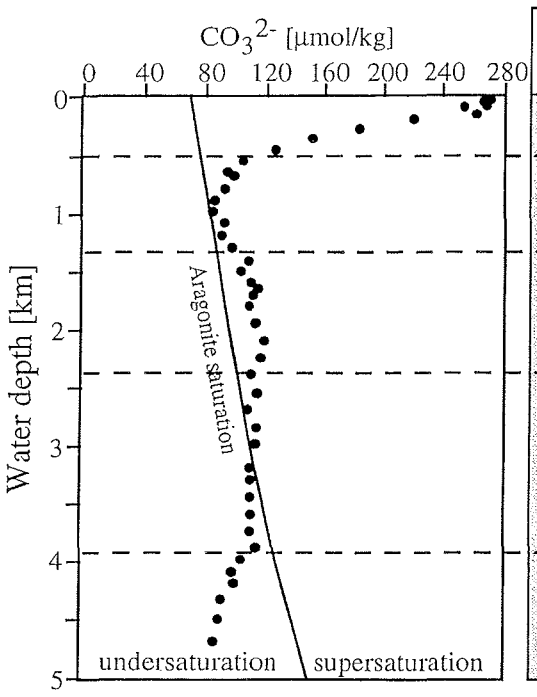

Water mass	Water-derived saturation state of aragonite	Observed aragonite-corrosiveness	Expected LDX stages
SACW	highly supersaturated	non-corrosive	0 - 2
AAIW + UCDW	close to saturation	corrosive	2 - >5
UNADW	supersaturated	non- to slight-corrosive	0 - 3
LNADW	close to saturation to undersaturated	corrosive	2 - >5
AABW	highly undersaturated	highly corrosive	>5

Fig. 3: Typical saturation profile for the western South Atlantic Ocean (GEOSECS Station 39, 7°57'N, 43°51'W; Bainbridge, 1981). Dots mark calculated CO_3^{2-} concentrations. Note that the $[CO_3^{2-}]$ minimum within the southern-source water masses AAIW/UCDW causes an S-shaped trend with increasing water depth. Also note that the water-derived aragonite saturation state and the observed aragonite preservation state (indicated by LDX stages) differ significantly. Increasing LDX values indicate worse preservation of aragonite.

One of the oldest and most strongly held theories in oceanography is that carbonate dissolution occurs only at great depths and that it increases regularly below the lysoclines. Yet in the last years, in situ microelectrode measurements of porewater oxygen, $CO_{2(aq)}$, and pH have demonstrated that calcite dissolution driven by metabolic CO_2 produced within the

sediments forms a significant part of the diagenesis of sedimentary calcite even above the lysocline ("supralysoclinal dissolution": e.g. Archer et al., 1989; Hales et al., 1994, Hales and Emerson, 1996, 1997). Recently, Milliman et al. (1999) have suggested that considerable dissolution (perhaps as much as 60-80%) occurs even in the upper 500-1000 m of the ocean. The LDX records suggest a large influence of supralysoclinal dissolution with respect to aragonite in the high-productivity areas of the eastern South Atlantic in recent times as well as during the LGM (part II-1, 2). However, predominant correspondence between the LDX and the GEOSECS $[CO_3^{2-}]$ data in the western South Atlantic and Caribbean (see part II-1) indicates that the bottom-water chemistry is responsible for the first-order variations in aragonite preservation. Therefore, examination of the differences in the corrosiveness of water masses through the use of preservation proxies provides a useful tool in order to reconstruct past water mass distributions.

2.5 Past intermediate water mass variability

During the late Pleistocene, large changes in deep and intermediate water circulation in the Atlantic occurred (e.g. Venz et al., 1999). The mean position of the northern and southern polar fronts are known to shift with time and the sources of deep and intermediate waters are variable (e.g. Duplessy et al., 1988). It is believed that the production of LNADW was greatly reduced during the last glaciation, whereas the production of Glacial North Atlantic Intermediate Water (GNAIW) was enhanced (e.g. Boyle and Keigwin, 1987; Oppo and Fairbanks, 1987; Duplessy et al., 1988; deMenocal et al., 1992; Oppo and Lehman, 1993). Moreover, it is assumed from many studies that the formation of nutrient-enriched, ^{13}C-depleted Southern Component Water (SCW) was significantly enhanced during glacial times (e.g. Boyle and Keigwin, 1982, 1987; Curry and Lohmann, 1982, 1983; Oppo and Fairbanks, 1987; Curry et al., 1988; Raymo et al., 1990; Sarnthein et al., 1994; Curry, 1996). Venz et al. (1999) determined benthic $\delta^{13}C$ values, calcium carbonate contents, and amounts of ice rafted debris (IRD) at ODP site 982 from the Rockall Plateau (Fig. 4) and indicated that the North Atlantic circulation underwent major reorganization during the past 1.0 Myr. The records suggest that during glacial periods, the intermediate-depth North Atlantic (<2200 m) was dominated by well-ventilated GNAIW. During terminations, production of LNADW increased and occupied the North Altantic below ≈2200 m. Melting of icebergs (high amounts of IRD) and production of low-salinity surface waters caused a shut-down in GNAIW production, creating poorly ventilated intermediate waters above ≈2200 m (low benthic $\delta^{13}C$ values). During interglacial periods, the intermediate-depth North Atlantic became ventilated again by UNADW.

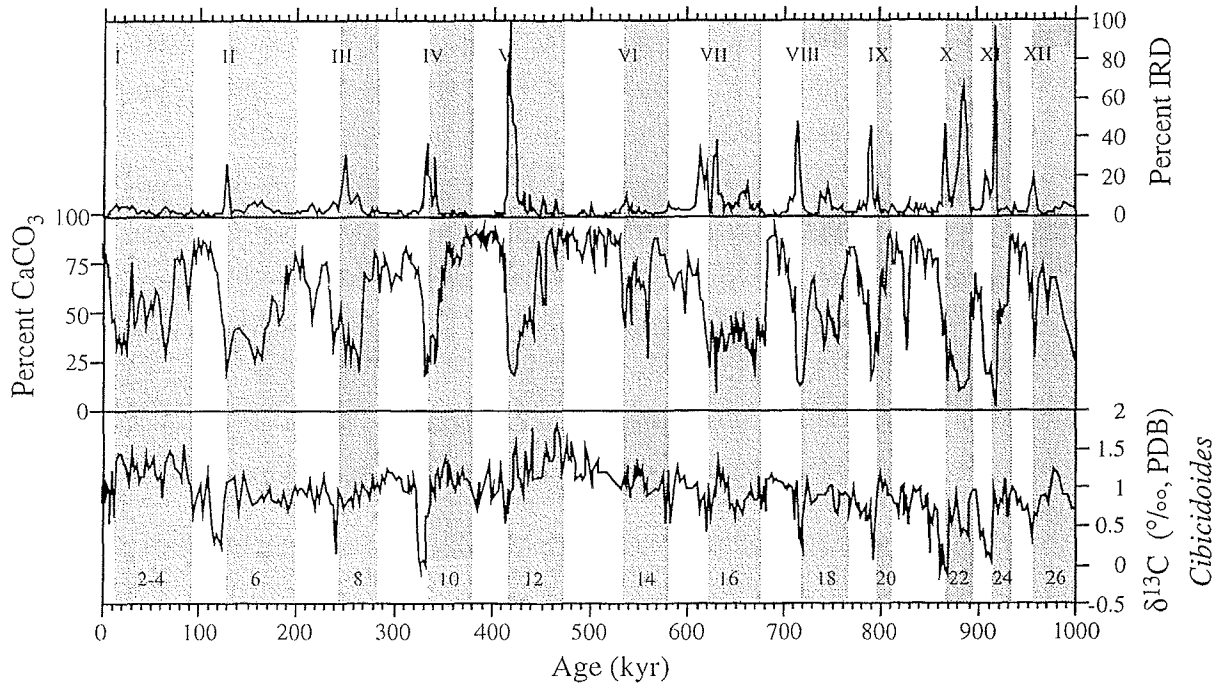

Fig. 4: Ice-rafted debris (%IRD), calcium carbonate (%$CaCO_3$) and benthic foraminifera $\delta^{13}C$ records from ODP site 982 (57°30.8'N, 15°52.5'W, 1145 m water depth; Venz et al., 1999). The records are shown with glacials and Terminations I-X labelled. Note that the shutdown of GNAIW during terminations is indicated by low benthic $\delta^{13}C$ values and high amounts of IRD.

Recently, Oppo and Horowitz (2000) inferred from $\delta^{13}C$ and Cd/Ca records that GNAIW extended at least as far south as 28°S during the LGM in the western South Atlantic, thereby replacing the southern-source intermediate waters AAIW and UCDW. However, the glacial distribution of AAIW and UCDW is not well understood. Droxler et al. (1991) and Haddad and Droxler (1996) suggested that during much of the late Quaternary, different water masses influenced the intermediate depth western North Atlantic and Caribbean, indicating strong fluctuations in AAIW/UCDW production. Boyle (1988) suggested that the switch from deep (NADW) to intermediate (GNAIW) water mass production during glaciations may have influenced the atmospheric CO_2 level. Therefore, improved knowledge of northern as well as southern intermediate water mass variability is important for understanding glacial to interglacial changes in climate.

3. Pteropods

3.1 Distribution patterns, fossil record, and systematic classification

Pteropods are marine gastropods adapted to pelagic life. The fin-shaped wings enable these animals to swim actively in the uppermost 500 m of the water column, migrating diurnally from great depths (during day time) to shallow positions (at night) (Herman, 1978). Pteropods are widely distributed and abundant in all oceans, although most species seem to prefer the circumglobal tropical and subtropical regions (see Fig. 5 for major biogeographic regions). Distribution of pteropods is limited by various physical and chemical parameters, such as temperature, salinity, food, oxygen content, and water depth (Herman, 1978).

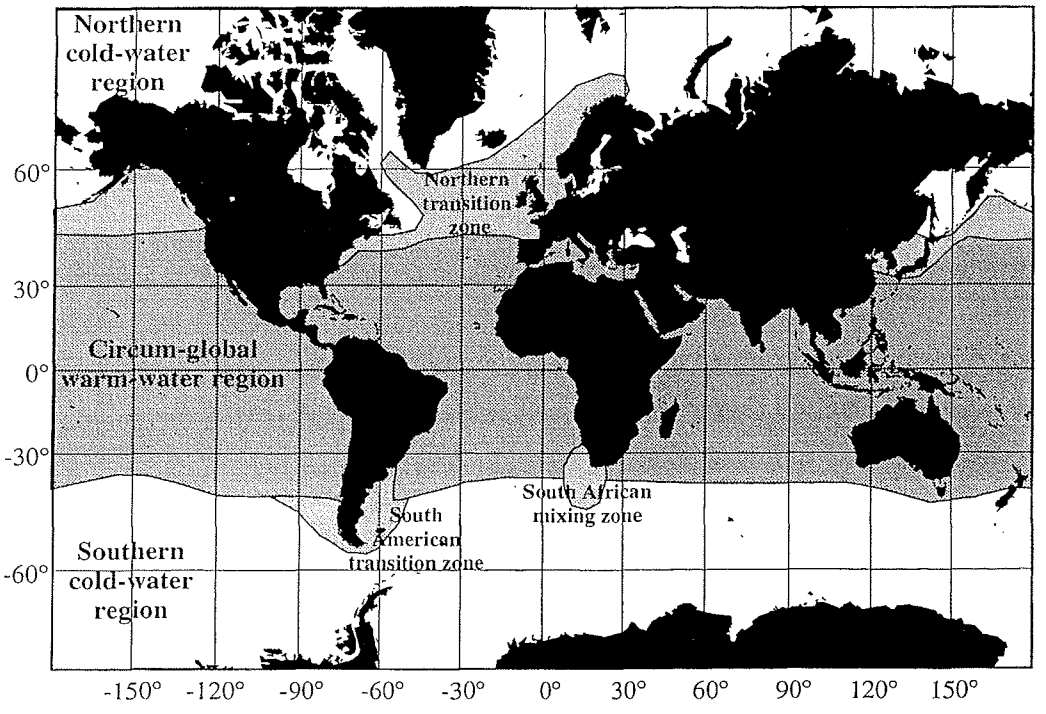

Fig. 5: Major biogeographic regions of pteropods in the modern oceans (modified after Bé and Gilmer, 1977).

The fossil record of shelled pteropods extends back to the Cretaceous, but the phylogenetic relationships among pteropods are still under discussion. Most likely, pteropods evolved from littoral gastropods through the lightening, reduction or even loss of the shell. The foot was transformed into two fin-shaped wings, which were uniquely adapted to enable the animals to swim (Bé and Gilmer, 1977; Herman, 1978). Just as the phylogenetic relationships among pteropods are not fully understood, the systematic classification (in particular on species level and below) is still under debate and often revised. In general, pteropods (with Peraclididae,

Limacinidae, and Cavoliniidae as the only shelled pteropod families) are classified as follows (according to Herman, 1978 and Bé and Gilmer, 1977):

Class GASTROPODA
  Subclass OPISTHOBRANCHIATA
    Order GYMNOSOMATA de Blainville, 1824 (naked pteropods; 6 families)
    Order THECOSOMATA de Blainville, 1824 (mainly shelled pteropods)
      Suborder PSEUDOTHECOSOMATA Meisenheimer, 1905
        Family PERACLIDIDAE Tesch, 1913
        Family CYMBULIIDAE Cantraine, 1841
        Family DESMOPTERIDAE Chun, 1889
        Family PROCYMBULIIDAE Tesch, 1913
      Suborder EUTHECOSOMATA Meisenheimer, 1905
        Family LIMACINIDAE Gray, 1847
        Family CAVOLINIIDAE Fischer, 1883

The systematic classification is based on shell characteristics and on the organization of the soft parts. Based on these features, it was believed that the coiled Limacinidae are more primitive, whereas the uncoiled Cavoliniidae are more advanced forms. Microstructural analysis revealed that the Limacinidae (excluding *L. inflata*) possess a similar microstructure to ancient gastropods (i.e. crossed-lamellar), which again has been interpreted as a rather primitive feature. On the other hand, the helical microstructure of the Cavoliniidae has been interpreted as more developed or even neomorph (Bé and Gilmer, 1977).

3.2 The biology and ecology of pteropods

Euthecosomatous pteropods feed on phyto- and zooplankton (Bé and Gilmer, 1977; Herman, 1978). An upper food size limit of approximately 200 µm was determined by Gilmer (1974) for the large pteropods *Creseis acicula* (shell length and diameter up to 33 and 1.5 mm, respectively; Van der Spoel, 1972) and *Cavolinia uncinata* (shell length 5.5-7.5 mm, width 4.0-6.6 mm; Van der Spoel, 1972). Moreover, it has been observed that there is a close connection between pteropod abundance, seasonal phytoplankton blooms, and nutrient levels (Bé and Gilmer, 1977). In the Bermuda and Barbados regions, for instance, it seems that pteropods are most abundant between March and June while January to February is the least productive period (Almogi-Labin, 1982).

Soft parts of pteropods consist of four regions: (1) the head; (2) the fin-shaped wings, used for swimming and gathering food; (3) the visceral mass; and (4) the mantle, which is responsible for the shell secretion (Herman, 1978). In addition, pteropods are hermaphroditic, i.e. each individual has both male and female sexual organs (Herman, 1978).

The pteropod shell is made of aragonite and serves as a refuge from predators (Bé and Gilmer, 1977). Pteropods can withdraw quickly into the shell and sink to another depth level (the sinking rate depends on shell shape and size). However, pteropods are also able to outswim their predators. In situ observations by Gilmer (1974) have revealed an average escape speed of 11-14 cm/s of larger pteropods (i.e. *Cavolinia longirostris*: shell length 2.0-10 mm, width 1.5-7.0 mm; *Cavolina tridentata*: shell length up to 20 mm; *C. acicula*; and *C. uncinata*: Van der Spoel, 1972) and 7 cm/s of the smaller form *Diacria quadridentata* (shell length 2.2-2.9 mm; Van der Spoel, 1972). The ability of some pteropods to sink and swim rapidly enables the animals to migrate vertically up to several hundred meters per day. Interestingly, this feature may also cause uncertainties in field sampling because large pteropods are able to escape from plankton nets or water samplers.

3.3 Pteropod shells

Shell formation takes place within two major phases: (1) cellular processes of ion transport, protein synthesis, and secretion, and (2) a series of physico-chemical processes in which $CaCO_3$ crystals are nucleated, orientated, and grow in intimate association with a secreted organic matrix (Wilbur and Saleuddin, 1983). Gastropod shells consist of minute particles of $CaCO_3$, which are secreted from the mantle epithelium. Aragonitic crystallites occur as approximately 0.2 µm-wide blocks, which are termed basic structural units (Bé and Gilmer, 1977; Bandel, 1990). In pteropods, these second-order blocks are arranged into first-order elongated rods, which themselves are arranged into special structural patterns such as crossed-lamellar, helical, and prismatic structures (Bé and Gilmer, 1977; Bandel, 1990). Among gastropods, crossed-lamellar structures are predominant and rather primitive, whereas helical structures are thought to be more advanced. Prismatic material is not very strong, but it can be deposited very quickly (Currey, 1990). Both the Limacinidae and Cavoliniidae possess aragonitic shells (Bé and Gilmer, 1977), but with strikingly different microstructures. The shells of the Limacinidae are spiral and always sinistrally coiled, and generally smaller than those of the Cavoliniidae which are mostly bilaterally symmetrical in the adult stages (Bé and Gilmer, 1977). Therefore, the Limacinidae can clearly be distinguished from the Cavoliniidae by their shell shapes. The Limacinidae (with the exception of *L. inflata*) possess a crossed-lamellar microstructure (Bé and Gilmer, 1977) with an inner prismatic aragonite layer. The

width of these layers varies within the individual and between the species. The Cavoliniidae have a helical aragonite microstructure (Bé and Gilmer, 1977). *Limacina inflata* possesses a helical microstructure just as the Cavoliniidae, but its shell shape is left-handed and spirally coiled in the same way as the other members of the Limacinidae. Because of the special microstructure of *L. inflata*, Richter (1976) suggested that this species should better be classified as belonging to the Cavoliniidae.

Shell formation of *L. inflata* and other pteropods takes place in the shallowest part of each pteropod's vertical range in the water column, and thus occurs mainly at night (Fabry and Deuser, 1992). After the animal's death, the shell rapidly settles to the sea floor due to its relatively large size (e.g. Herman and Rosenberg, 1969). Initial settling velocities, determined in the laboratory by Byrne et al. (1984), range from 1.0 cm/s (*L. inflata*, juvenile form) to 5.0 cm/s (*Cuvierina columnella*, adult stage). At a mid-range settling rate of 1.4 cm/s (Byrne et al., 1984), pteropod shells in transit to the sea floor will therefore pass the Aragonite Compensation Depth (≈3400 m in the western South Atlantic; see part II-1) after less than three days. Byrne et al. (1984) observed that pteropods at a mid-range settling rate experience substantial dissolution during settling in the Pacific Ocean. This is in contrast to the findings from the South Atlantic Ocean, where dissolution of the pteropod tests mainly occurs at the sea floor (part II-1). This is probably due to the "aging" of the deep waters, since Pacific Ocean deep waters are more undersaturated with respect to aragonite. Preservation of pteropod shells is restricted to shallow parts of the ocean, i.e. shelf regions, continental slopes, ridges, and rises, as the aragonitic shells of pteropods are much more susceptible to solution than the calcitic remains of foraminifera and coccolithophorids. Preservation of pteropods in the geological record (especially in pre-Pleistocene sediments) is rare because of their very thin and fragile shells.

3.4 Limacinidae

The Limacinidae inhabit all oceanic regions, although most species are found in the circumglobal warm-water regions (Bé and Gilmer, 1977; see also Fig. 5). In the present study, four members of the family Limacinidae were recognized in the South Atlantic and Caribbean sediments (see part II), which belong to the suptropical/tropical species (*L. inflata*, *L. bulimoides*, *L. lesueuri*, and *L. trochiformis*). These species are mostly found together (Van der Spoel, 1967), and the first three were chosen for the LDX due to their relatively high abundance and their apparently alternating modes of preservation. The four species will be described in the following.

Limacina inflata (d'Orbigny, 1836; Fig. 6) is one of the most common warm-water cosmopolitans adapted to epiplanktonic life. It is widely distributed in tropical and subtropical

regions (Bé and Gilmer, 1977). Yet, it seems to avoid the eastern South Atlantic upwelling regions, probably due to cold surface water temperatures (Bonnevie, 1913; Tesch, 1946). *Limacina inflata* lives primarily in the upper 300 m of the water column (Bé and Gilmer, 1977) and oxygen isotope studies on adult specimens suggest rapid growth and a life span of merely several weeks to a few months (Fischer et al., 1999). The almost planispiral shell has three whorls coiled in one level with shell diameters up to 1.5 mm (Van der Spoel, 1972). Its unaffected shell surface is smooth, transparent, and lustrous, with gently developed growth lines from the second whorl onwards (Bandel et al., 1984). *Limacina inflata* appears to be highly reliable with respect to the LDX in surface sediments (see part II-1) and LGM sediments (see part II-2). However, since it is more fragile than *L. bulimoides* and *L. lesueuri*, its downcore use is questionable (see LDX results in Fig. 6 of part II-3). It is generally more susceptible to solution than the other three Limacinidae species.

Limacina bulimoides (d'Orbigny, 1836; Fig. 6) is very abundant in the subtropical regions of all oceans. It is generally less abundant in tropical regions and in the boundary currents, with the exception of high concentrations in the BC in the western South Atlantic (Bé and Gilmer, 1977). *Limacina bulimoides* seems to prefer a shallower depth range than *L. inflata*. The shell is spirally coiled with six whorls, large (height and width are up to 2 and 1.4 mm, respectively), and conical (Van der Spoel, 1972). It is not as fragile as *L. inflata* and the shell preservation state is always about one stage better than that of *L. inflata* (see LDX results in Figs. 5, 6 of part II-3).

Limacina lesueuri (d'Orbigny, 1836; Fig. 6) prefers the subtropical regions of all oceans and is predominantly found in oligotrophic, central water masses. This species seems to avoid equatorial waters and appears to be less common than the other three Limacinidae. Bé and Gilmer (1977) proposed that its rarity may in part be an artifact because of its large size (height and width are up to 0.8 and 1.3 mm, respectively: Van der Spoel, 1972), which enables it to escape more efficiently. The shell has 4.5 whorls and is significantly more broad than high (Van der Spoel, 1972). In the LDX records (see Fig. 6 of part II-3), *L. bulimoides* and *L. lesueuri* appear to be more reliable with increasing core depth because they are less fragile than *L. inflata*. *Limacina lesueuri* is just as susceptible to solution as *L. bulimoides*.

Limacina trochiformis (d'Orbigny, 1836; Fig. 6) is a very abundant tropical species, which particularly prefers upwelling regions and a close proximity to land masses (Bé and Gilmer, 1977). The shell has five rapidly increasing whorls and is quite small, with a shell height up to 1 mm (Van der Spoel, 1972). It is much more fragile than *L. bulimoides* and *L. lesueuri*, but nevertheless it seems to be more resistant to solution (Almogi-Labin et al., 1986). This species was not used for the LDX studies.

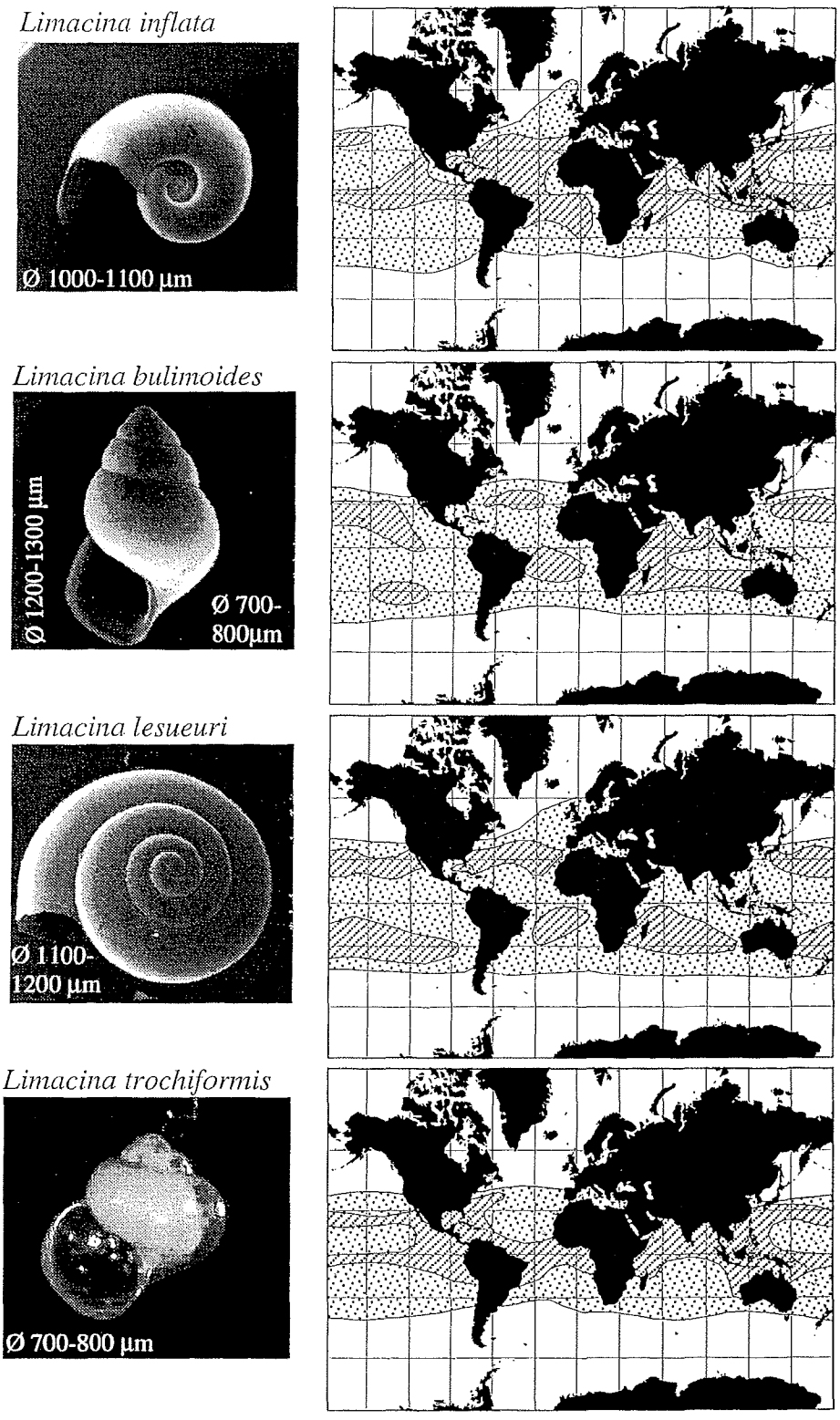

Fig. 6: SEM and light microscope pictures of *L. inflata*, *L. bulimoides*, *L. lesueuri*, and *L. trochiformis* with average shell sizes. The recent distribution in the world's oceans is modified after Bé and Gilmer, 1977. Note that these species prefer the subtropical/tropical regions of all oceans. Dotted = present; hatched = common or abundant.

4. Material and study area

The sediment material used in this thesis was recovered during various RV *Meteor*, RV *Sonne*, and RV *Victor Hensen* cruises between 1988 and 1998 and was derived from different water depths and latitudes throughout the South Atlantic Ocean and the Caribbean Sea (Table 1, Fig. 7). In total, 310 surface sediment samples, 87 sediment samples from 38 gravity cores representing the LGM, and sections of the late Quaternary of six sediment cores (Table 1) were investigated in order to obtain both spatial and temporal information on aragonite preservation patterns. The stratigraphic ranges given in Table 1 are based on different dating methods which have been obtained from various sources (for details see the respective sections of the manuscripts).

Table 1: Sediment material investigated.

Samples	Core type	Latitude	Longitude	Water depth [m]	Stratigraphic range investigated	Reference
Surface *1	MC, MIC, BC, VG	18°N-38°S	78°W-15°E	23-5684	<1 ka	Gerhardt & Henrich, in press
LGM *2	GC	06°N-37°S	46°W-15°E	767-4588	19-23 ka	Gerhardt & Henrich, subm.
GeoB 2202-4	GC	08°12'S	34°16'W	1156	0-240.8? ka	Gerhardt & Henrich, in press
GeoB 2204-1	MC	08°32'S	34°01'W	2080	0-18 ka	Gerhardt et al. (2000)
GeoB 2204-2	GC	08°32'S	34°01'W	2072	6.9-426.1 ka	Gerhardt et al. (2000)
GeoB 2205-4	MC	08°34'S	34°21'W	1790	0-18? ka	Gerhardt et al. (2000)
GeoB 2207-2	MC	08°44'S	34°08'W	2585	0-13? ka	Gerhardt et al. (2000)
GeoB 3910-2	GC	04°15'S	36°21'W	2362	0-11 ka	Arz et al., in press

BC - Box corer; GC - Gravity corer; MC - Multicorer; MIC - Minicorer; VG - Van Veen Grab
*1 - see Appendix 1 in Gerhardt and Henrich, in press; *2 - see Appendix 1 in Gerhardt and Henrich, subm.

The study area stretches from 20°N to 40°S and 80°W to 15°E (Fig. 7), including most of the Central and South Atlantic Ocean and the Caribbean Sea. The sediments were recovered in different regions with various oceanographic and environmental conditions, such as shelf regions with large amounts of benthic organisms and lithogenous material, continental slope regions with turbidites and contourites, deep-sea basins with strong aragonite dissolution beneath the aragonite compensation depth, and various ridges and rises. Particularly, the latter two favor pteropod accumulation and aragonite preservation. The investigated sediments have accumulated in coastal and equatorial upwelling regions as well as in oligotrophic regions and contain varying amounts of organic material.

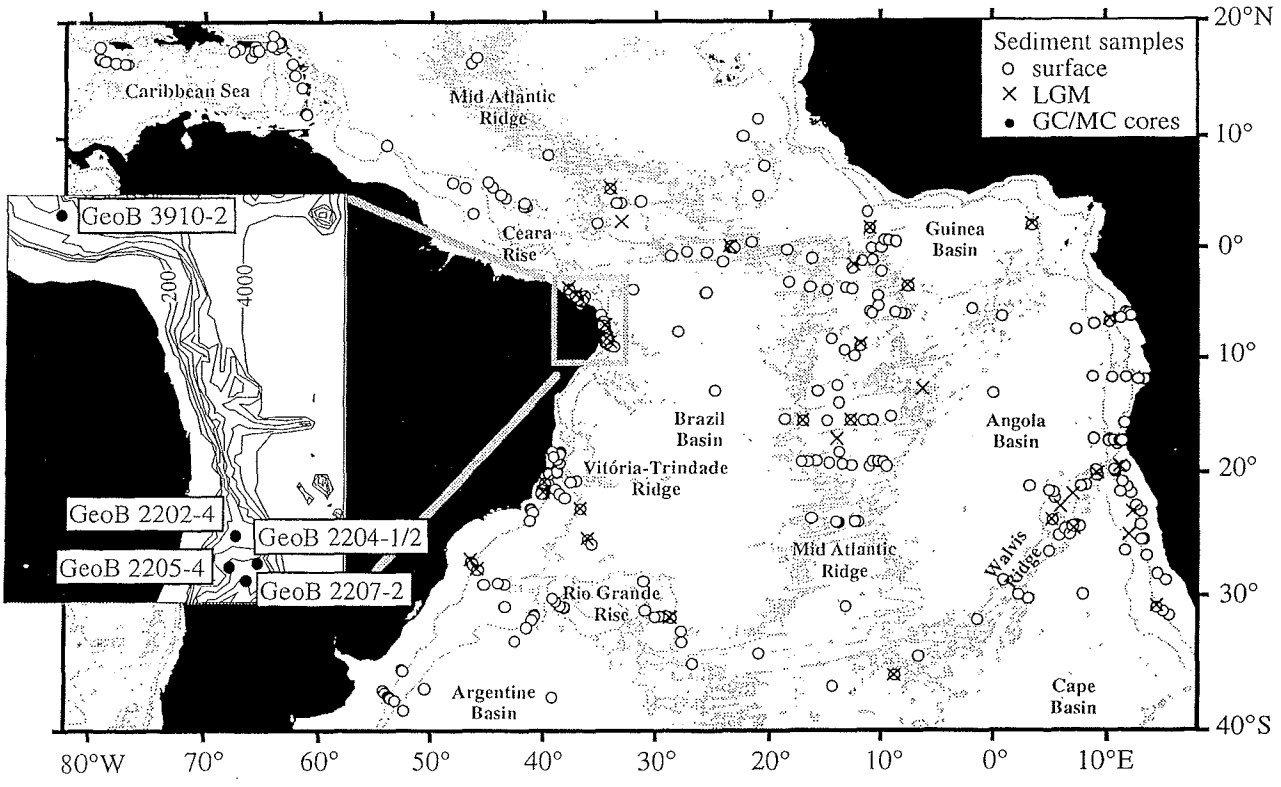

Fig. 7: Overview of the sediment samples investigated. Surface samples (open circles; mostly the uppermost cm) were collected with multicorer (MC), minicorer (MIC), box corer (BC), or Van Veen Grab (VG). Last glacial maximum (LGM) samples (crosses; 23-19 cal-ka-BP) were collected with Gravity corer (GC). Black dots mark gravity cores and multicores, which were studied entirely (GeoB 2202-4, GeoB 2204-1/2, GeoB 2205-4, GeoB 2207-2) or of which only the Holocene section was studied (GeoB 3910-2).

5. Methods

As the methods used in this thesis are described in detail in the respective manuscripts, they will only be briefly described in the following section (see also Fig. 8). The stratigraphic control of sediments was obtained by $\delta^{18}O$ and accelerator mass spectrometry (AMS) ^{14}C datings. Calcium carbonate and total organic carbon (TOC) contents were measured using a LECO element analyzer, and the sand content (>63 µm fraction) was weighed. These basic parameters were combined with pteropodal counts, preservation studies (LDX), and aragonite contents (x-ray diffraction analysis: XRD) to obtain a multi-proxy approach.

In order to determine gastropodal and foraminiferal abundances, particle counts were carried out using a binocular microscope (see part II-3 for a detailed description). Each particle was counted as whole (intact), damaged (at least 50% of the shell existing) or as a fragment. The counted particle number varied strongly due to changing amounts of whole and damaged

gastropod shells, as most pteropods are highly fragile. Pteropodal fragility affects the assemblage records in several ways, resulting in possible uncertainties in paleoecologic reconstructions: (1) since the susceptibility to fragmentation varies among pteropod species, less fragile pteropods will be enriched depending on sedimentary preservation state and preparation; (2) reconstruction of the original assemblage is difficult because most pteropods lack surface shell ornamentation, hence fragments are nearly unidentifiable; (3) since most pteropods break in an indefinite number of fragments, it is difficult to determine the original number of shells from the number of fragments; and (4) fragmentation increases downcore and with increasing aragonite dissolution.

Pteropods are not only affected by mechanical factors causing fragmentation, but also by changes in water chemistry causing dissolution. Therefore, pteropodal preservation patterns were investigated by developing and establishing a new method: the *Limacina* Dissolution Index (LDX; see part II-1 for a detailed description). Briefly, at least 10 adult tests per sample of *L. inflata*, *L. bulimoides*, or *L. lesueri* were picked from the coarse fraction and classified using a binocular microscope after the following six preservation stages: (0) transparent, (1) milky/cloudy, (2) opaque-white, lustrous shell surface, (3) opaque-white, partly lustreless shell surface, (4) opaque-white, totally lustreless shell surface, and (5) opaque-white, totally lustreless and perforated. *Limacina inflata* appears to be most reliable because of its abundance and its variability in the preservation stages. On the other hand, *L. bulimoides* and *L. lesueri* are not as fragile as *L. inflata*, so that their applicability increases downcore and when aragonite dissolution becomes stronger. The LDX is a reliable method to indicate aragonite dissolution as changes in carbonate production in the surface waters as well as dilution in the sediment may only lead to a lack of pteropod tests (and hence lead to LDX failure), but does not influence the preservation of tests in the sediment.

Bulk aragonite contents were determined using XRD (see part II-1, 3 for a detailed description). Even in sediments containing poorly preserved pteropods (e.g. when LDX failure occurs due to a lack of tests), the XRD still displays consistent aragonite values (with a minimum detection limit of 5%). In contrast to the LDX, however, changes in the bulk aragonite content are due to a combination of aragonite preservation changes and varying aragonite production in the surface water. Since dilution of the sediment by terrigenous material also affects the aragonite content, relative aragonite contents (percent of bulk carbonate) were used. Calcite and aragonite ratios in surficial sediments and in GeoB 2202-4 (part II-1) were measured with a Philips PW1830 goniometer, whereas the aragonite records in cores GeoB 2204-1/2 and GeoB 2207-2 (part II-3) were determined with a Siemens D-500 diffractometer.

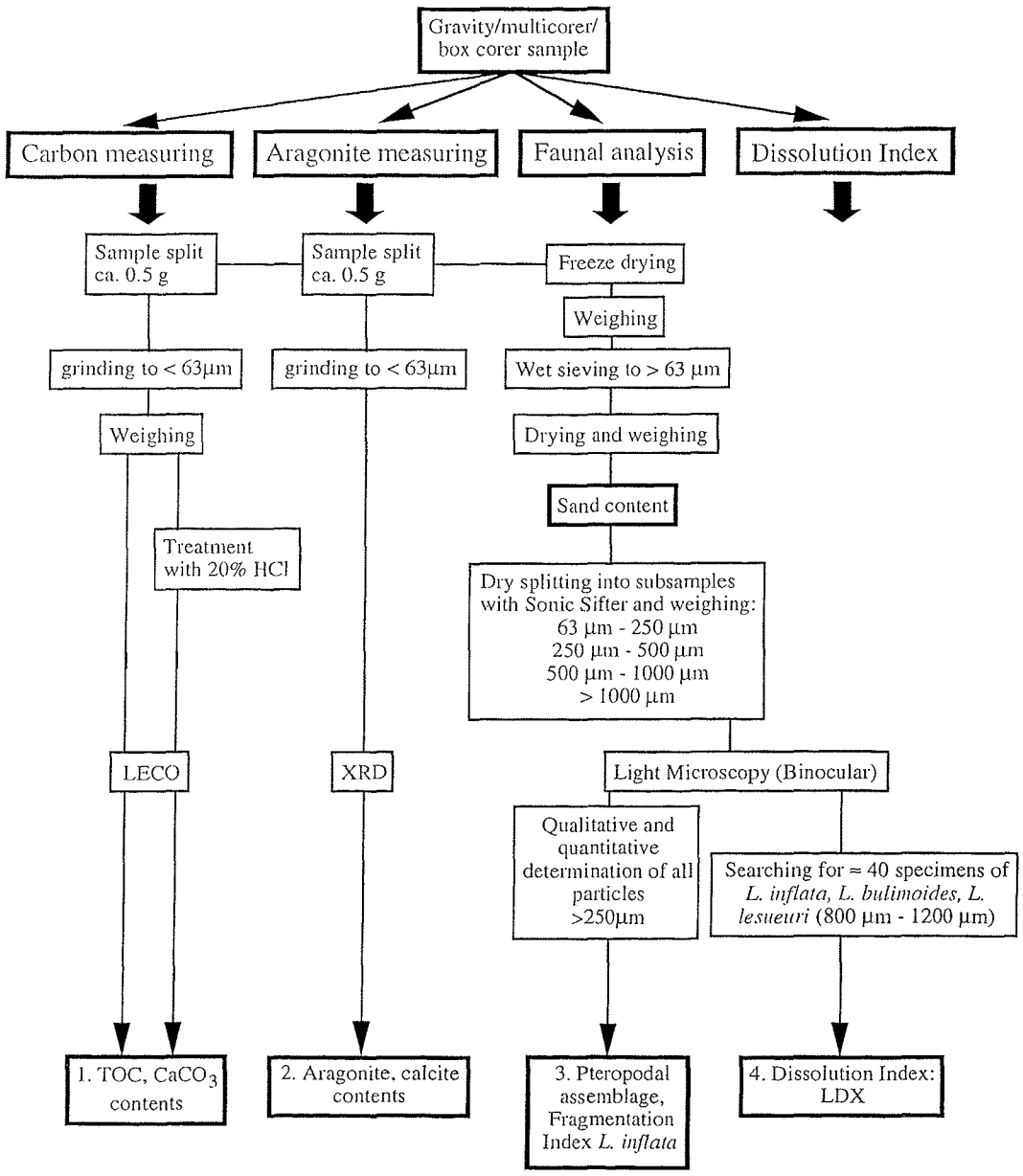

Fig. 8: Flow-chart of all routines carried out. The investigation of sediment material is based on four methods: (1) determination of bulk carbonate and TOC contents using a LECO element analyzer; (2) determination of aragonite/calcite ratios using x-ray diffraction analysis (XRD); (3) determination of sand contents as well as particle counts and the *Limacina* Fragmentation Index on *L. inflata* using light microscopy; and (4) the determination of preservation states of *L. inflata*, *L. bulimoides* and *L. lesueuri* also using light microscopy.

6. References

Almogi-Labin, A., 1982. Distribution of euthecosomatous pteropods in plankton tows, trap and surface sediment off Bermuda and Barbados (Northern Atlantic). In: Hemleben, C. (Ed.), Cytologic and Ecologic Aspects of Morphogenesis. Neues Jahrbuch der Geologie und Paläontologie 164 (1), pp. 92-95.

Almogi-Labin, A., Luz, B., Duplessy, J.-C., 1986. Quaternary paleo-oceanography, pteropod preservation and stable-isotope record of the Red Sea. Palaeogeography, Palaeoclimatology, Palaeoecology 57, 195-211.

Archer, D.E., 1996. An atlas of the distribution of calcium carbonate in sediments of the deep sea. Global Biogeochemical Cycles 10 (1), 159-174.

Archer, D., Emerson, S., Reimers, C., 1989. Dissolution of calcite in deep-sea sediments: pH and O_2 microelectrode results. Geochimica et Cosmochimica Acta 53, 2831-2845.

Arz, H.W., Gerhardt, S., Pätzold, J., Röhl, U., 2001. Millennial-scale changes of surface- and deep-water flow in the western tropical Atlantic linked to Northern Hemisphere high-latitude climate during the Holocene. Geology, in press.

Bainbridge, A.E., 1981. GEOSECS Atlantic Expedition, Hydrographic Data, 1972-1973. National Science Foundation, Superintendent of Documents, US Government Printing Office, Washington DC, pp. 1-121.

Bandel, K., 1990. Shell structure of the Gastropoda excluding Archaegastropoda. In: Carter, J.G. (Ed.), Skeletal Biomineralization: Patterns, Processes and Evolutionary Trends. Volume 1. Van Nostrand Reinhold, New York, pp. 117-134.

Bandel, K., Almogi-Labin, A., Hemleben, Chr., Deuser, W.G., 1984. The conch of *Limacina* and *Peraclis* (Pteropoda) and a model for the evolution of planktonic gastropods. Neues Jahrbuch Geologisch-Paläontologische Abhandlungen 168 (1), 87-107.

Barnola, J.-M., Pimienta, P., Raynaud, D., Korotkevich, 1991. CO_2-climate relationship as deduced from the Vostok ice core: a re-examination based on new measurements and on a re-evaluation of the air dating. Tellus 43B, 83-90.

Bé, A.W.H., Gilmer, R.W., 1977. A zoographic and taxonomic review of euthecosomatous pteropoda. In: Ramsay, A.T.S. (Ed.), Oceanic Micropalaeontology, volume 1. Academic Press, London, pp. 733-808.

Berner, R.A., Honjo, S., 1981. Pelagic sedimentation of aragonite: its geochemical significance. Science 211: 940-942.

Bickert, T., Wefer, G., 1996. Late Quaternary deep water circulation in the South Atlantic: Reconstruction from carbonate dissolution and benthic stable isotopes. In: Wefer, G., Berger, W.H., Siedler, G., Webb, D. (Eds.), The South Atlantic: Present and Past Circulation. Springer-Verlag, Berlin, Heidelberg, pp. 599-620.

Bonnevie, K., 1913. Pteropoda from the Michael Sars North Atlantic deep- sea expedition. Report and Scientific Results. "Michael Sars" North Atlantic Deep-Sea Expedition 1910 III (1), pp. 1-69.

Boyle, E.A., 1988. Cadmium: chemical tracer of deepwater paleoceanography. Paleoceanography 3, 471-490.

Boyle, E.A., Keigwin, L.D., 1982. Deep circulation of the North Atlantic over the last 200,000 years: geochemical evidence. Science 218, 784-787.

Boyle, E.A., Keigwin, L.D., 1987. North Atlantic thermohaline circulation during the past 20,000 years linked to high-latitude surface temperature. Nature 30, 35-40.

Broecker, W.S., Clark, E., McCorkle, D.C., Peng, T.-H., Hajdas, I., Bonani, G., 1999. Evidence for a reduction in the carbonate ion content of the deep sea during the course of the Holocene. Paleoceanography 14 (6), 744-752.

Broecker, W.S., Peteet, D.M., Rind, D., 1985. Does the ocean-atmosphere system have more than one stable mode of operation? Nature 315, 21-26.

Broecker, W.S., Takahashi, T., 1978. The relationship between lysocline depth and in situ carbonate ion concentration. Deep-Sea Research 25, 65-95.

Byrne, R.H., Acker, J.G., Betzer, P.R., Feely, R.A., Cates, M.H.,1984. Water column dissolution of aragonite in the Pacific Ocean. Nature 312, 321-326.

Charles, C.D., Fairbanks, R.G., 1992. Evidence from Southern Ocean sediments for the effect of North Atlantic deep-water flux on climate. Nature 355, 416-419.

Chester, R., 1990. Marine Geochemistry. Unwin Hyman, London, Boston, Sydney, Wellington, pp. 1-698.

Currey, J.D., 1990. Biomechanics of mineralized skeletons. In: Carter, J.G. (Ed.), Skeletal Biomineralization: Patterns, Processes and Evolutionary Trends. Volume 1. Van Nostrand Reinhold, New York, pp. 11-25.

Curry, W.B., 1996. Late Quaternary deep circulation in the western equatorial Atlantic. In: Wefer, G., Berger, W.H., Siedler, G., Webb, D. (Eds.), The South Atlantic: Present and Past Circulation. Springer-Verlag, Berlin, Heidelberg, pp. 577-598.

Curry, W.B., Duplessy, J.C., Labeyrie, L.D., Shackleton, N.J., 1988. Changes in the distribution of $\delta^{13}C$ of deep water ΣCO_2 between the last glaciation and the Holocene. Paleoceanography 5, 487-506.

Curry, W.B., Lohmann, G.P., 1982. Carbon isotopic changes in benthic foraminifera from the western South Atlantic: reconstruction of glacial abyssal circulation patterns. Quaternary Research 18, 218-235.

Curry, W.B., Lohmann, G.P., 1983. Reduced advection into Atlantic Ocean deep eastern basins during last glaciation maximum. Nature 306, 577-580.

Dansgaard, W., Johnsen, S.J., Clausen, H.B., Dahl-Jensen, D., Gundestrup, N.S., Hammer, C.U., Hvidberg, C.S., Steffensen, J.P., Sveinbjörnsdottir, A.E., Jouzel, J., Bond, G., 1993. Evidence for general instability of past climate from a 250 kyr ice-core record. Nature, 364, 218-220.

deMenocal, P.B., Oppo, D.W., Fairbanks, R.G., Prell, W.L., 1992. Pleistocene $\delta^{13}C$ variability of North Atlantic intermediate water. Paleoceanography 7 (2), 229-250.

Droxler, A.W., Morse, J.W., Glaser, K.S., Haddad, G.A., Baker, P.A., 1991. Surface sediment carbonate mineralogy and water column chemistry: Nicaragua Rise versus the Bahamas. Marine Geology 100, 277-289.

Duplessy, J.C., Shackleton, N.J., Fairbanks, R.G., Labeyrie, L.D., Oppo, D., Kallel, N., 1988. Deepwater source variations during the last climatic cycle and their impact on the global deepwater circulation. Paleoceanography 3, 343-360.

Fabry, V.J., 1990. Shell growth rates of pteropod and heteropod molluscs and aragonite production in the open ocean: implications for the marine caronate system. Journal of Marine Research 48, 209-222.

Fabry, V.J., Deuser, W.G., 1991. Aragonite and magnesian calcite fluxes to the deep Sargasso Sea. Deep-Sea Research 38, 713-728.

Fabry, V.J., Deuser, W.G., 1992. Seasonal changes in the isotopic compositions and sinking fluxes of euthecosomatous pteropod shells in the Sargasso Sea. Paleoceanography 7 (2), 195-213.

Fischer, G., Kalberer, M., Donner, B., Wefer, G., 1999. Stable isotopes of pteropod shells as recorders of sub-surface water conditions: comparison to the record of *G. ruber* and to measured values. In: Fischer, G., Wefer, G. (Eds.), Use of Proxies in Paleoceanography: Examples from the South Atlantic. Springer-Verlag, Berlin, Heidelberg, pp. 191-206.

Gerhardt, S., Groth, H., Rühlemann, C., Henrich, R., 2000. Aragonite preservation in late Quaternary sediment cores on the Brazilian Continental Slope: implications for intermediate water circulation. International Journal of Earth Sciences 88 (4), 607-618.

Gerhardt, S., Henrich, R., 2001. Shell preservation of *Limacina inflata* (Pteropoda) in surface sediments from the Central and South Atlantic Ocean: a new proxy to determine the aragonite saturation state of water masses. Deep-Sea Research I, in press.

Gerhardt, S., Henrich, R., 2001. Intermediate water circulation during the last glacial maximum in the South Atlantic Ocean inferred from changes in the shell preservation of *Limacina inflata* (Pteropoda). Submitted to Deep-Sea Research I.

Gilmer, R.W., 1974. Some aspects of feeding in thecosomatous pteropod molluscs. Journal of Marine Biology and Ecology 15, 127-144.

Gordon, A.L., 1986. Interocean exchange of thermocline water. Journal of Geophysical Research 91, 5037-5046.

Gordon, A.L., Ray, F.W., Smethie Jr., W.M., Warner, M.J., 1992. Thermocline and intermediate water communication between the South Atlantic and Indian Oceans. Journal of Geophysical Research 97C, 7223-7240.

Grootes, P.M., Stuiver, M., White, J.W.C., Johnsen, S., Jouzel, J., 1993. Comparison of oxygen isotopes records from the GISP 2 and GRIP Greenland ice cores. Nature 366, 552-554.

Grootes, P.M., Stuiver, M., 1997. Oxygen 18/16 variability in Greenland snow and ice with 10^{-3}- to 10^{5}-year time resolution. Journal of Geophysical Research 102 (C12), 26,455-26,470.

Haddad, G.A., Droxler, A.W., 1996. Metastable $CaCO_3$ dissolution at intermediate water depths of the Caribbean and western North Atlantic: implications for intermediate water circulation during the past 200,000 years. Paleoceanography 11 (6), 701-716.

Hales, B., Emerson, S., 1996. Calcite dissolution in sediments of the Ontong-Java Plateau: in situ measurements of pore water O_2 and pH. Global Geochemical Cycles 10 (3), 527-541.

Hales, B., Emerson, S., 1997. Calcite dissolution in sediments of the Ceara Rise: in situ measurements of porewater O_2, pH, and $CO_{2(aq)}$. Geochimica et Cosmochimica Acta 61 (3), 501-514.

Hales, B., Emerson, S., Archer, D., 1994. Respiration and dissolution in the sediments of the western North Atlantic: estimates from models of in situ microelectrode measurements of porewater oxygen and pH. Deep-Sea Research I 41 (4), 695-719.

Herman, Y., 1978. Pteropods. In: Haq, B., Boersma, A. (Eds.), Introduction to Marine Micropaleontology. Elsevier, North-Holland, Ney York, pp. 151-159.

Herman, Y., Rosenberg, P.E., 1969. Pteropods as bathymetric indicators. Marine Geology 7, 169-173.

Kaese, R.H., Zenk, W., 1987. Reconstructed Mediterranean salt lens trajectories. Journal of Physical Oceanography 17, 158-163.

Kawase, M., Sarmiento, J., 1986. Circulation and nutrients in mid-depth Atlantic waters. Journal of Geophysical Research 91, 9749-9770.

Kroopnick, P.M., 1985. The distribution of ^{13}C of ΣCO_2 in the world oceans. Deep-Sea Research Part I 32 (1), 57-84.

Lea, D.W., 1999. Innovations in monitoring ocean history. In: Abrantes, F., Mix, A. (Eds.), Reconstructing Ocean History: A Window into the Future. Kluwer Academic/Plenum Publishers, New York, pp. 321-327.

Mercier, H., Speer, K.G., Honnorez, J., 1994. Tracing the Antarctic Bottom Water through the Romanche and Chain Fracture Zones. Deep-Sea Research 41, 1457-1477.
Millero, F.J., 1996. Chemical oceanography. CRC Press, Boca Raton, pp. 1-469.
Milliman, J.D., 1993. Production and accumulation of calcium carbonate in the ocean: budget of a nonsteady state. Global Biogeochemical Cycles 7 (4), 927-957.
Milliman, J.D., Troy, P.J., Balch, W.M., Adams, A.K., Li, Y.-H., Mackenzie, F.T., 1999. Biologically mediated dissolution of calcium carbonate above the chemical lysocline? Deep-Sea Research I 46, 1653-1669.
Morse, J.W., Mucci, A., Millero, F.J., 1980. The solubility of calcite and aragonite in seawater at various salinities, temperatures and 1 atmosphere total pressure. Geochimica et Cosmochimica Acta 44, 85-94.
Oppo, D.W., Fairbanks, R.G., 1987. Variability in the deep and intermediate water circulation of the Atlantic Ocean during the past 25,000 years: Northern Hemisphere modulation of the Southern Ocean. Earth and Planetary Science Letters 86, 1-15.
Oppo, D.W., Horowitz, M., 2000. Glacial deep water geometry: South Atlantic benthic foraminiferal Cd/Ca and $\delta^{13}C$ evidence. Paleoceanography 15 (2), 147-160.
Oppo, D.W., Lehman, S.J., 1993. Mid-depth circulation of the subpolar North Atlantic during the last glacial maximum. Science 259, 1148-1152.
Peterson, R.G., Stramma, L., 1991. Upper-level circulation in the South Atlantic Ocean. Progress in Oceanography 26, 1-73.
Raymo, M.E., Ruddiman, W.F., Shackleton, N.J, Oppo, D.W., 1990. Evolution of Atlantic-Pacific $\delta^{13}C$ gradients over the last 2.5 m.y. Earth and Planetary Science Letters 97, 353-368.
Reid, J.L., 1989. On the total geostrophic circulation of the South Atlantic Ocean: flow patterns, tracers, and transports. Program of Oceanography 23 (3), 149-244.
Reid, J.L., 1994. On the total geostrophic circulation of the North Atlantic Ocean: flow patterns, tracers, and transports. Progress in Oceanography 33 (1), 1-92.
Reid, J.L., 1996. On the circulation of the South Atlantic Ocean. In: Wefer, G., Berger, W.H., Siedler, G.,
Webb, D. (Eds.), The South Atlantic: Present and Past Circulation. Springer-Verlag, Berlin, Heidelberg, pp. 13-44.
Richter, G., 1976. Zur Frage der Verwandtschaftsbeziehungen von Limacinidae und Cavolinidae. Archiv für Molluskenkunde 107 (1/3), 137-144.
Sarnthein, M., Winn, K., Jung, S.J.A., Duplessy, J.C., Labeyrie, L.D., Erlenkeuser, H., Ganssen, G., 1994. Changes in East Atlantic deepwater circulation over the last 30,000 years: eight time slice reconstructions. Paleoceanography 9, 209-267.
Shannon, L.V., Chapman, P., 1991. Evidence of Antarctic Bottom Water in the Angola Basin at 32°S. Deep-Sea Research 38, 1299-1304.
Schlitzer, R., 1996. Mass and heat transports in the South Atlantic derived from historical hydrographic data. In: Wefer, G., Berger, W.H., Siedler, G., Webb, D. (Eds.), The South Atlantic: Present and Past Circulation. Springer-Verlag, Berlin, Heidelberg, pp. 305-323.
Talley, L.D., 1996. Antarctic Intermediate Water in the South Atlantic. In: Wefer, G., Berger, W.H., Siedler, G., Webb, D. (Eds.), The South Atlantic: Present and Past Circulation. Springer-Verlag, Berlin, Heidelberg, pp. 219-238.
Tesch, J.J., 1946. The thecosomatous pteropods. I. The Atlantic. Dana-Report No. 5 (28), pp. 1-82.
Van der Spoel, S.,1967. Euthecosomata, a group with remarkable development stages (Gastropoda, Pteropoda). Ph.D. thesis, Univ. Amsterdam, J. Noorduijn en Zoon, Gorinchem, pp. 1-375
Van der Spoel, S., 1972. Pteropoda Thecosomata. Conseil Internatational Pour Exploration De La Mer. Zooplankton Sheet 140-142, pp. 1-12.
Venz, K.A., Hodell, D.A., Stanton, C., Warnke, D.A., 1999. A 1.0 Myr record of Glacial North Atlantic Intermediate Water variability from ODP site 982 in the northeast Atlantic. Paleoceanography 14 (1), 42-52.
Volbers, A.N.A., Niebler, H.-S., Giraudeau, J., Schmidt, H., Henrich, R., 2001. Palaeoceanographic changes in the Northern Benguela Upwelling System over the last 245.000 years as derived from planktic foraminifera assemblages. Submitted to Progress in Oceanography.
Wefer, G., Berger, W.H., Bijma, J., Fischer, G., 1999. Clues to ocean history: a brief overview of proxies. In: Fischer, G., Wefer, G. (Eds.), Use of Proxies in Paleoceanography: Examples from the South Atlantic. Springer-Verlag, Berlin, Heidelberg, pp. 1-68.
Wilbur, K.M., Saleuddin, A.S.M., 1983. Shell formation. In: Saleuddin, A.S.M., Wilbur, K. (Eds.), The Mollusca, Volume 4, Physiology, Part 1. Academic Press, New York, London, pp. 235-287.
Wüst, G., 1935. Schichtung und Zirkulation des altantischen Ozeans. Deutsche Atlantische Expedition "Meteor", 1925-1927, Wissenschaftliche Ergebnisse 2.

Part II *Publications*

Four manuscripts were submitted to international journals as a major part of this study. The content of these papers will be described briefly in the following section:

(1) Shell preservation of *Limacina inflata* (Pteropoda) in surface sediments from the Central and South Atlantic Ocean: a new proxy to determine the aragonite saturation state of water masses. Gerhardt, S. and Henrich, R. (Deep-Sea Research I, in press)

The *Limacina* Dissolution Index (LDX) was developed in order to improve our understanding about intermediate water mass variability. In this paper, the reliability of the LDX is tested in surface sediments under modern hydrographic conditions. For this purpose, 310 surface sediment samples from the Central and South Atlantic Ocean and the Caribbean Sea were investigated. The LDX reflects the aragonite saturation state at the sediment-water interface. In the western South Atlantic Ocean, poor preservation is found within aragonite-corrosive intermediate water masses of southern origin (i.e. AAIW and UCDW), whereas good preservation is observed within the surface water and the UNADW. In the eastern Atlantic Ocean, in particular along the African continental margin, the LDX fails in most cases. In the Caribbean Sea, a more complex preservation pattern is observed based on the interaction between different water masses, which invade the Caribbean basins through several channels and sills.

(2) Intermediate water circulation during the last glacial maximum in the South Atlantic Ocean inferred from changes in the shell preservation of *Limacina inflata* (Pteropoda). Gerhardt, S. and Henrich, R. (Submitted to Deep-Sea Research I)

In this manuscript, the LDX is applied on the LGM (23-19 cal-ka-BP). 87 sediment samples derived from 38 South Atlantic cores were investigated in order to reconstruct the western South Atlantic intermediate circulation. The LDX records indicate very good to moderate preservation at intermediate water depths during the LGM, which is in contrast to the modern situation. This indicates the presence of non- or only slightly aragonite-corrosive GNAIW at intermediate depths at least as far south as 20°S in the western South Atlantic. Speculation on the glacial distribution of AAIW and UCDW in the South Atlantic assumes three models: (1) the southward restriction of AAIW and UCDW; (2) the complete

elimination of AAIW and UCDW; or (3) the relative change in position with NADW with or without mixing with SCW.

(3) Aragonite preservation in late Quaternary sediment cores on the Brazilian Continental Slope: implications for intermediate water circulation. Gerhardt, S., Groth, H., Rühlemann, C., and Henrich, R. International Journal of Earth Sciences 88 (4), 607-618.

In order to determine intermediate water variability during the late Quaternary, four sediment cores were studied, which were recovered from the Brazilian Continental Slope between 1790 m and 2585 m water depth. Besides various ecological and preservational indices, the LDX was applied on three pteropod species (i.e. *L. inflata*, *L. bulimoides*, and *L. lesueuri*). Excellent preservation was found during the Holocene, whereas aragonite dissolution gradually increases downcore. This general pattern is attributed to an overall increase in the aragonite-corrosiveness of pore waters. Overprinted on this early diagenetic trend are high-frequency fluctuations of aragonite preservation, which may be related to climatically induced variations of intermediate water masses.

(4) Millennial-scale changes of surface- and deep-water flow in the western tropical Atlantic linked to Northern Hemisphere high-latitude climate during the Holocene. Arz, W.H., Gerhardt, S., Pätzold, J. , Röhl, U. (Geology, in press)

Here, a well-dated, high-resoluted Holocene marine record from the tropical western Atlantic is presented. Changes in Ca intensity and in preservation of *L. inflata* record changes in the corrosiveness of the bottom water at the core site due to changing influence of northern versus southern water masses. The $\delta^{18}O$ difference between the shallow-living planktonic foraminifera *Globigerinoides sacculifer* and the deep-living *Globorotalia tumida* is used as proxy for changes in the vertical stratification of the surface water, hence for the trade wind strength at this latitude. Comparison to high-latitude records of the North Atlantic region reveals good agreement between aragonite dissolution and the strength in the Iceland-Scotland Overflow Water (ISOW), which significantly contributes to the NADW. This strongly suggests that large-scale variations in the Atlantic thermohaline circulation occurred throughout the Holocene. Concurrently, the comparison of the $\Delta\delta^{18}O$ with the GISP2 glaciochemical records points to global Holocene atmospheric reorganizations seen both in the tropics and high northern latitudes.

1. Shell preservation of *Limacina inflata* (Pteropoda) in surface sediments from the Central and South Atlantic Ocean: a new proxy to determine the aragonite saturation state of water masses

Sabine Gerhardt and Rüdiger Henrich

Dept. of Geosciences, University of Bremen, P.O. Box 33 04 40, D-28334 Bremen, Germany

Abstract

Over 300 surface sediment samples from the Central and South Atlantic Ocean and the Caribbean Sea were investigated for the preservation state of the aragonitic test of *Limacina inflata*. Results are displayed in spatial distribution maps and are plotted against cross-sections of vertical water mass configurations, illustrating the relationship between preservation state, saturation state of the overlying waters, and overall water mass distribution. The microscopic investigation of adults of *L. inflata* yielded the *Limacina* Dissolution Index (LDX), and revealed three regional dissolution patterns. In the western Atlantic Ocean, sedimentary preservation states correspond to saturation states in the overlying waters. Poor preservation is found within intermediate water masses of southern origin (i.e. Antarctic Intermediate Water = AAIW, Upper Circumpolar Water = UCDW), which are distinctly aragonite-corrosive, whereas good preservation is observed within the surface waters above and within the Upper North Atlantic Deep Water (UNADW) beneath the AAIW. In the eastern Atlantic Ocean, in particular along the African continental margin, the LDX fails in most cases (i.e. less than 10 tests of *L. inflata* per sample were found). This is most probably due to extensive "metabolic" aragonite dissolution at the sediment-water interface combined with a reduced abundance of *L. inflata* in the surface waters. In the Caribbean Sea, a more complex preservation pattern is observed based on the interaction between different water masses, which invade the Caribbean basins through several channels and varying input of bank-derived fine aragonite and magenesian calcite material.

The solubility of aragonite increases with increasing pressure, but aragonite dissolution in the sediments does not simply increase with water depth. Worse preservation is found in intermediate water depths following an S-shaped curve. As a result, two aragonite lysoclines are observed one above the other. In four depth transects, we show that the western Atlantic and Caribbean LDX records resemble surficial calcium carbonate data, and water-derived $\delta^{13}C$ and carbonate ion concentration profiles. Moreover, preservation of *L. inflata* within AAIW and UCDW improves significantly to the north, whereas carbonate-corrosiveness

diminishes due to increased mixing of AAIW and UNADW. The close relationship between LDX values and aragonite contents in the sediments shows much promise for the quantification of the aragonite loss under the influence of different water masses.

Keywords: Pteropods, *Limacina inflata*, aragonite, carbonate dissolution, water masses, Atlantic Ocean, Caribbean Sea

1. Introduction

A large research effort has been directed towards the investigation of physical and chemical properties of water masses in order to decipher the main controls and climatic signals of the oceans. Global programs such as the Geochemical Ocean Section Study (GEOSECS) and the World Ocean Circulation Experiment (WOCE) produced an extensive data set (e.g. Bainbridge, 1981; Siedler et al., 1996). In particular, the modern water mass configuration in the Atlantic Ocean was and still is a high priority topic of numerous studies (e.g. Kroopnick, 1985; Reid, 1989, 1996; Siedler et al., 1996). These studies have consolidated our understanding of the world's oceans. All these investigations are based on both measured and calculated data (e.g. temperature, salinity, alkalinity, potential density, oxygen, phosphate, silica, pH, TCO_2, pCO_2, ^{13}C of ΣCO_2, and $[CO_3^{2-}]$). This is most effective with respect to the modern water mass configuration, but in order to reconstruct ocean history reliable proxies have to be applied (a recent review of proxies is given by Wefer et al., 1999). Among these proxies, the use of carbon isotopes ($^{12}C/^{13}C$) and the Cd/Ca ratio incorporated in the calcitic tests of benthic foraminifera have been perhaps the most important and successful (e.g. Curry and Lohmann, 1982; Boyle, 1988, 1994; Curry et al., 1988; Raymo et al., 1990, 1997; deMenocal et al., 1992; Bickert and Wefer, 1996; Curry, 1996; Rosenthal et al., 1997; Martin and Lea, 1998). The applicability of these tracers is based on their relationships to nutrient cycles, and to the carbon chemistry of the oceans and deep water circulation (Curry et al., 1988; Curry, 1996).

Differences in the water mass corrosiveness with respect to carbonate due to variations in CO_2 content also show much promise for the development of reliable water mass proxies. The degree of dissolution that a sample has experienced has been determined by numerous authors using qualitative and quantitative indices, such as variations in the percentages of non-carbonate, carbonate, coarse fraction (>63 μm), and resistant planktic foraminifera (e.g. Ruddiman and Heezen, 1967). Dissolution-sensitive micropaleontological parameters, such as foraminiferal dissolution indices (e.g. the *Globigerina bulloides* dissolution index, BDX'; Volbers and Henrich, subm.), the planktic to benthic foraminiferal ratio (e.g. Berger, 1975),

the planktic foraminifera to radiolarians ratio (e.g. Diester-Haass, 1977), and the planktic foraminifera fragments to complete tests ratio (i.e. fragmentation index, FI; Peterson and Prell, 1985) have been used to measure carbonate-corrosiveness. Nevertheless, most of these proxies are not only influenced by dissolution, but also by changes in the carbonate production of the surface waters, and by dilution by other sediment components as well as by lateral transport of particles. Thus their reliability is questionable if a single variable approach is used (Thunell, 1976). For this reason, several experimental studies have related the progressive ultrastructural breakdown of selected planktic foraminifera species to the loss of carbonate from an assemblage undergoing dissolution (e.g. Bé et al., 1975; Hecht et al., 1975; Henrich, 1989; Henrich et al., 1989; Van Krefeld-Alfane, 1996; Dittert et al., 1999). Proxies based on calcite dissolution have been successfully used to reconstruct deep water circulation patterns, such as shifts of the calcite lysocline in the South Atlantic Ocean, which coincides with the water mass boundary between North Atlantic Deep Water (NADW) and Antarctic Bottom Water (AABW) (e.g. Bickert and Wefer, 1996). However, methods which are successfully applied to reconstruct deep water circulation patterns mostly fail with respect to reconstructions of intermediate water circulation patterns because calcite dissolution is mainly restricted to deep water levels. In contrast, aragonitic shelled pteropods are particularly useful at intermediate water depths because aragonite is much more soluble than calcite, thus aragonite dissolution is found at shallower water depths.

Pteropods have received much taxonomic and biogeographic attention (reviewed by Tesch, 1946, 1948, 1966; Van der Spoel, 1967; Bé and Gilmer, 1977). Numerous studies have focused on such themes as pteropod ecology and occurrences, changes in the isotopic composition, relative abundances and seasonal variations in abundance, vertical and horizontal distributions, and diurnal migrations by net tow, sediment trap, and surface sediment comparisons (e.g. Wormelle, 1962; Chen, 1964; Chen and Bé, 1964; Rottman, 1980; Wormuth, 1981; Cifelli and McCloy, 1983; Almogi-Labin et al., 1988; Meinecke and Wefer, 1990; Fabry and Deuser, 1992; Kalberer et al., 1993; Fischer et al., 1999). The applicability of proxies based on pteropods is evident since pteropods are used for instance as bathymetric indicators (Herman and Rosenberg, 1969), and for the reconstruction of the Aragonite Compensation Depth (ACD) in the oceans by fixing the water depth at which pteropod shells disappear in seafloor sediments (e.g. Chen, 1964; Berger, 1977, 1978; Berner, 1977; Rottman, 1979).

Droxler et al. (1991) found a strong correspondence between the carbonate mineralogy of surface sediments and the saturation state of the overlying waters on the northern Nicaragua Rise (Caribbean Sea) and the Bahamas (western North Atlantic). They also observed striking variations in the in situ pCO_2 values, which are reflected in a 2.2 km difference of the levels at which the water column reaches saturation with respect to aragonite on the northern

Nicaragua Rise (1800 m) and in the Bahamas (4000 m). This contrast is probably due to the mixing of aragonite-corrosive Antarctic Intermediate Water (AAIW) with non-corrosive Upper North Atlantic Deep Water (UNADW) within the Caribbean (Droxler et al., 1991; Haddad and Droxler, 1996).

Haddad and Droxler (1996) have first used metastable carbonate dissolution indices (%Mg calcite, pteropod abundance, %whole pteropods, and %clear pteropods) analogous to deep-sea calcite dissolution indices, which yielded a composite dissolution index (CDI). They also performed binocular and Scanning Electron Microscope (SEM) examinations of pteropod shells to establish a reliable measure of aragonite dissolution. This is based on the observation of Almogi-Labin et al. (1986), who related pteropod shell opacity to aragonite dissolution, since unaltered shells are transparent. Gerhardt et al. (2000) developed the *Limacina* Dissolution Index (LDX) in order to trace aragonite dissolution in late Quaternary sediments. It thus appears that pteropods show much promise as proxies to determine the aragonite saturation state of water masses.

This paper deals with preservation variations of *L. inflata* according to the LDX (Gerhardt et al., 2000) in surface sediments from the Atlantic Ocean and the Caribbean Sea. The aim of this study is to demonstrate the applicability of the LDX as a water mass indicator under present oceanographic conditions in order to obtain a reliable proxy for the reconstruction of past water masses. For this purpose, we compare LDX values with other parameters, including carbonate and aragonite contents of surface sediments, and water-derived $\delta^{13}C$ and $[CO_3^{2-}]$ profiles.

1.1. Limacina inflata*: present distribution, shell features, and initial dissolution*

Limacina inflata (d'Orbigny, 1836) is one of the most common warm-water cosmopolitan pteropods and is widely distributed in the tropical and subtropical regions of all oceans. In the Atlantic Ocean, it is present between 40°-60°N and 40°S and very abundant between 40°N and 15°-20°S (Bé and Gilmer, 1977; Fig. 1). *Limacina inflata* is most abundant in the Caribbean Sea (Haagensen, 1976) and it is less common along the eastern Atlantic margin (Bonnevie, 1913; Tesch, 1946) due to relatively cold surface water temperatures in these regions (Tesch, 1946). *Limacina inflata* is an epiplanktonic species living primarily in the upper 300 m of the water column (Bé and Gilmer, 1977). Oxygen isotope studies on adult specimens suggest rapid growth and a life span of merely several weeks to a few months (Fischer et al., 1999). After the animals death shells rapidly settle to the sea floor, thus initial dissolution mostly occurs at the sediment-sea water interface (Adelseck and Berger, 1975).

Limacina inflata possesses a sinistrally coiled shell with shell diameters up to 1.5 mm (see Fig. 5). The aperture border of the adult is protruded to the so-called aperture tooth (Van der Spoel, 1972). The thin aragonitic shell, which is covered by the organic Periostracum, consists of an innermost prismatic layer (Bé and Gilmer, 1977) and a central helical layer (Richter, 1976). In contrast, all other Limacinidae possess a central crossed-lamellar aragonite layer. These central layers consist of elongated aragonite rods (see Fig. 5, preservation stages 3 to 5), which themselves consist of basic structural units with approximate dimensions of 0.2 µm x 0.2 µm x 0.4 µm (Bé and Gilmer, 1977; Bandel, 1990). The unaffected shell surface of *L. inflata* is smooth, transparent, and lustrous with gently developed growth lines (see Fig. 5, preservation stage 0) from the second whorl onwards (Bandel et al., 1984).

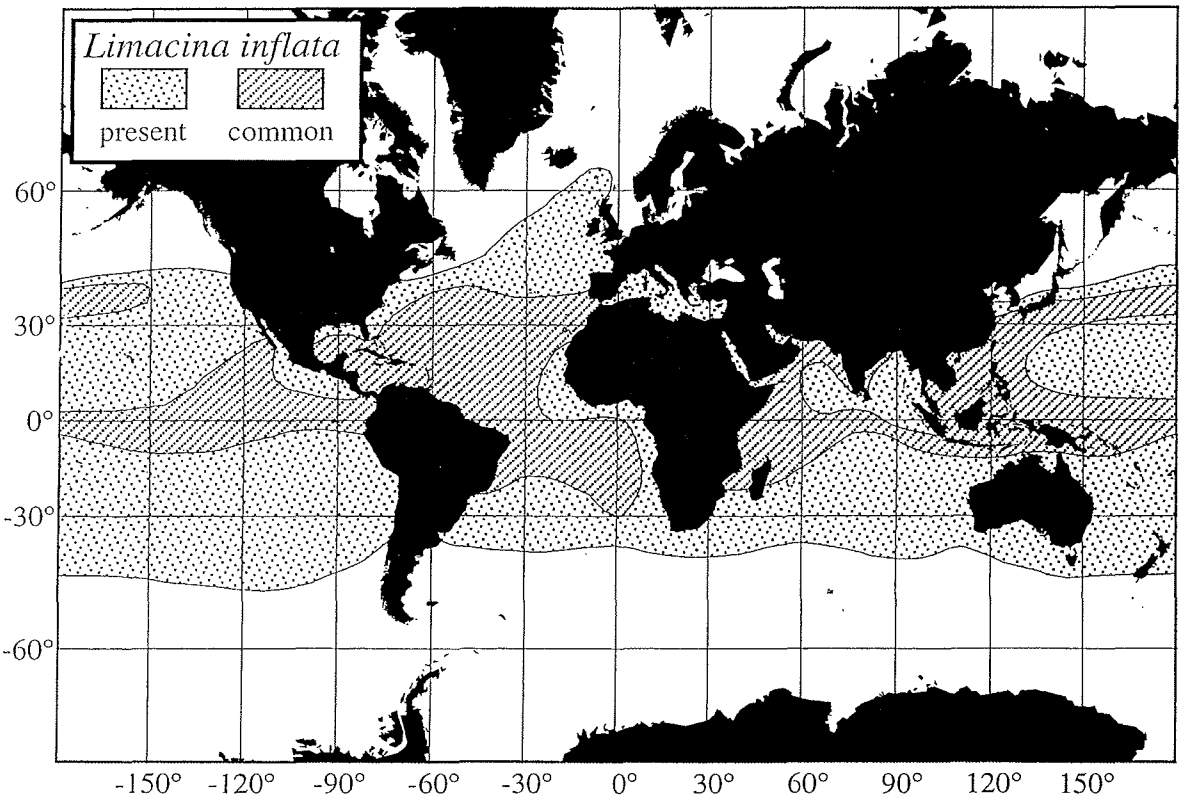

Fig. 1: Distribution of *Limacina inflata* in the world's oceans (adapted from Bé and Gilmer, 1977). Note that *L. inflata* is most common in the western parts of the Atlantic, Indian, and Pacific Oceans, whereas it seems to be less common in the eastern Atlantic upwelling regions.

1.2. Environmental setting, hydrography, and carbonate chemistry of the water column

The investigated area stretches from 20°N to 40°S and from 80°W to 18°E which comprises parts of the Central and South Atlantic Ocean and the Caribbean Sea (Fig. 2).

Various topographic structures are covered, including the Mid-Atlantic Ridge, the Rio Grande Rise, the Walvis Ridge, the Brazil Basin, and the Angola Basin. Pteropod-rich sediments are restricted to the shallow parts of the ocean, i.e. continental slopes, ridges, and rises.

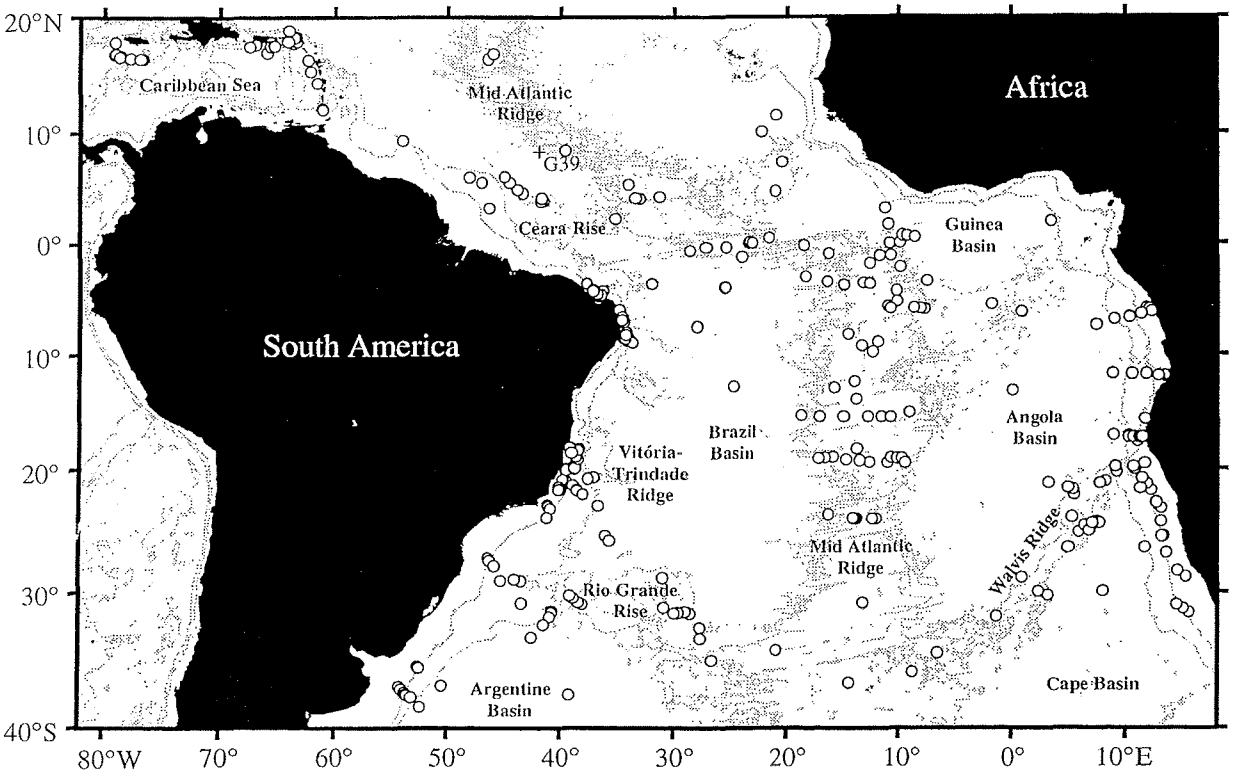

Fig. 2: Map of surface sediment sample distribution, comprising multicorer, minicorer, box corer, and Van Veen Grab sites (see Appendix 1 for detail). Also included is the location of GEOSECS station 39 used to draw the saturation profile of Fig. 4.

The South Atlantic Ocean receives waters from the North Atlantic, the Weddell Sea, and from the Circumpolar Current. Figure 3 illustrates the modern water masses configuration in the western Atlantic Ocean section. The description below follows the definitions by Reid (1989) and Siedler et al. (1996). Accordingly, the deepest water mass is the Weddell Sea Deep Water (WSDW), which flows northward through the Argentine Basin and enters the Brazil Basin through the Vema Channel and the Hunter Channel. Above the WSDW, we find the Lower Circumpolar Deep Water (LCDW), which also has its origin in the South. WSDW and LCDW are often linked together and hence called Antarctic Bottom Water (AABW; e.g. Siedler et al., 1996). On top of the AABW, the broad core of North Atlantic Deep Water (NADW) flows southward, which can be divided into several sublayers (e.g. Lower and Upper NADW). The northward flowing Upper Circumpolar Deep Water (UCDW) separates

the NADW from the Antarctic Intermediate Water (AAIW), which can be clearly distinguished from UCDW by its low salinity and high oxygen values (Siedler et al., 1996). Finally, South Atlantic Central Water (SACW) covers the AAIW. Mediterranean Overflow Water (MOW) spreads out west- and southwestward from the Straits of Gibraltar at depths between 800 and 1500 m (e.g. Kaese and Zenk, 1987). MOW enters the Caribbean Sea between 10° and 20°N.

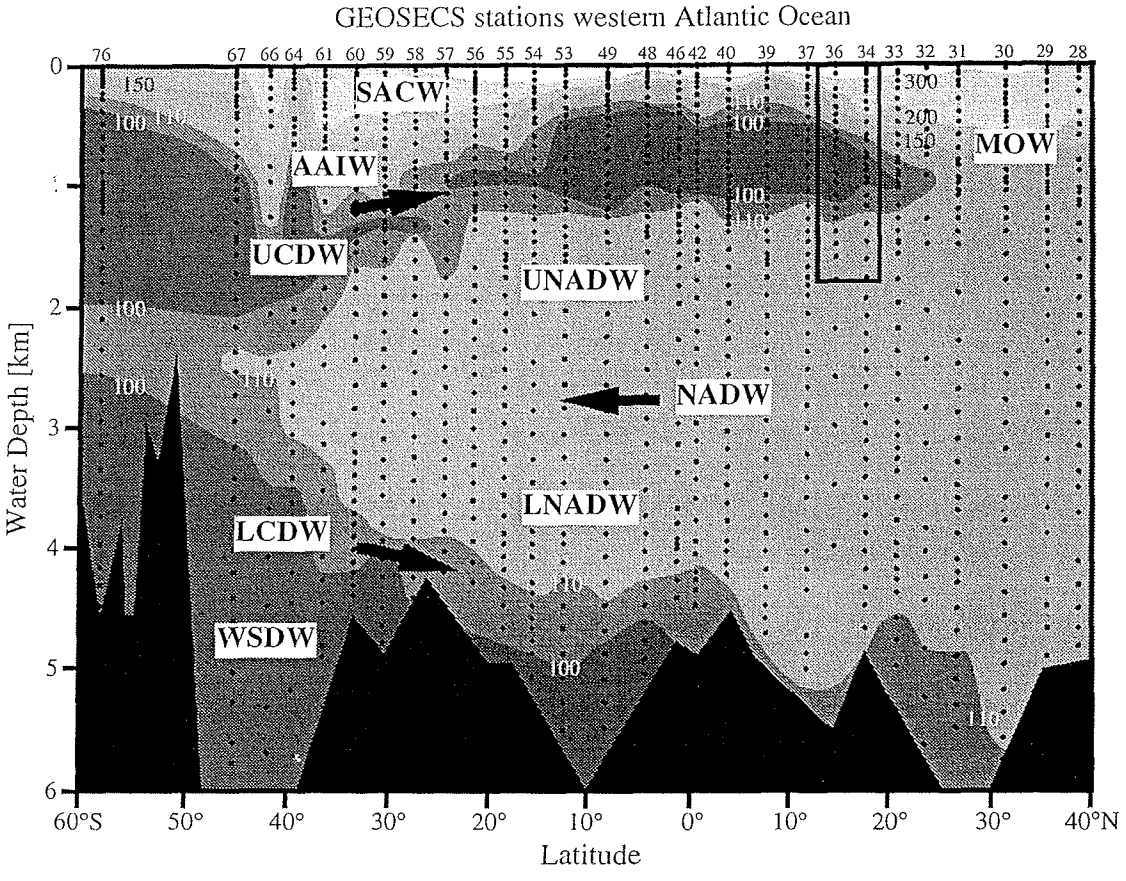

Fig. 3: Present water mass distribution in the western Atlantic Ocean between 40°N and 60°S interpolated between calculated CO_3^{2-} concentrations (in µmol/l; redrawn from GEOSECS, Bainbridge, 1981). Each GEOSECS station used to draw the cross section is labeled at the top by its number and the measured CO_3^{2-} values down the water column are displayed by dots. Arrows mark flow directions of the main water masses. Rectangular box shows the waters entering the Caribbean Sea. WSDW = Weddell Sea Deep Water; LCDW = Lower Circumpolar Deep Water; NADW = North Atlantic Deep Water; LNADW = Lower North Atlantic Deep Water; UNADW = Upper North Atlantic Deep Water; UCDW = Upper Circumpolar Deep Water; AAIW = Antarctic Intermediate Water; MOW = Mediterranean Overflow Water; SACW = South Atlantic Central Water. Note that the $[CO_3^{2-}]$ values for the AAIW/UCDW are as low as the values for the WSDW (<100 µmol/l). The $[CO_3^{2-}]$ profile at station 39 is shown in Fig. 4.

The Caribbean Sea is a marginal basin which receives intermediate waters from the adjacent western North Atlantic (Wüst, 1964) through several channels and sills. Kawase and Sarmiento (1986) and deMenocal et al. (1992) calculated that Atlantic intermediate waters adjacent to the Caribbean Sea at 1800 m contain approximately 85% UNADW, 10%

AAIW/UCDW, and a small portion of MOW (≈5%). A near vertical [CO_3^{2-}] profile near the Nicaragua Rise suggests that there is mixing between AAIW/UCDW and UNADW within the Caribbean Basin (Droxler et al., 1991; Haddad and Droxler, 1996). The mixing between AAIW/UCDW and UNADW may be largely responsible for the poor preservation of carbonate observed today in the Caribbean (Haddad and Droxler, 1996).

Carbonate dissolution in the oceans is primarily controlled by the saturation state of seawater with respect to carbonate minerals. It is related to the ratio of the carbonate ion concentration in seawater to the saturation concentration. In fact, in most parts of the deep sea, the in situ CO_3^{2-} concentration changes little with water depth. The saturation concentration increases with water depth because of the pressure dependence of the solubility of calcite and aragonite. Therefore, the in situ CO_3^{2-} concentration exeeds the saturation concentration at shallower depths and, at great depth, the reverse is true. Due to their differing crystal structures, calcite and aragonite have dissimilar thermodynamic and chemical properties. In seawater, aragonite is more soluble than calcite (by an approximate factor of 1.5; Morse et al., 1980; Millero, 1996), which is reflected in different saturation concentrations (see Fig. 4). This situation is clearly imprinted in the sediments. Differences in the CO_3^{2-} concentration of bottom waters are believed to be responsible for the first-order variations in the depth of the lysoclines between and within the oceans.

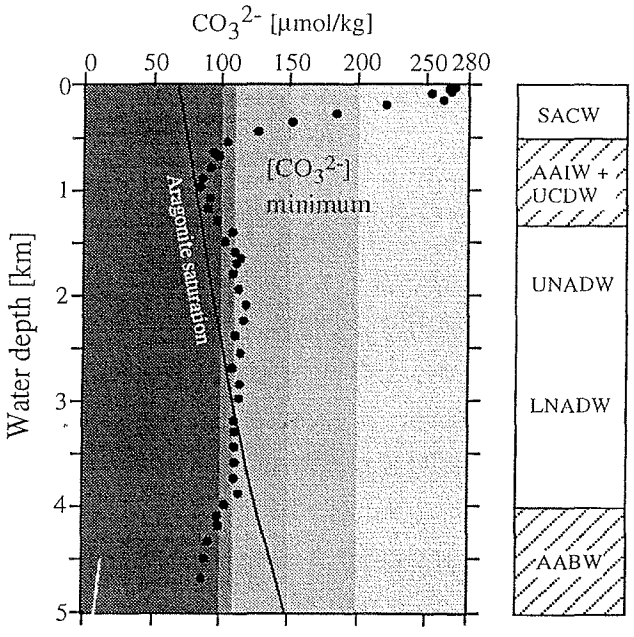

Fig. 4: Typical saturation profile for the western South Atlantic Ocean (GEOSECS Station 39, 7°57'N, 43°51'W, located in Fig. 2; Bainbridge, 1981). Dots mark calculated CO_3^{2-} concentrations. Note that the [CO_3^{2-}] minimum (<100 µmol/kg) at ≈600-1300 m coincides with the southern-source intermediate water masses AAIW/UCDW. Also note the resulting S-shaped [CO_3^{2-}] trend with increasing water depth. Near aragonite saturation within AAIW/UCDW is also reflected in the LDX records presented in this study (see Figs. 7, 9). The worse preservation defines an upper aragonite lysocline within the AAIW/UCDW and a lower aragonite lysocline within the LNADW. Overall LDX failure beneath ≈3400 m water depth (see Figs. 7, 9) corresponds to the level below which saturation with respect to aragonite has been reached.

As can be seen in an example from the western tropical Atlantic Ocean, illustrated in Fig. 4, AABW is undersaturated with respect to both aragonite and calcite, whereas the NADW is supersaturated with respect to calcite in this region. Aragonite saturation is reached in the lower part of the NADW. As a consequence, aragonite dissolution, indicating a deep

aragonite lysocline, is observed in surface sediments within the LNADW. However, Fig. 4 displays that the rate of decrease of $[CO_3^{2-}]$ is not regular with water depth, but follows an S-shaped curve. The minimum $[CO_3^{2-}]$ within the AAIW and UCDW can be attributed to the oxic degradation of organic matter in the water column, which increases the CO_2 content in intermediate depths. Thereby, it lowers the pH of the waters, which makes them more corrosive to calcium carbonate material (Chester, 1990). Actually, Fig. 4 displays that the CO_3^{2-} content exceeds the saturation concentration with respect to calcite, but is close to aragonite saturation. This situation is reflected in poor aragonite preservation of surface sediments that are in contact with AAIW and UCDW (this study).

In theory, the depths of the local lysoclines, based on analyses of sediment samples, should coincide with the depths calculated from adjacent GEOSECS saturation profiles. In practice, the sedimentary and hydrographic lysoclines may vary significantly due to strong differences in water chemistry between bottom water and water column. Recently, in situ electrode measurements of porewater O_2, pH, and $CO_{2(aq)}$ demonstrated that calcite dissolution driven by metabolic CO_2 produced within the sediments is a significant part of the diagenesis of sedimentary calcite even in supralysocline waters (e.g. Hales and Emerson, 1996, 1997). In some areas, "metabolic dissolution" may account for 65-80% of the total dissolution (Hales and Emerson, 1996), but its role is still under discussion.

2. Materials and methods

Comparison of sediment surfaces with recent hydrography is a clear way of testing the usefulness of a paleoceanographic proxy. We thus studied 310 sediment surfaces collected with multicorer, minicorer, box corer, or Van Veen Grab during RV *Meteor* cruises M6/6 (Wefer et al., 1988), M9/4 (Wefer et al., 1989), M12/1 (Wefer et al., 1990), M15/2 (Pätzold et al., 1993), M16/1 (Wefer et al., 1991), M16/2 (Schulz et al., 1991), M20/1 (Wefer et al., 1992), M20/2 (Schulz et al., 1992), M23/1 (Spieß et al., 1994), M23/2 (Bleil et al., 1994), M23/3 (Wefer et al., 1994), M29/2 (Bleil et al., 1994), M29/3 (Henrich et al., 1995), M34/2 (Schulz et al., 1996), M34/3 (Wefer et al., 1996), M34/4 (Fischer et al., 1996), M35/1, M38/1 (Fischer et al., 1998), M38/2 (Bleil et al., 1998), M41/2 (Devey et al., 1999), M41/3 (Pätzold et al., 1999), RV *Sonne* cruise SO-84 (Devey et al., 1993), and RV *Victor Hensen* cruises VH/JOPS II-6 and VH/JOPS II-8 (Pätzold et al., 1996). The samples were recovered in the Atlantic Ocean from 23 to 5684 m water depths and in the Caribbean Sea from 889 to 4710 m water depths (see Fig. 2 and Appendix 1 for sample locations). All sediment surfaces are assumed to be of Holocene age. Variations up to several hundred to thousand years may occur depending on the local sedimentation rate.

2.1. Sample preparation and Limacina *Dissolution Index (LDX)*

Commonly, the uppermost centimetre of every surface sample was carefully wet sieved to separate the fine (< 63 µm) and the coarse fraction (> 63 µm). After drying the coarse fraction, at least 10 adult tests (about 1 mm in size) of *L. inflata* were picked and examined according to the LDX (Gerhardt et al., 2000) (see Appendix 1 for respective shell numbers). The determination of pteropodal preservation stages is based on the observation that pteropod shells loose their integrity with increasing dissolution (e.g. Almogi-Labin et al., 1986; Acker and Byrne, 1989; Haddad and Droxler, 1996; Gerhardt et al., 2000). The LDX is represented by six preservation stages, which are briefly described in the following (see also Fig. 5):

Stage 0: Transparent shells
This stage indicates best preservation. Only the shells of living pteropods and originally preserved pteropod assemblages in the sediments show this mode of preservation.
Stage 1: Milky and cloudy shells, lustrous shell surface
This stage is reached when either slight shell corrosion has taken place or the organic parts of the shell have become cloudy through oxidation (Haddad and Droxler, 1996).
Stage 2: Opaque-white shells, lustrous shell surface
In this stage, pteropod shells are opaque and white, not just milky, which means they have truly experienced initial dissolution on the surface.
Stage 3: Opaque-white shells, partly lustreless shell surface
In this stage, parts of the surface layer have disappeared by dissolution. Consequently, the shell surface seems to be lustreless in those areas where the helical aragonite layer is exposed.
Stage 4: Opaque-white shells, totally lustreless shell surface
This stage is reached when the surface layer has been entirely removed by corrosion.
Stage 5: Opaque-white, totally lustreless and perforated shells
This stage is characterized by additional shell damage of any kind, neglecting the absence of the aparture tooth of *L. inflata* which is often broken off during sample preparation.

Each sample is represented by preservation values showing a Gaussian distribution. Samples that did not provide a Gaussian distribution were supposed to be influenced by lateral transport and were excluded from this study. The LDX was calculated according to the equation:

$$LDX=\Sigma(n_p*p)/\Sigma n_p$$

where n_p is the number of investigated tests per preservation stage p (with p = 0 to 5) and Σn_p is at least 10.

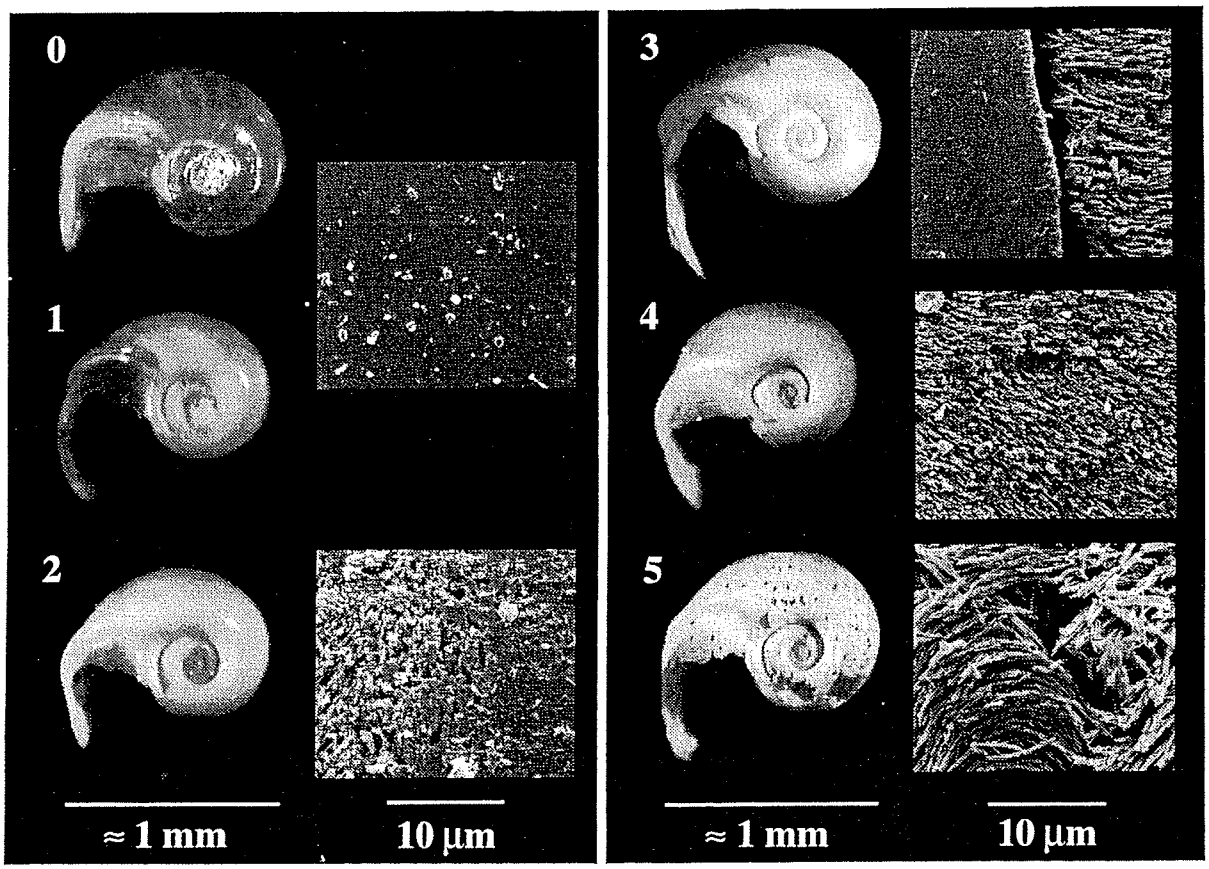

Fig. 5: Preservation stages (worsening from 0 to 5) of *Limacina inflata* (adult) according to the *Limacina* Dissolution Index (LDX) of Gerhardt et al. (2000). Whole shell photographs were taken under the optical microscope, whereas the enlargements were carried out by SEM. (0) transparent and lustrous shell with smooth surface, hence no solution, (1) as (0) but milky and lustrous shell with smooth surface, (2) opaque-white and lustrous shell with slightly corroded surface, (3) opaque-white and partly lustreless shell showing incipient loss of the surface layer, thus elongated aragonite rods from the central layer are partly exposed, (4) opaque-white and completely lustreless shell with loss of the surface layer, (5) as (4) with additional damage, hence worst preservation. Note the characteristic smooth surface layer (0, 1) and the central helical layer with elongated aragonite rods (3, 4, 5).

2.2. Determination of aragonite/calcite ratios and bulk carbonate contents

For determining the relation between LDX and aragonite content, calcite and aragonite ratios were measured in several surface samples and additionally on one gravity core (GeoB 2202-4: 8°12'S/ 34°16'W, 1156 m water depth) from the Atlantic Ocean using x-ray diffraction analysis (XRD). After freeze drying, about 0.5 g bulk sediment of each sample was carefully ground to obtain a grain size <63 µm. All samples were measured with a Philips PW1830 goniometer (Crystallography, Bremen University) equipped with a fix

divergence slit, using Cu Kα radiation (40 kV, 30 mA). The XRD measurements were carried out between 20-50° 2Θ with a step size of 0.02° and a scan time of 2 seconds per step. The quantitative analyses of the diffractograms were made by determining aragonite and calcite peak heights and areas using the graphic oriented computer program "MacDiff" (Petschick, unpublished) and subsequent comparisons with calibration curves (for details see Klug and Alexander, 1954; Cullity, 1956; Milliman, 1974). Core-top $\%CaCO_3$ data were determined by using a LECO-CS 300 element analyzer. Additional $\%CaCO_3$ and %aragonite data come from several sources (see Appendix 2 for data and references).

3. Results and discussion

It appears that differences in pteropod shell preservation in sediments correspond to the saturation states of the bottom water masses.

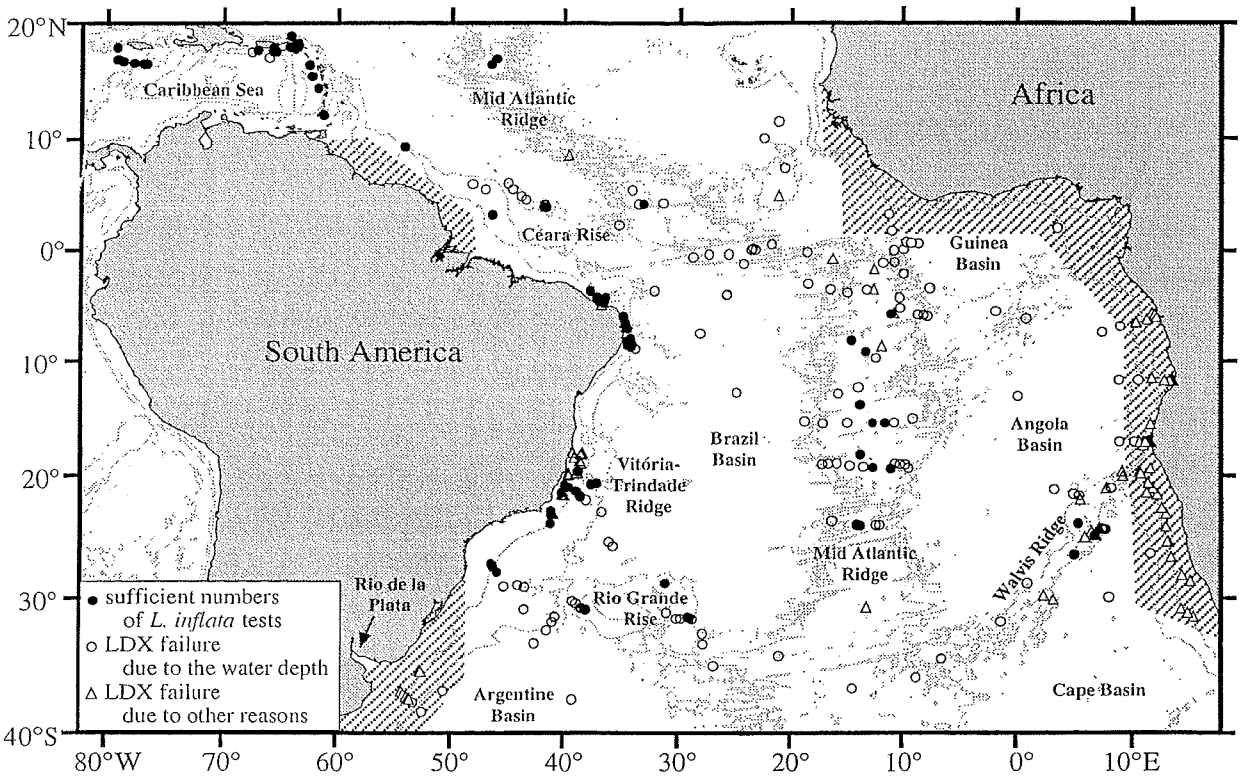

Fig. 6: Map of surficial LDX results. Sufficient shell numbers of *Limacina inflata* (filled dots) are restricted to shallow parts of the ocean, i.e. to the western Atlantic slope, to the Mid-Atlantic Ridge, to the Rio Grande Rise, to the Walvis Ridge, to the Ceara Rise, and to the Caribbean Sea. LDX failure due to undersaturation with respect to aragonite (circles) is found beneath ≈3400 m water depth. Lack of supply of *L. inflata*, dilution of the sediments by terrigenous material, or aragonite dissolution due to enhanced degradation of organic matter leads to LDX failure near the Rio de la Plata, the Vitória-Trindade Ridge, and along the western African Continental Margin. Hatched: absence of pteropods recorded in any depth according to Berger (1978).

Three regional dissolution patterns were observed in the Atlantic and Caribbean LDX records. In the western Atlantic Ocean including the Mid-Atlantic Ridge, the LDX predominantly displays good correlation with aragonite-corrosive AAIW/UCDW and non-corrosive UNADW presence (Fig. 7). Contrary to the western Atlantic Ocean, the LDX in the eastern Atlantic Ocean fails in most cases (Fig. 6). Within the Caribbean Sea the LDX reveals a more complex aragonite dissolution pattern (Figs. 6 and 8).

The applicability of the LDX is primarily dependent on the availability of *L. inflata* tests, hence less than 10 tests per sample lead to LDX failure (see Appendix 1 for relation to each sample location). Presuming that milky shells (LDX stage 1) predominantly indicate perfect preservation and opaque-white shells (LDX stage 2) have truly experienced initial dissolution (according to Haddad and Droxler, 1996), then more severe dissolution occurs from LDX stage 2 onwards. The transition from milky to opaque-white shells is therefore assumed to mark the top of the aragonite lysoclines as illustrated in Fig. 7. Correspondingly, the transition from very poor aragonite preservation (LDX stages 4-5) to LDX failure is assumed to indicate the position of the ACD as displayed in Fig. 7.

3.1. Western Atlantic Ocean and Mid-Atlantic Ridge preservation pattern

Figure 7 illustrates the relationship between water mass distribution represented by calculated CO_3^{2-} concentrations and preservation of *L. inflata* (LDX) in sediment surfaces from the western Atlantic Ocean and Mid-Atlantic Ridge (≈55°W to 5°W). In Fig. 7 and 8, the preservation stages were grouped (from excellent = stages 0-1 to very poor = stages 4-5) to better graphically display this relationship. Excellent preservation of *L. inflata* corresponds to high [CO_3^{2-}] within SACW. Within the low [CO_3^{2-}] core of AAIW and UCDW, preservation is found to be very good or moderate. The transition zone between very good to moderate aragonite preservation around 750 m can be considered to represent an upper aragonite lysocline (defined as top of the dissolution zone). However, the lysocline depth proposed around 750 m is inferred graphically from the preservation data (Fig. 7) and represents a mean depth level. Most likely, the depth of the upper aragonite lysocline is not constant, but corresponds to the local depth level of the [CO_3^{2-}] minimum zone within AAIW/UCDW. However, considering the GEOSECS data compiled in Fig. 7, aragonite dissolution should not occur in intermediate depths since the intermediate waters are supersaturated (though close to saturation) with respect to aragonite. Separating the effects on aragonite dissolution due to bottom water undersaturation from those due to metabolic addition of CO_2 is difficult without in situ measurements of bottom water pH, but it can be assumed that dissolution driven by metabolic CO_2 production could play a significant role.

Apparently, a group of shallow samples (≈4°-7°S, 350-525 m water depth) displays very good preservation, although the GEOSECS data imply that the locations are influenced by aragonite-corrosive AAIW. Again, this inconsistency may result from different water chemistry of bottom water (sedimentary data) and water column (GEOSECS data).

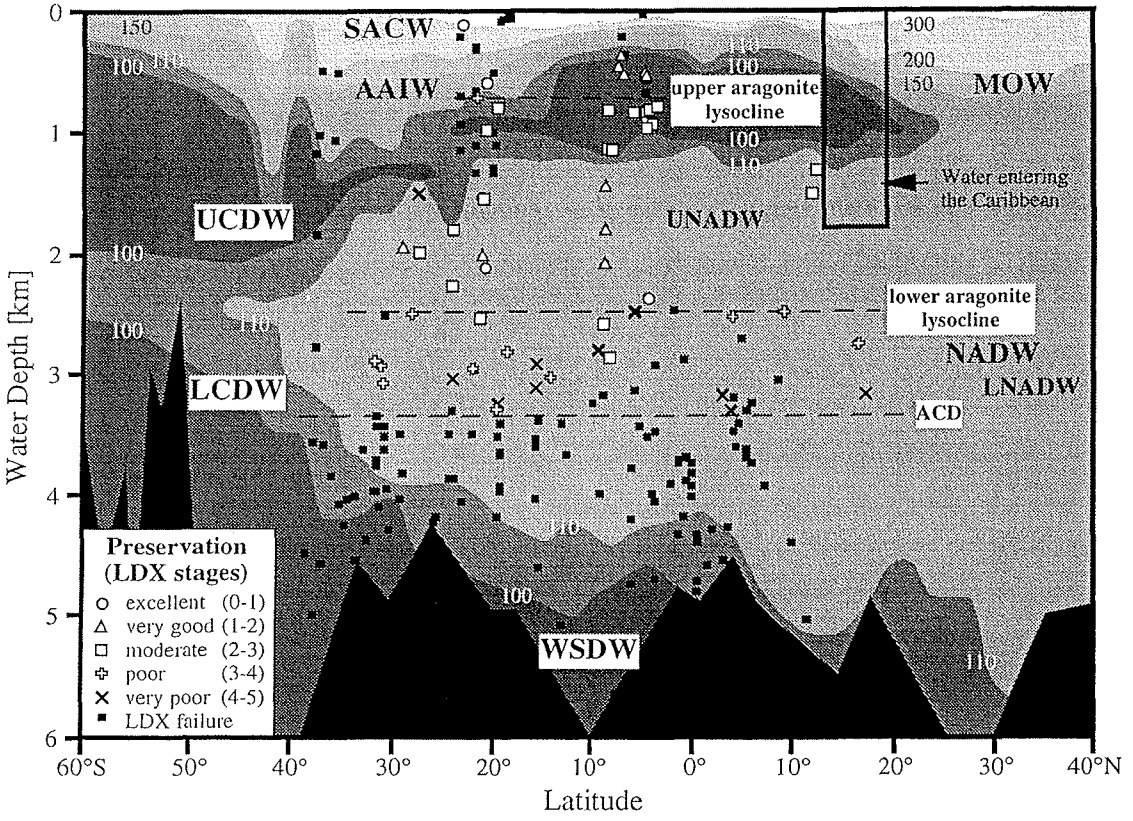

Fig. 7: LDX results in the western Atlantic Ocean including the Mid-Atlantic Ridge compared with the present water mass distribution (interpolated between calculated $[CO_3^{2-}]$ after Bainbridge, 1981). Perfect preservation (LDX <2) is found within SACW, within the upper part of AAIW/UCDW (although possibly these data point not to AAIW/UCDW influence, see description in the text), and partly within the UNADW. Dissolution (LDX >2) is observed in the lower part of AAIW/UCDW, suggesting an upper aragonite lysocline at ≈750 m, within LNADW beneath ≈2500 m, and in the southern regions within the UNADW. Overall LDX failure below ≈3400 m may be considered to mark the Aragonite Compensation Depth (ACD).

Beneath the zone of minimum $[CO_3^{2-}]$, there is a window of aragonite preservation within the UNADW. Sediment surfaces within UNADW display very good to moderate preservation. In particular, significantly improved preservation within UNADW is found around 5°S to 9°S (see also depth transect C, Fig. 9), which is in contrast with worse preservation within UCDW. Within the LNADW (below about 2500 m) preservation becomes worse, indicated by moderate to very poor modes of preservation, suggesting that a lower aragonite lysocline is developed at about 2500 m water depth. Again, the mean depth of the lower lysocline shown in Fig. 7 is inferred from the preservation data. Broecker and

Takahashi (1978) determined the lysocline topography in the western Atlantic from the crossover between the critical and observed carbonate ion curves at the stations along the GEOSECS track. They obtained a near constant depth of the aragonite lysocline varying from ≈2500 to 3100 m (≈2750 m on average) between 40°N to 40°S, which they attributed to the dominance of the NADW throughout the entire length of the Atlantic in the 2- to 4-km depth range. Apparently, our data reveal a ≈250 m shallower depth level for the lower lysocline on average.

Overall LDX failure below about 3400 m water depths indicates strong aragonite dissolution, hence 3400 m can be considered to represent the ACD. Apparently, LDX failure is also observed at shallower water depths in supersaturated waters along the western continental margin (e.g. close to the shelf between ≈5°-7°S in 23-565 m water depth as well as close to the Vitória-Trindade Ridge between ≈18°-23°S in 23-1330 m , and near the mouth of the Rio de la Plata between ≈35°-38°S in 490-1836 m). We suspect that this type of LDX failure may be mostly related to the metabolic addition of CO_2 to the bottom water. The discharge of nutrients by rivers enhances the primary production in the adjacent euphotic zone. Therefore, high amounts of organic matter are found in the vicinity of the river mouths of the Rio de la Plata and the Amazon River, which promote the dissolution of calcium carbonate at the sediment-seawater interface. This is consistent with the findings of Berger (1978), who observed total absence of pteropod tests in these regions (see Fig. 6). Additionally, LDX failure on the shelf may be due to a lack of supply of *L. inflata*, since the present distribution of *L. inflata* in the world's oceans indicates their main abundance in offshore regions, where water depth exceeds 200 m (Herman and Rosenberg, 1969). On the other hand, a lack of tests may be also due to dilution by both terrigenous material and benthic organisms.

3.2. Eastern Atlantic Ocean preservation pattern

In most areas of the eastern Atlantic Ocean, with the exception of the Mid-Atlantic Ridge, the LDX fails (Fig. 6). Only three locations on the Walvis Ridge (GeoB 1203-2, GeoB 1217-1, GeoB 1220-2) reveal poor or very poor preservation of *L. inflata*. Berger (1978) also mentioned the absence of pteropod tests in surface sediments of any depth along the southwestern African continental margin. LDX failure may be caused by a considerably reduced occurrence of *L. inflata* in upwelling regions (Bé and Gilmer, 1977; Fig. 1) and thus a lack of supply into the sediment. Dilution by terrigenous material delivered by great rivers such as the Congo River may also contribute to the apparent overall LDX failure. However, the main reason for LDX failure in these regions is increased aragonite dissolution due to

degradation of organic matter and hence CO_2 supply at the sediment-water interface. The large supply of organic matter into the sediment is characteristic of high productivity areas such as offshore SW Africa (Berger and Wefer, 1996). In these areas, the degradation of organic matter plays the more important role than the bottom water chemistry on aragonite preservation.

3.3. Caribbean Sea preservation pattern

Surface samples within and near the Caribbean Sea (Fig. 8) particularly reflect the combined effects of local differences in water circulation, in carbonate production, and in dilution. Although all studied surface samples are located relatively close together, three different preservation patterns (Fig. 8b: regions A-C) are observed. The LDX results are apparently consistent with %$CaCO_3$ and %aragonite data (see Lembke, 1997 and Appendix 2 for data) and Fig. 10 illustrates differences in the proportional aragonite contents between the three Caribbean regions.

In the Lesser Antilles island arc (SE Caribbean), the preservation of *L. inflata* is found to be moderate or very poor (Fig. 8: region A). Comparison between the regions shows that preservation (LDX 2.34 to 4.45) as well as calcium carbonate contents (12.5 to 64.0 wt.-% of bulk sediment) and the proportions of aragonite (33.8 to 55.9% of bulk carbonate) are lowest. In addition, it appears that the carbonate contents increase northward along the Lesser Antilles arc. Our findings agree with the results of Reid et al. (1996) from this region, such that average calcium carbonate contents are low and increasing to the north. Deep-water carbonate sedimentation in the Lesser Antilles region includes deposition of both shallow-water carbonate, which is mainly delivered from the insular shelves on the arc platform and pelagic carbonate, which is formed throughout the arc in open-ocean surface waters (Reid et al., 1996). We therefore suspect that the relatively low amounts of carbonate and aragonite in the SE Caribbean result from the interplay of two main controls: (1) less input of bank-derived fine aragonite and Mg calcite because the sources are limited, and (2) increased dissolution of metastable carbonates due to greatest AAIW/UCDW influence.

In the NE Caribbean (Fig. 8: region B), AAIW/UCDW influence is minor and the nearby Anegada Passage represents one of the most important passages for UNADW inflow. Consequently, very good preservation of *L. inflata* is observed, even though three samples above 2000 m show moderate preservation (LDX values 2.02-2.06). Below the aragonite saturation depth, moderate preservation is found and LDX failure was only observed in two samples below 3800 m water depth due to aragonite undersaturation. The NE Caribbean shows better preservation (LDX 1.71 to 2.94) as well as higher carbonate (62.2 to 90.6%) and

aragonite contents (58.4 to 72.6%) than the SE Caribbean, which may be attributed to an increase of input of bank-derived fine aragonite and Mg calcite and an increase in UNADW influence.

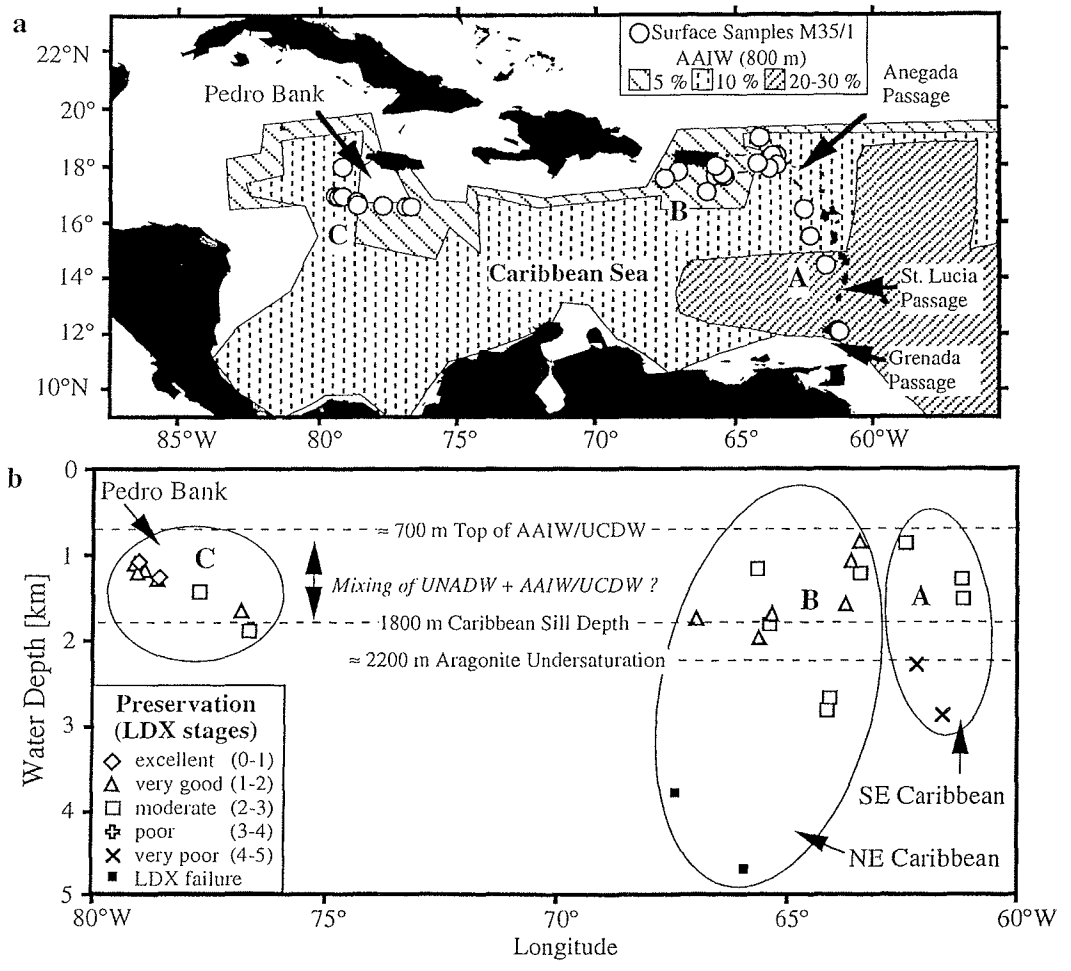

Fig. 8a-b: (a) Map of surface samples and percentage amount of AAIW at its core layer (≈800 m) in the Caribbean Sea (adapted from Wüst, 1964 and Haddad and Droxler, 1996). Note that the highest AAIW concentrations (20-30%) are found in the SE Caribbean Sea. (b) LDX results within the Caribbean Sea versus water depth, displaying the mixing between AAIW/UCDW and UNADW within the Caribbean Basin. Best preservation is found near the Pedro Bank (C). Very good to moderate preservation is found in the NE Caribbean (B), whereas moderate preservation can be observed in the SE Caribbean (A) in the region of highest AAIW/UCDW influence.

A third aragonite dissolution pattern is developed near the Pedro Bank (Fig. 8: region C). The southern Pedro Bank region shows the best preservation (LDX 0.57 to 2.14) as well as the highest carbonate contents (92.7 to 96.8%) and also the highest proportions of aragonite (72.6 to 79.3%). Apparently, preservation is best down to 1313 m water depth and is worse beneath. The findings agree with previous research by Droxler et al. (1991) and Glaser and Droxler (1993), who determined aragonite and Mg calcite contents in the fine fraction (<63

µm) in the Walton Basin (a deep seaway between Pedro Bank and the southern shelf of Jamaica). Accordingly, proportions of fine aragonite average 70% (ranging between 60 and 80%) and decrease strongly below 1800 m (Droxler et al., 1991). Interestingly, the fine Mg calcite record from the Walton Basin (averaging 20%, ranging between 10 and 30%) shows an S-shaped trend with increasing water depth, which Droxler et al. (1991) related to the large value of the PCO_2 concentration at the base of the thermocline (core of the AAIW). We suppose that aragonite preservation in the study area is improved due to the additional input of bank-derived fine aragonite and Mg calcite material, locally depressing the aragonite saturation depth. Results of studies in the Bahamian basins and northern Nicaragua Rise show that the depression of the regional carbonate saturation depth is a typical feature of periplatform environments (Droxler et al., 1991; Glaser and Droxler, 1993).

3.4. LDX versus $CaCO_3$, aragonite percentages, and CO_3^{2-} and $\delta^{13}C$ concentrations

$CaCO_3$ data from surface sediments compiled in Fig. 9 (see Appendix 2 for data) vary strongly in the western South Atlantic Ocean and the Caribbean Sea, depending on the degree of carbonate production, dissolution, and dilution. Comparison between LDX and %CaCO3 versus water depth in four depth transects (Fig. 9: regions A-D) reveals two important findings: firstly, both LDX values and $\%CaCO_3$ display S-shaped trends due to increased aragonite dissolution (i.e. LDX > 2) where sediments are in contact with AAIW/UCDW in contrast to improved preservation (i.e. LDX < 2) under NADW influence. Secondly, the S-shape of the LDX curve becomes narrower from transect A to D. The water-derived concentrations of CO_3^{2-} and $\delta^{13}C_{DIC}$ also display S-shaped trends and minima within AAIW/UCDW. The results may be attributed to a combination of both northward aging of AAIW/UCDW and mixing with overlying saline waters and UNADW (Talley, 1996). [CO_3^{2-}] and $\delta^{13}C_{DIC}$ do not become narrower from transect A to D, which is in contrast to the LDX curves, and instead [CO_3^{2-}] and $\delta^{13}C_{DIC}$ show lowest values within the AAIW/UCDW minimum in the northernmost transects C and D (see Fig. 9). This trend may be attributed to the passage of the AAIW/UCDW under the high equatorial productivity zone. However, predominant agreement of two surface sediment parameters (LDX and $\%CaCO_3$) with two water-derived parameters ([CO_3^{2-}] and $\delta^{13}C$) in the western Atlantic Ocean suggests a close relationship between LDX and saturation state of the overlying waters that might be used for the reconstruction of water masses.

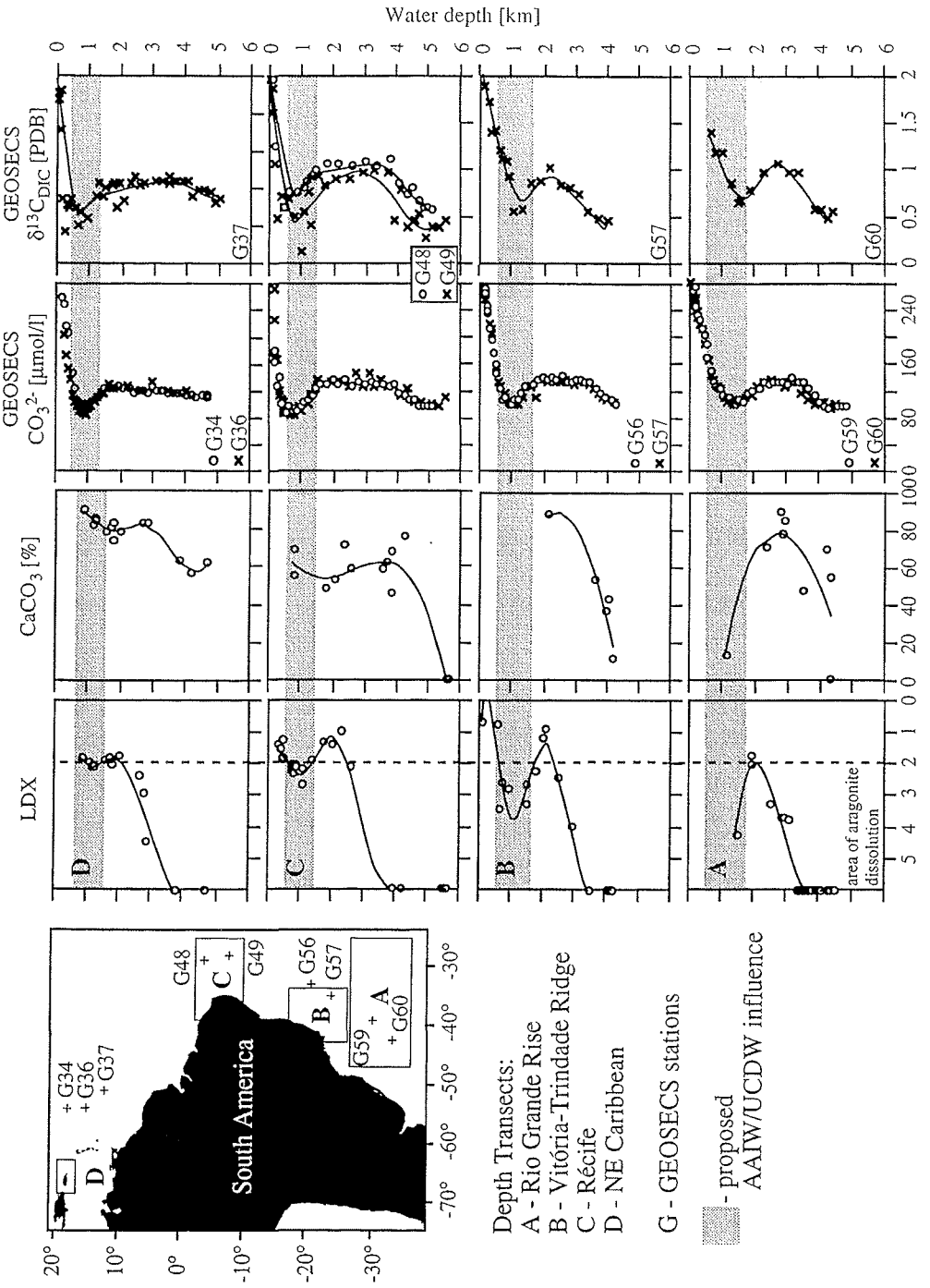

Fig. 9: Comparison between LDX data (see Appendix 1 for data), carbonate contents (see Appendix 2 for data and references), and water-derived $[CO_3^{2-}]$ and $\delta^{13}C$ data (GEOSECS; Bainbridge, 1981) in four depth transects along the South American Continental Margin to the NE Caribbean Sea. The curves display a characteristic S-shape due to a minimum in preservation (LDX), in $CaCO_3$ content, in CO_3^{2-} as well as in $\delta^{13}C$ within AAIW/UCDW. Note that the S-shape of the LDX curve becomes narrower from transect A to D (however, this is not observed in the $[CO_3^{2-}]$ and $\delta^{13}C$ data), which may be due to northward aging as well as mixing of AAIW/UCDW with UNADW and surface waters (Talley, 1996). Also note, that the depth level of the AAIW/UCDW in transect D seems to differ slightly between the inner Caribbean (LDX and $\%CaCO_3$ data) and the adjacent North Atlantic (GEOSECS data).

Comparison of LDX stages with aragonite contents (Fig. 10) should reveal significant correlation because both parameters are indicative for aragonite dissolution. In fact, variations in aragonite content may be due to regional differences of three main controls: (1) changes in aragonite production rates in the surface waters and changes in the input of bank-derived fine aragonite, (2) variations in the extent of dilution by terrigenous material, and (3) changes in aragonite loss due to dissolution at the sediment-water interface. In order to obtain the true dissolution signal, surface samples from small geographic areas were compiled and assumed to have been formed under similar production rates. In addition, to avoid the influence of dilution, LDX values are expressed versus aragonite percentages balanced to bulk carbonate contents (a ratio which is independent of dilution). The resulting relationship between aragonite preservation state (represented by the LDX) and aragonite content is therefore assumed to indicate aragonite dissolution. Additionally, data from four sediment cores from the western South Atlantic Ocean (GeoB 2204-1/2 and GeoB 2207-2 from Gerhardt et al., 2000) are also included in Fig. 10, assuming that aragonite production did not vary considerably during the past 240 ka.

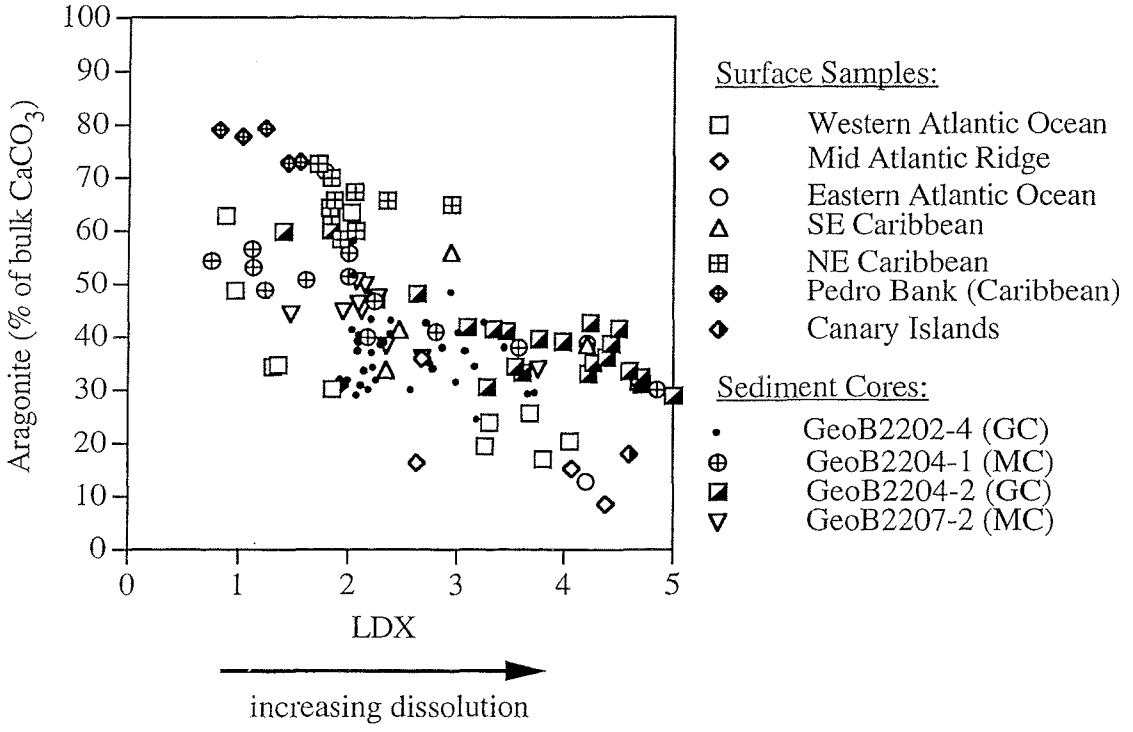

Fig. 10: Correlation between aragonite content (expressed as % of bulk carbonate) and LDX in several regions of the South Atlantic Ocean and Caribbean Sea. See Appendix 2 for data and references for surficial sediment samples and GeoB 2202-4. Additional sediment core data were taken from Gerhardt et al. (2000). Initial aragonite values strongly vary in different ecological regimes based on differences in aragonite production in the surface waters. A general trend of decreasing aragonite contents with decreasing preservation and vice versa can be observed. MC = Multicorer, GC = Gravity Corer.

The close relationship between LDX values and aragonite proportions is apparent, although initial aragonite amounts strongly vary in different geographic regimes (e.g. ≈80% near the Pedro Bank and ≈63% in the western Atlantic Ocean). In all regions, surface samples as well as sediment cores show a general trend of decreasing aragonite contents with decreasing preservation (i.e. higher LDX values) and vice versa. Most regions follow this general trend, but differences in the aragonite loss do occur between the LDX stages. That is, we suspect that the aragonite loss from LDX stage 2 to 3 is greater than from stage 1 to 2. Dissolution experiments on pteropod tests may provide the exact aragonite loss between the LDX stages. However, we suggest that taking the difference between the aragonite contents of dissolution affected samples (LDX > 2) and those of dissolution unaffected samples (LDX < 2) within distinct geographic regimes might be considered as a reliable estimation of the aragonite loss.

In summary, we have demonstrated that the LDX is a reliable indicator of aragonite dissolution. The predominant correspondence between the LDX and the GEOSECS $[CO_3^{2-}]$ data in the western South Atlantic and Caribbean implies that the bottom water chemistry is responsible for the first-order variations in aragonite preservation. An increase in bottom water CO_2, such as results from the degradation of organic matter at the sediment-water interface and within the sediment, tends to drive the aragonite dissolution to greater extent. Thus high productivity areas, which produce mainly LDX failure, should be avoided to obtain the true bottom water signal. It would be interesting to calculate the exact value at which the "rain ratio" (= organic to inorganic carbon ratio) superimposes the bottom water signal.

4. Conclusions

We have applied the LDX (Gerhardt et al., 2000) on 310 surficial sediments and one sediment core (GeoB 2202-4) from the Central and South Atlantic Ocean and the Caribbean Sea based on microscopic shell surface investigations. The resulting preservation stages closely reflect the respective saturation states of the overlying waters, indicated by good preservation within surface waters (SACW) and UNADW and worse preservation within AAIW, UCPW, and LNADW. This rather complex aragonite preservation pattern is indicated by an S-shaped curve trend with increasing water depth, which was also observed in Mg calcite studies from the northern Nicaragua Rise (Droxler et al., 1991). Moreover, our results suggest that two aragonite lysoclines are developed under modern conditions, i.e. an upper lysocline within AAIW/UCDW (mean depth: 750 m) and a lower lysocline within LNADW (mean depth: 2500 m). Along four depth transects in the western South Atlantic Ocean and the Caribbean Sea, we found a close connection between LDX values, $[CO_3^{2-}]$ and $\delta^{13}C$

values from the water column and calcium carbonate contents from sediment surfaces, indicated by similar S-shaped trends. Aragonite preservation within AAIW/UCDW improves significantly northwards from the Rio Grande Rise region to the NE Caribbean Sea. LDX values display a close relationship to proportions of aragonite, suggesting that both parameters are predominantly influenced by dissolution. The close relationship between LDX values and aragonite contents might be used for the quantification of the aragonite loss. LDX failure and uncertainties may be attributed to (1) aragonite dissolution due to bottom water corrosiveness, (2) aragonite dissolution due to additional CO_2 release into the bottom water by the degradation of organic matter based on an enhanced supply of organic matter into the sediment, (3) variations in the distribution of *L. inflata* and hence a lack of supply into the sediment, (4) dilution of the sediments and hence a lack of tests of *L. inflata*, (5) redeposition of sediment particles. Since the LDX appears to be most reliable in the western South Atlantic Ocean and in the Caribbean Sea, we are able to present a new proxy for the reconstruction of past water masses in these regions. High productivity regions such as along the African Continental Margin and near the mouths of great rivers should be avoided since these regions are susceptible to metabolic dissolution, which may superimpose the bottom water signal.

Acknowledgements

We thank the members of the SFB 261 ("The South Atlantic in the late Quaternary: Reconstruction of Material Budget and Current Systems") and especially B. Donner, S. Mulitza, and H.W. Arz for making most of the coarse fraction samples available for our study. We also thank R. Fischer (Crystallography, Bremen University) for giving us the opportunity to use the X-ray diffractometer (XRD). Special thanks are due to M. Wendschuh-Josties and Chr. Vogt for their support with the XRD and the interpretation of the diffractograms. J. Schönfeld, Kiel and P. Müller, Bremen kindly provided data on calcium carbonate contents, which we appreciate. We also thank L. Lembke, who provided data on aragonite contents from the Caribbean Sea. Finally, we would like to thank A. Volbers, S. Rath, and two anonymous reviewers for valuable comments on the manuscript and C. Devey for correcting the English in an earlier version. This research was funded by the Deutsche Forschungsgemeinschaft (Graduierten-Kolleg "Stoff-Flüsse in marinen Geosystemen"). This is contribution no. 299 of the SFB 261 (Bremen University).
All data presented in Appendices 1 and 2 are available electronically under www.pangaea.de/Projects/SFB261/SGerhardt_RHenrich_2000/.

References

Acker, J.G., Byrne, R.H., 1989. The influence of surface state and saturation state on the dissolution kinetics of biogenetic aragonite in seawater. American Journal of Science 289, 1098-1116.

Adelseck, C.G., Berger, W.H., 1975. On the dissolution of planktonic foraminifera and associated microfossils during settling and on the sea floor. In: Sliter, W.V., Bé, A.W.H., Berger, W.H. (Eds.), Dissolution of Deep-Sea Carbonates. Cushman Foundation, Foraminiferal Research, Special Publication 13, Ithaka, NY, pp. 70-81.

Almogi-Labin, A., Hemleben, Ch., Deuser, W.G., 1988. Seasonal variation in the flux of euthecosomatous pteropods collected in a deep sediment trap in the Sargasso Sea. Deep-Sea Research I 35 (3), 441-464.

Almogi-Labin, A., Luz, B., Duplessy, J.-C., 1986. Quaternary paleo-oceanography, pteropod preservation and stable-isotope record of the Red Sea. Paleogeography, Paleoclimatology, Paleoecology 57, 195-211.

Bainbridge, A.E., 1981. GEOSECS Atlantic Expedition, Hydrographic Data, 1972-1973. National Science Foundation, Superintendent of Documents, US Government Printing Office, Washington DC, pp. 1-121.

Bandel, K., 1990. Shell structure of the gastropoda excluding archaegastropoda. In: Carter, J.G. (Ed.), Skeletal Biomineralization: Patterns, Processes, and Evolutionary Trends, volume 1. Van Nostrand Reinhold, New York, pp 1-832.

Bandel, K., Almogi-Labin, A., Hemleben, Chr., Deuser, W.G., 1984. The conch of *Limacina* and *Peraclis* (Pteropoda) and a model for the evolution of planktonic gastropods. Neues Jahrbuch Geologisch Paläontologische Abhandlungen 168 (1), 87-107.

Bé, A.W.H., Gilmer, R.W., 1977. A zoographic and taxonomic review of euthecosomatous pteropoda. In: Ramsay, A.T.S. (Ed.), Oceanic Micropalaeontology, volume 1. Academic Press, London, pp. 733-808.

Bé, A.W.H., Morse, J.W., Harrison, S.M., 1975. Progressive dissolution and ultrastructural breakdown in planktonic foraminifera. In: Sliter, W.V., Bé, A.W.H., Berger, W.H. (Eds.), Dissolution of Deep-Sea Carbonates. Cushman Foundation, Foraminiferal Research, Special Publication 13, Ithaka, NY, pp. 27-55.

Berger, W.H., 1975. Deep-sea carbonates: dissolution profiles from foraminiferal preservation. In: Sliter, W.H., Bé, A.W.H., Berger, W.H. (Eds.), Dissolution of Deep-Sea Carbonate, Cushman Foundation, Special Publication 13, 82-86.

Berger, W.H., 1977. Deep-sea carbonate and the deglaciation preservation spike in pteropods and foraminifera. Nature 269, 301-304.

Berger, W.H., 1978. Deep-sea carbonate: pteropod distribution and the Aragonite Compensation Depth. Deep-Sea Research I 25, 447-452.

Berger, W.H., Wefer, G., 1996. Central themes of South Atlantic circulation. In: Wefer, G., Berger, W.H., Siedler, G., Webb, D. (Eds.), The South Atlantic: Present and Past Circulation, Springer-Verlag, Berlin, Heidelberg, pp. 3-11.

Berner, R.A., 1977. Sedimentation and dissolution of pteropods in the ocean. In: Anderson, N.R., Malahoff, A. (Eds.), The Fate of Fossil Fuel CO_2 in the Oceans. Plenum Press, New York, NY, pp. 243-260.

Bickert, T., Wefer, G., 1996. Late Quaternary deep water circulation in the South Atlantic: Reconstruction from carbonate dissolution and benthic stable isotopes. In: Wefer, G., Berger, W.H., Siedler, G., Webb, D. (Eds.), The South Atlantic: Present and Past Circulation. Springer-Verlag, Berlin, Heidelberg, pp. 599-620.

Bleil, U., cruise participants, 1994. Report and preliminary results of METEOR-Cruise M23/2, Rio de Janeiro-Récife, 27.2.-19.3.1993. Berichte Fachbereich Geowissenschaften, Universität Bremen 43, pp. 1-133.

Bleil, U., cruise participants, 1994. Report and preliminary results of METEOR-Cruise M29/2, Montevideo-Rio de Janeiro, 15.7.-8.8.1994. Berichte Fachbereich Geowissenschaften, Universität Bremen 59, pp. 1-153.

Bleil, U., cruise participants, 1998. Report and preliminary results of METEOR-Cruise M38/2, Récife-Las Palmas, 4.3.-14.4.1997. Berichte Fachbereich Geowissenschaften, Universität Bremen 95, pp. 1-126.

Bonnevie, K., 1913. Pteropoda from the Michael Sars North Atlantic deep- sea expedition. Report and Scientific Results. "Michael Sars" North Atlantic Deep-Sea Expedition 1910 III (1), pp. 1-69.

Boyle, E.A., 1988. Cadmium: chemical tracer of deepwater paleoceanography. Paleoceanography 3, 471-490.

Boyle, E.A., 1994. A comparison of carbon isotopes and cadmium in the modern and glacial maximum ocean: can we account for the discrepancies? In: Zahn, R., Pedersen, T.F., Kaminski, M.A., Labeyrie, L. (Eds.), Carbon Cycling in the Glacial Ocean: Constraints on the Ocean's Role in Global Change, NATO ASI Serie C 117, pp. 105-144.

Broecker, W.S., Takahashi, T., 1978. The relationship between lysocline depth and in situ carbonate ion concentration. Deep-Sea Research 25, 65-95.

Chen, C., 1964. Pteropod ooze from Bermuda Pedestal. Science 144, 60-62.

Chen, C., Bé, A.W.H., 1964. Seasonal distribution of euthecosomatous pteropods in the surface waters of five stations in the western North Atlantic. Bulletin of Marine Science of the Gulf and Caribbean 14 (2), 185-220.

Chester, R., 1990. Marine Geochemistry. Unwin Hyman, London, Boston, Sydney, Wellington, pp. 1-698.

Cifelli, R., McCloy, C., 1983. Planktonic foraminifera and euthecosomatus pteropods in the surface waters of the North Atlantic. Journal of Foraminiferal Research 13 (2), 91-107.

Cullity, B.D., 1956. Elements of x-ray diffraction. Addison-Wesley Publication Co, Inc, Reading, Massachusetts; Menlo Park, California; London; Amsterdam; Don Mills, Ontario; Sydney, pp. 1-555.

Curry, W.B., 1996. Late Quaternary deep circulation in the western equatorial Atlantic. In: Wefer, G., Berger, W.H., Siedler, G., Webb, D. (Eds.), The South Atlantic: Present and Past Circulation. Springer-Verlag, Berlin, Heidelberg, pp. 577-598.

Curry, W.B., Duplessy, J.C., Labeyrie, L.D., Shackleton, N.J., 1988. Changes in the distribution of $\delta^{13}C$ of deep water $\sum CO_2$ between the last glaciation and the Holocene. Paleoceanography 5, 487-506.

Curry, W.B., Lohmann, G.P., 1982. Carbon isotopic changes in benthic foraminifera from the western South Atlantic: reconstruction of glacial abyssal circulation patterns. Quaternary Research 18, 218-235.

deMenocal, P.B., Oppo, D.W., Fairbanks, R.G., Prell, W.L., 1992. Pleistocene $\delta^{13}C$ variability of North Atlantic intermediate water. Paleoceanography 7 (2), 229-250.

Devey, C.W., cruise participants, 1993. Cruise report SO-84: The St Helena hotspot, Las Palmas-Cape Town, 2.1.-20.2.1993. Reports, Geologisch-Paläontologisches Institut der Universität Kiel 64, pp. 1-103.

Devey, C.W., cruise participants, 1999. Report and shipboard results from METEOR-Cruise M41/2, Libreville-Vítoria, 18.3.-15.4.1998. Berichte Fachbereich Geowissenschaften, Universität Bremen 137, pp. 1-50.

Diester-Haass, 1977. Radiolarian/planktonic foraminiferal ratios in a coastal upwelling region. Journal of Foraminiferal Research 7 (1), 26-33.

Dittert, N., Baumann, K.-H., Bickert, T., Henrich, R., Huber, R., Kinkel, H., Meggers, H., 1999. Carbonate dissolution in the deep-sea: methods, quantification, and paleoceanographic application. In: Fischer, G., Wefer, G. (Eds.), Use of Proxies in Paleoceanography: Examples from the South Atlantic. Springer-Verlag, Berlin, Heidelberg, pp. 255-284.

Droxler, A.W., Morse, J.W., Glaser, K.S., Haddad, G.A., Baker, P.A., 1991. Surface sediment carbonate mineralgoy and water column chemistry: Nicaragua Rise versus the Bahamas. Marine Geology 100, 277-289.

Fabry, V.J., Deuser, W.G., 1992. Seasonal changes in the isotopic compositions and sinking fluxes of euthecosomatous pteropod shells in the Sargasso Sea. Paleoceanography 7 (2), 195-213.

Fischer, G., cruise participants, 1996. Report and preliminary results of METEOR-Cruise M34/4, Récife-Bridgetown, 19.3.-15.4.1996. Berichte Fachbereich Geowissenschaften, Universität Bremen 80, pp. 1-105.

Fischer, G., cruise participants, 1998. Report and preliminary results of METEOR-Cruise M38/1, Las Palmas-Récife, 25.1.-1.3.1997. Berichte Fachbereich Geowissenschaften, Universität Bremen 94, pp. 1-178.

Fischer, G., Kalberer, M., Donner, B., Wefer, G., 1999. Stable isotopes of pteropod shells as recorders of sub-surface water conditions: comparison to the record of *G. ruber* and to measured values. In: Fischer, G., Wefer, G. (Eds.), Use of Proxies in Paleoceanography: Examples from the South Atlantic. Springer-Verlag, Berlin, Heidelberg, pp. 191-206.

Gerhardt, S., Groth, H., Rühlemann, C., Henrich, R., 2000. Aragonite preservation in late Quaternary sediment cores on the Brazilian Continental Slope: implications for intermediate water circulation. International Journal of Earth Sciences 88 (4), 607-618.

Glaser, K.S., Droxler, A.W., 1993. Controls and development of late Quaternary periplatform carbonate stratigraphy in Walton Basin (northeastern Nicarague Rise, Caribbean Sea). Paleoceanography 8 (2), 243-274.

Haagensen, D.A., 1976. Caribbean zooplankton. Part II - Thecosomata. U.S. Government Printing Office, pp. 551-712.

Haddad, G.A., Droxler, A.W., 1996. Metastable $CaCO_3$ dissolution at intermediate water depths of the Caribbean and western North Atlantic: implications for intermediate water circulation during the past 200,000 years. Paleoceanography 11 (6), 701-716.

Hales, B., Emerson, S., 1996. Calcite dissolution in sedimetns of the Ontong-Java Plateau: In situ measurements of pore water O_2 and pH. Global Biogeochemical Cycles 10 (3), 527-541.

Hales, B., Emerson, S., 1997. Calcite dissolution in sediments of the Ceara Rise: In situ measurements of porewater O_2, pH, and $CO_{2(aq)}$. Geochimica et Cosmochimica Acta 61 (3), 501-514.

Hecht, A.D., Eslinger, E.V., Garmon, L.B., 1975. Experimental studies on the dissolution of planctonic foraminifera. In: Sliter, W.V., Bé, A.W.H., Berger, W.H. (Eds.), Dissolution of Deep-Sea Carbonates. Cushman Foundation, Foraminiferal Research, Special Publication 13, Ithaka, NY, pp. 56-69.

Henrich, R., 1989. Glacial/interglacial cycles in the Norwegian Sea: sedimentology, paleoceanography, and evolution of late Pliocene to Quaternary northern hemisphere climate. In: Eldholm, O., Thiede, J., Taylor, E. (Eds.), Proceedings of ODP, Scientific Results 104. College Station, TX, pp. 189-232.

Henrich, R., cruise participants, 1995. Report and preliminary results of METEOR-Cruise M29/3, Rio de Janeiro-Las Palmas, 11.8.-5.9.1994. Berichte Fachbereich Geowissenschaften, Universität Bremen 60, pp. 1-100.

Henrich, R., Kassens, H., Vogelsang, E., Thiede, J., 1989. Sedimentary facies of glacial-interglacial cycles in the Norwegian Sea during the last 350 ka. Marine Geology 86, 283-319.

Herman, Y., Rosenberg, P.E., 1969. Pteropods as bathymetric indicators. Marine Geology 7, 169-173.

Kaese, R.H., Zenk, W., 1987. Reconstructed Mediterranean salt lens trajectories. Journal of Physical Oceanography 17, 158-163.

Kalberer, M., Fischer, G., Pätzold, J., Donner, B., Segl, M., Wefer, G., 1993. Seasonal sedimentation and stable isotope records of pteropods off Cap Blanc. Marine Geology 113, 305-320.

Kawase, M., Sarmiento, J., 1986. Circulation and nutrients in mid-depth Atlantic waters. Journal of Geophysical Research 91, 9749-9770.

Klug, H.P., Alexander, L.E., 1954. X-ray diffraction procedures for polycrystalline and amorphous materials. John Wiley & Sons, New York, London, Sydney, Toronto, pp. 1-966.

Kroopnick, P.M., 1985. The distribution of ^{13}C of ΣCO_2 in the world oceans. Deep-Sea Research Part I 32 (1), 57-84.

Lembke, L., 1997. Paläozeanographische Rekonstruktion karibischer Tiefenwassermassen anhand von stabilen Kohlenstoffisotopen aus Benthosforaminiferen und metastabilen Karbonatlösungsindizes. Thesis, University of Kiel, Germany, unpublished.

Martin, P.A., Lea, D.W., 1998. Comparison of water mass changes in the deep tropical Atlantic derived from Cd/Ca and carbon isotope records: implications for changing Ba composition of deep Atlantic water masses. Paleoceanography 13 (6), 572-585.

Meinecke, G. ,Wefer, G., 1990. Seasonal pteropod sedimentation in the Norwegian Sea. Palaeogeography, Palaeoclimatology, Palaeoecology 79, 129-147.

Millero, F.J., 1996. Chemical oceanography. CRC Press, Boca Raton, pp. 1-469.

Milliman, J.D., 1974. Marine Carbonates. Springer-Verlag, New York, pp. 1-363.

Morse, J.W., Mucci, A., Millero, F.J., 1980. The solubility of calcite and aragonite in seawater at various salinities, temperatures and 1 atmosphere total pressure. Geochimica et Cosmochimica Acta 44, 85-94.

Pätzold, J., cruise participants, 1993. Bericht und erste Ergebnisse über die METEOR-Fahrt M15/2, Rio de Janeiro-Vitória, 18.1.-7.2.1991. Berichte Fachbereich Geowissenschaften, Universität Bremen 17, pp. 1-46.

Pätzold, J., cruise participants, 1996. Report and preliminary results of VICTOR HENSEN cruise JOPS II, Leg 6, Fortaleza-Récife, 10.3.-26.3.1995 and Leg 8, Vitoria-Vitoria, 10.4.-23.4.1995. Berichte Fachbereich Geowissenschaften, Universität Bremen 76, pp. 1-87.

Pätzold, J., cruise participants, 1999. Report and preliminary results of METEOR-Cruise M41/3, Vitória-Salvador, 18.4.-15.5.1998. Berichte Fachbereich Geowissenschaften, Universität Bremen 129, pp. 1-160.

Peterson, L.C., Prell, W.L., 1985. Carbonate dissolution in recent sediments of the eastern equatorial Indian Ocean: preservation patterns and carbonate loss above the lysocline. Marine Geology 64, 259-290.

Petschick, R., 1996. MacDiff. Computer software, http://servermac.geologie.uni-frankfurt.de/MacDiff.html.

Raymo, M.E., Oppo, D.W., Curry, W., 1997. The mid-Pleistocene climate transition: a deep sea carbon isotopic perspective. Paleoceanography 12 (4), 546-559.

Raymo, M.E., Ruddiman, W.F., Shackleton, N.J, Oppo, D.W., 1990. Evolution of Atlantic-Pacific $\delta^{13}C$ gradients over the last 2.5 m.y. Earth and Planetary Science Letters 97, 353-368.

Reid, J.L., 1989. On the total geostrophic circulation of the South Atlantic Ocean: flow patterns, tracers, and transports. Program of Oceanography 23 (3), 149-244.

Reid, J.L., 1996. On the circulation of the South Atlantic Ocean. In: Wefer, G., Berger, W.H., Siedler, G., Webb, D. (Eds.), The South Atlantic: Present and Past Circulation, Springer-Verlag, Berlin, Heidelberg, pp. 13-44.

Reid, R.P., Carey, S.N., Ross, D.R., 1996. Late Quaternary sedimentation in the Lesser Antilles island arc. Geological Society of America Bulletin 108 (1), 78-100.

Richter, G., 1976. Zur Frage der Verwandtschaftsbeziehungen von Limacinidae und Cavolinidae. Archiv für Molluskenkunde 107 (1/3), 137-144.

Rosenthal, Y., Boyle, A., Labeyrie, L., 1997. Last glacial maximum paleochemistry and deepwater circulation in the Southern Ocean: evidence from foraminiferal cadmium. Paleoceanography 12 (6), 787-796.

Rottman, M.L., 1979. Dissolution of planktonic foraminifera and pteropods in South China Sea sediments. Journal of Foraminiferal Research 9 (1), 41-49.

Rottman, M.L., 1980. Net tow and surface sediment distributions of pteropods in the South China Sea region: comparison and oceanographic implications. Marine Micropaleontology 5, 71-110.

Ruddiman, W.F., Heezen, B.C., 1967. Differential solution of planktonic foraminifera. Deep-Sea Research 14, 801-808.

Schulz, H.D., cruise participants, 1991. Bericht und erste Ergebnisse über die METEOR-Fahrt M16/2, Récife-Belem, 28.4.-20.5.1991. Berichte Fachbereich Geowissenschaften, Universität Bremen 19, pp. 1-149.

Schulz, H.D., cruise participants, 1992. Bericht und erste Ergebnisse der METEOR-Fahrt M20/2, Abidjan-Dakar, 27.12.1991-3.2.1992. Berichte Fachbereich Geowissenschaften, Universität Bremen 25, pp. 1-173.

Schulz, H.D., cruise participants, 1996. Report and preliminary results of METEOR-Cruise M34/2, Walvis Bay-Walvis Bay, 29.1.-18.2.1996. Berichte Fachbereich Geowissenschaften, Universität Bremen 78, pp. 1-133.

Siedler, G., Müller, T.J., Onken, R., Arhan, M., Mercier, H., King, B.A., Saunders, P.M., 1996. The Zonal WOCE Sections in the South Atlantic. In: Wefer, G., Berger, W.H., Siedler, G., Webb, D. (Eds.), The South Atlantic: Present and Past Circulation, Springer-Verlag, Berlin, Heidelberg, pp. 83-104.

Spieß, V., cruise participants, 1994. Report and preliminary results of METEOR-Cruise M23/1, Kapstadt-Rio de Janeiro, 4.-25.2.1993. Berichte Fachbereich Geowissenschaften, Universität Bremen 42, pp. 1-139.

Talley, L.D., 1996. Antarctic Intermediate Water in the South Atlantic. In: Wefer, G., Berger, W.H., Siedler, G., Webb, D. (Eds.), The South Atlantic: Present and Past Circulation, Springer-Verlag, Berlin, Heidelberg, pp. 219-238.

Tesch, J.J., 1946. The thecosomatous pteropods. I. The Atlantic. Dana-Report No. 5 (28), pp. 1-82.

Tesch, J.J., 1948. The thecosomatous pteropods. II. The Indo-Pacific. Dana-Report No. 5 (30), pp. 1-45.

Tesch, J.J., 1966. Das Tierreich. Eine Zusammenstellung und Kennzeichnung der rezenten Tierformen. Mollusca. Pteropoda. Verlag von Friedländer und Sohn, Berlin, pp. 1-154.

Thunell, R.C., 1976. Optimum indices of calcium carbonate dissolution in deep-sea sediments. Geology 4, 525-528.
Van Der Spoel, S., 1967. Euthecosomata, a group with remarkable development stages.(Gastropoda, Pteropoda). Ph.D. thesis, Univ. Amsterdam, J. Noorduijn en Zoon, Gorinchem, pp. 1-375.
Van Der Spoel, S., 1972. Pteropoda Thecosomata. Conseil Internatational Pour Exploration De La Mer. Zooplankton Sheet 140-142, pp. 1-12.
Van Krefeld-Alfane, S., 1996. Late Quaternary sediment records of mid-latitude Northeast Atlantic calcium carbonate production and dissolution. FEBO B.V., Enschede, pp. 1-212.
Volbers, A.N.A., Henrich, R., 2000. Late Quaternary variations in calcium carbonate preservation of deep-sea sediments in the northern Cape Basin: results from a multiproxy approach. Submitted to Marine Geology.
Wefer, G., Berger, W.H., Bijma, J., Fischer, G., 1999. Clues to ocean history: a brief overview of proxies. In: Fischer, G., Wefer, G. (Eds.), Use of Proxies in Paleoceanography: Examples from the South Atlantic. Springer-Verlag, Berlin, Heidelberg, pp. 1-68.
Wefer, G., cruise participants, 1988. Bericht über die METEOR-Fahrt M6/6, Libreville-Las Palmas, 18.2.-23.3.1988. Berichte Fachbereich Geowissenschaften, Universität Bremen 3, pp. 1-97.
Wefer, G., cruise participants, 1989. Bericht über die METEOR-Fahrt M9/4, Dakar-Santa Cruz, 19.2.-16.3.1989. Berichte Fachbereich Geowissenschaften, Universität Bremen 7, pp. 1-103.
Wefer, G., cruise participants, 1990. Bericht über die METEOR-Fahrt M12/1, Kapstadt-Funchal, 13.3.-14.4.1990. Berichte Fachbereich Geowissenschaften, Universität Bremen 11, pp. 1-66.
Wefer, G., cruise participants, 1991. Bericht und erste Ergebnisse über die METEOR-Fahrt M16/1, Point Noire-Récife, 27.3.-25.4.1991. Berichte Fachbereich Geowissenschaften, Universität Bremen 18, pp. 1-120.
Wefer, G., cruise participants, 1992. Bericht und erste Ergebnisse der METEOR-Fahrt M20/1, Bremen-Abidjan, 18.11.-22.12.1991. Berichte Fachbereich Geowissenschaften, Universität Bremen 24, pp. 1-74.
Wefer, G., cruise participants, 1994. Report and preliminary results of METEOR-Cruise M23/3, Récife-Las Palmas, 21.3.-12.4.1993. Berichte Fachbereich Geowissenschaften, Universität Bremen 44, pp. 1-71.
Wefer, G., cruise participants, 1996. Report and preliminary results of METEOR-Cruise M34/3, Walvis Bay-Récife, 21.2.-17.3.1996. Berichte Fachbereich Geowissenschaften, Universität Bremen 79, pp. 1-168.
Wormelle, R.L., 1962. A survey of the standing crop of plankton of the Florida Current. VI. A study of the distribution of the pteropods of the Florida Current. Bulletin of Marine Science of the Gulf and the Caribbean 12 (1), 95-136.
Wormuth, J.H., 1981. Vertical distributions and diel migrations of euthecosomata in the northwest Sargasso Sea. Deep-Sea Research 28A (12), 1493-1515.
Wüst, G., 1964. Stratification and circulation of the Antillean-Caribbean Basins, part 1; spreading and mixing of the water types with an oceanographic atlas. Columbia University Press, New York, pp. 1-202.

2. Intermediate water circulation during the last glacial maximum in the South Atlantic Ocean inferred from changes in the shell preservation of *Limacina inflata* (Pteropoda)

Sabine Gerhardt and Rüdiger Henrich

Dept. of Geosciences, University of Bremen, P.O. Box 33 04 40, D-28334 Bremen, Germany

Abstract

We present last glacial maximum (LGM, 23-19 cal-ka-BP) data of aragonite preservation determined from 38 South Atlantic sediment cores. Microscopic investigation of tests of *Limacina inflata* were used to produce the *Limacina* Dissolution Index (LDX), which displays very good to moderate aragonite preservation at intermediate water depths during the LGM. This preservation pattern indicates the presence of non- to slightly aragonite-corrosive water at intermediate depths at least as far south as 20°S in the western South Atlantic. This is in contrast to the present situation where aragonite-corrosive Antarctic Intermediate Water (AAIW) and Upper Circumpolar Deep Water (UCDW) dominate the intermediate depth level. Past work on $\delta^{13}C$ and Cd/Ca of benthic foraminifera tests suggests that Glacial North Atlantic Intermediate Water (GNAIW) occupied the glacial intermediate depth level and extended at least as far south as 28°S in the western South Atlantic (Oppo and Horowitz, 2000). The southward intrusion of GNAIW implies either (1) a southward restriction or complete elimination of AAIW and UCDW; or (2) a relative change in the position of AAIW and UCDW, with or without mixing with the Southern Component Water (SCW) below. Our data suggest that the corrosive southern component intermediate waters extended at most as far north as 20°S. Our results further show that the position of the deep aragonite lysocline was much shallower during the LGM than it is today, indicating upward expansion of SCW. The aragonite lysocline was situated above the GNAIW/SCW-boundary, which itself is considered to mark the Aragonite Compensation Depth (ACD) of that time.

Keywords: Pteropods, *Limacina inflata*, aragonite dissolution, last glacial maximum, Antarctic Intermediate Water, Glacial North Atlantic Intermediate Water, Northern Component Water, Southern Component Water, South Atlantic Ocean

1. Introduction

Deep-sea circulation changes have been typically inferred from $\delta^{13}C$ and Cd/Ca records of benthic foraminifera (e.g. Curry and Lohmann, 1982; Boyle and Keigwin, 1987; Boyle, 1988, 1994; Curry et al., 1988; Oppo and Fairbanks, 1990; Raymo et al., 1990, 1997; deMenocal et al., 1992; Bickert and Wefer, 1996; Curry, 1996; Rosenthal et al., 1997; Martin and Lea, 1998; Oppo and Horowitz, 2000). The utility of $\delta^{13}C$ and Cd is based on the observation that these parameters are inversely and directly correlated to nutrients, respectively (Curry et al., 1988; Curry, 1996). Carbonate dissolution proxies such as the percentages of carbonate, coarse fraction (> 63 μm), and planktic foraminifera, as well as foraminiferal dissolution proxies (e.g. the *Globigerina bulloides* dissolution index, BDX'; Volbers and Henrich, subm.), foraminiferal fragmentation indices (e.g. the fragmentation index FI; Peterson and Prell, 1985), the planktic to benthic foraminifera ratio (e.g. Berger, 1975), and the planktic foraminifera to radiolarians ratio (e.g. Diester-Haass, 1977) have been widely used in order to reconstruct deep-ocean history. However, most of these proxies are not only steered by a single process, but have multiple interacting control mechanisms. To extract the true bottom water signal, variations in abyssal circulation as well as in bottom water chemistry, in organic and inorganic productivity of the surface waters, in shell shape or structure of the examined species, in dilution of the sediments by terrigenous material, in lateral transport of particles, and in bioturbation all have to be evaluated in their relative extent. Moreover, in situ electrode measurements of porewater O_2, pH, and $CO_{2(aq)}$ suggested recently that calcite dissolution driven by metabolic CO_2 produced within the sediments may be an important part of the diagenesis of sedimentary calcite even in supralysoclinal waters (e.g. Hales and Emerson, 1996, 1997).

Dissolution proxies inferred from aragonitic skeletons may yield essential information about intermediate water variability as aragonite is ≈1.5 times more soluble than calcite in seawater (Morse et al., 1980; Millero, 1996) and thus dissolves at much shallower water depths. This difference is based on the dissimilar thermodynamic and chemical properties of calcite and aragonite due to their differing crystal structures, and is clearly imprinted in the sediments. Haddad and Droxler (1996) established a composite dissolution index (CDI), consisting of % Mg calcite, pteropod abundance, % whole pteropods, and % clear pteropods, which revealed that different water masses occupied the intermediate depth western North Atlantic and Caribbean during much of the late Quaternary. These CDI records suggest that variations in aragonite preservation are most probably related to changes in the flow of Antarctic Intermediate Water (AAIW) into the Caribbean Sea. Mixing between low $[CO_3^{2-}]$ water from the base of the AAIW and high $[CO_3^{2-}]$ North Atlantic Deep Water (NADW) may

be largely responsible for the poor preservation of carbonate sediment observed today in the Caribbean (Droxler et al., 1991; Haddad and Droxler, 1996).

In two separate papers, Gerhardt et al. (2000) and Gerhardt and Henrich (in press) have introduced and tested the *Limacina* Dissolution Index (LDX). Gerhardt et al. (2000) found that variations in late Quaternary aragonite preservation on the Brazilian continental margin may be attributed to temporal shifts in intermediate water mass structure. Gerhardt and Henrich (in press) have shown that today's aragonite preservation patterns in western Atlantic Ocean and Caribbean Sea sediments are closely tied to the distribution of aragonite-corrosive/less corrosive water masses. The core-top calibrations permit us to apply the LDX on other time slices in order to reconstruct glacial to interglacial variations in intermediate water geometry. In the present paper we determine aragonite preservation patterns in South Atlantic sediments of the last glacial maximum (LGM). In comparison with the modern situation, we show that variations in aragonite preservation are directly linked to changes in NADW and AAIW/UCDW distribution. It appears that the LDX is a reliable measure to distinguish between present aragonite-corrosive and less corrosive water masses. However, before it can be accepted as a valid paleo-proxy, it must be tested in the past.

1.1. The present Atlantic circulation mode and its imprint on the surficial LDX record

The present Atlantic circulation has been described by numerous authors (e.g. Reid, 1989, 1996; Siedler et al., 1996). Figure 1 (Gerhardt and Henrich, in press) illustrates the western Atlantic water mass configuration as determined from differing CO_3^{2-} concentrations. The water masses which contribute to the South Atlantic circulation include (from deep to shallow) the northward flowing Weddell Sea Deep Water (WSDW) and Lower Circumpolar Deep Water (LCDW), which are mostly linked together and hence termed Antarctic Bottom Water (AABW). Above the AABW, the broad core of NADW flows southwards and can be divided into a lower (LNADW) and an upper (UNADW) sub-layer. UNADW is covered by two northward moving, mid-depth water masses termed Antarctic Intermediate Water (AAIW) and Upper Circumpolar Deep Water (UCDW). South Atlantic Central Water (SACW) covers the AAIW. AAIW can be traced as far north as 25°N, whereas the UCDW reaches 25-30°N (Talley, 1996), as indicated by a silica maximum. AAIW and UCDW enter the Caribbean Sea through several channels and sills and mix with NADW (Droxler et al., 1991; Haddad and Droxler, 1996). Mediterranean Overflow Water (MOW) spreads out west- and southwestward from the Straits of Gibraltar at depths between 800 and 1500 m (e.g. Kaese and Zenk, 1987) and enters the Caribbean Sea between 10° and 20°N.

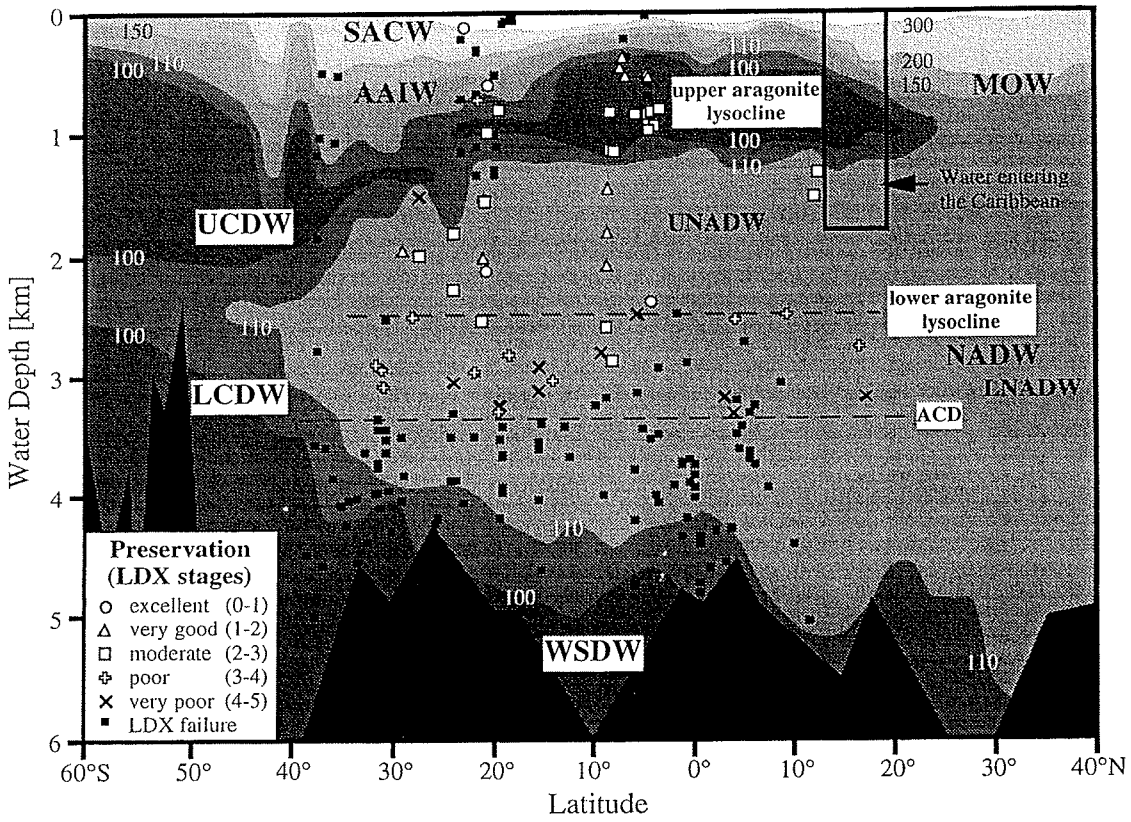

Fig. 1: Modern water mass distribution in the western Atlantic Ocean between 40°N and 60°S and LDX values determined from pteropods in surface sediments of the western Atlantic Ocean including the Mid-Atlantic Ridge (Gerhardt and Henrich, in press). Perfect aragonite preservation (LDX <2) is found within the SACW, within the upper part of the AAIW/UCDW, and partly within the UNADW. Dissolution (LDX >2) is observed in the lower part of the AAIW/UCDW with an upper aragonite lysocline developed at ≈750 m, within the LNADW beneath the lower lysocline at ≈2500 m, and in southern regions within the UNADW. The Aragonite Compensation Depth (ACD) occurs at ≈3400 m. WSDW = Weddell Sea Deep Water; LCDW = Lower Circumpolar Deep Water; NADW = North Atlantic Deep Water; LNADW = Lower North Atlantic Deep Water; UNADW = Upper North Atlantic Deep Water; UCDW = Upper Circumpolar Deep Water; AAIW = Antarctic Intermediate Water; MOW = Mediterranean Overflow Water; SACW = South Atlantic Central Water.

The aragonite preservation state at the sediment-water interface is primarily controlled by the saturation state of the overlying bottom water with respect to aragonite (Gerhardt and Henrich, in press). The local saturation state depends on the carbonate ion concentration under the given in situ p/T-conditions, as the solubility of both calcite and aragonite increases with pressure. The saturation concentration increases with water depth, whereas the in situ CO_3^{2-} concentration changes little with water depth in most parts of the deep sea. In the South Atlantic, the rate of decrease of $[CO_3^{2-}]$ is not regular with water depth, but follows an S-shaped curve (with a distinct minimum within AAIW/UCDW). Preservation occurs where the in situ CO_3^{2-} concentration exeeds the saturation concentration, whereas dissolution occurs below the cross-point of the two curves. Differences in the CO_3^{2-} concentration of bottom

waters are believed to be responsible for the first-order variations in the depth of the lysoclines between and within the oceans. In the western South Atlantic, near saturation is first reached within AAIW/UCDW. As a result, aragonite particles at the sediment-water interface that are in contact with AAIW or UCDW are worse preserved than those within the SACW above or the UNADW below (Fig. 1 and Gerhardt and Henrich, in press). Aragonite saturation is reached next in the lower part of the NADW layer. The LDX reveals that two aragonite lysoclines are developed one above the other (Fig. 1). The first (or upper) lysocline is indicated at ≈750 m water depth while the second (or lower) lysocline is found at ≈2500 m (Gerhardt and Henrich, in press).

1.2. Glacial Atlantic circulation pattern

The modern hydrological situation has not been constant over the Pleistocene climatic cycles. The mean position of the northern and southern polar front is known to shift with time and the sources of deep and intermediate waters are variable (e.g. Duplessy et al., 1988). In many previous studies, the glacial distribution of northern and southern source waters was discussed (mainly based on $\delta^{13}C$ and Cd/Ca records). Benthic foraminiferal $\delta^{13}C$ records suggest that the NADW contribution to the deep South Atlantic was significantly reduced during the LGM (e.g. Curry and Lohmann, 1982; Oppo and Fairbanks, 1987), but Southern Ocean Cd/Ca records do not (Boyle, 1992). The formation of nutrient-enriched, ^{13}C-depleted southern source water may have been significantly enhanced during the LGM (e.g. Boyle and Keigwin, 1982, 1987; Curry and Lohmann, 1982, 1983; Oppo and Fairbanks, 1987; Curry et al., 1988; Raymo et al., 1990; Sarnthein et al., 1994; Curry, 1996). As a result, southern ocean deep water penetrated farther into the North Atlantic and crossed several fracture zones into the eastern Atlantic Ocean. The glacial counterpart of NADW is termed GNAIW because of its intermediate level in the water column, or simply Northern Component Water (NCW) because of its source area. In this paper, we refer to glacial NADW as GNAIW. Likewise, the glacial equivalent for AABW is called Southern Component Water (SCW). The SCW can be divided into a lower (LSCW) and an upper part (USCW; Fig. 2b and Bickert and Wefer, 1996). During the LGM, the boundary between SCW and GNAIW, marked also by the calcite lysocline, was situated at 3800 m water depth near the equator and rose slightly toward the Southern Ocean (Bickert and Wefer, 1996).

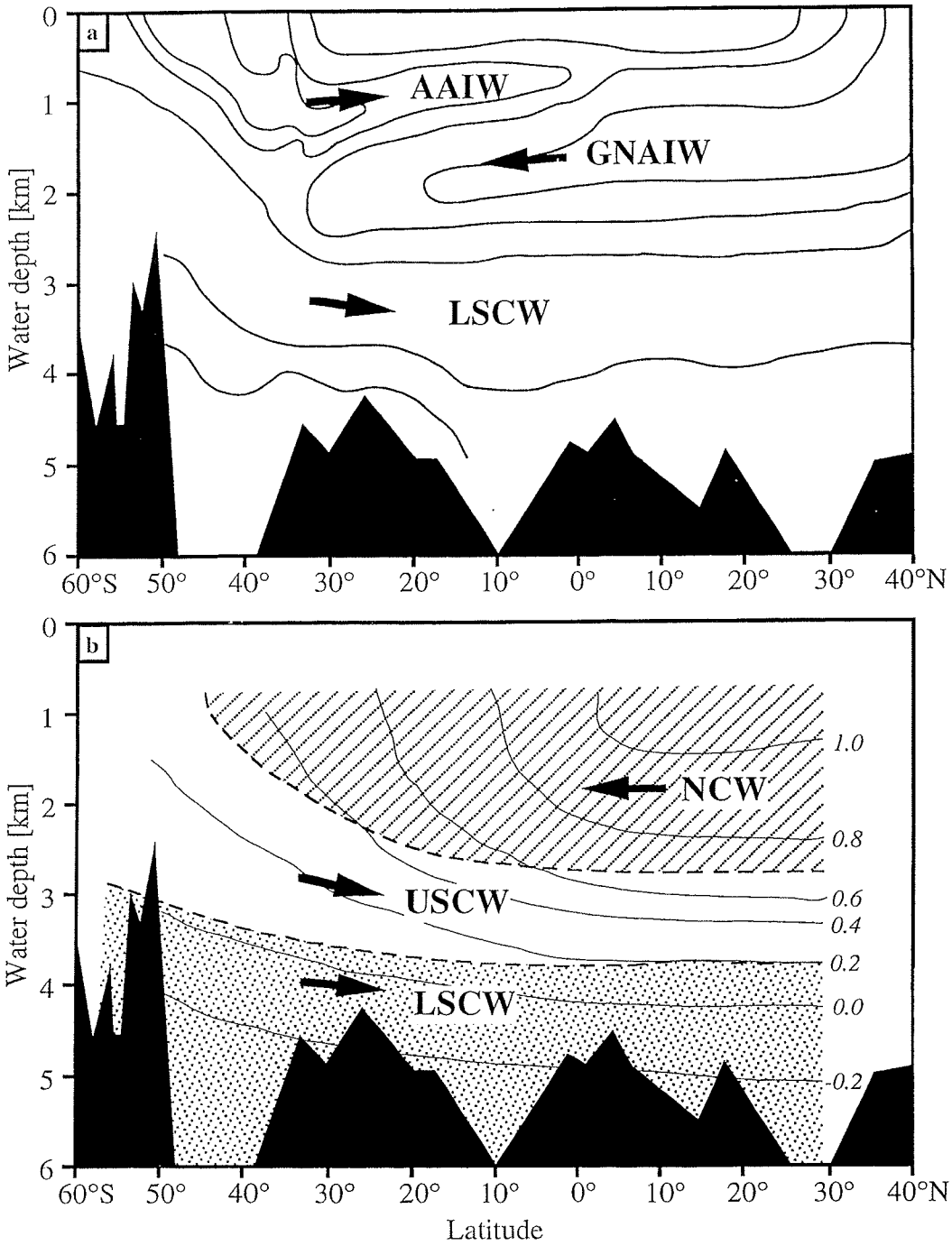

Fig. 2a-b: Models of western Atlantic circulation modes during the last glacial maximum (LGM). (a) Based on benthic foraminifera $\delta^{13}C$ and Cd/Ca data, Antarctic Intermediate Water (AAIW) is assumed to spread northward above Glacial North Atlantic Intermediate Water (GNAIW) similar to today (though significantly reduced), but with a northern boundary close to the equator (modified after Haddad and Droxler, 1996). (b) Based on benthic foraminifera $\delta^{13}C$ (labelled with italic numbers), Bickert (1992) presented a LGM circulation model consisting of three independent water masses, i.e. Northern Component Water (NCW) overlying Upper and Lower Southern Component Water (USCW/LSCW). Arrows mark flow directions.

In the last years, rapid shifts in the contribution of varying northern sources of deep and intermediate waters during glacial and deglacial periods have been recognized (e.g. Venz et al., 1999), whereas much less is known about the variability of intermediate southern source waters. Recently, Oppo and Horowitz (2000) inferred from $\delta^{13}C$ and Cd/Ca data that GNAIW extended at least as far south as 28°S in the western South Atlantic during the LGM. Yet, if GNAIW was situated at the intermediate depth level during the LGM and hence replaced southern source AAIW and UCDW, then AAIW and UCDW must have changed their relative position and/or strength. It is believed that these intermediate waters were restricted to the southern hemisphere, but whether they were reduced (Fig. 2a; Haddad and Droxler, 1996), completely eliminated, or whether they changed their relative positions with NADW, with or without mixing with SCW (Fig. 2b; Bickert, 1992), is not well understood.

2. Materials and methods

2.1. Core selection and study area

We studied 87 LGM sediment samples from 38 core locations, which were collected with a gravity corer during RV Meteor cruises M6/6 (Wefer et al., 1988), M9/4 (Wefer et al., 1989), M12/1 (Wefer et al., 1990), M15/2 (Pätzold et al., 1993), M16/1 (Wefer et al., 1991), M16/2 (Schulz et al., 1991), M20/2 (Schulz et al., 1992), M23/1 (Spieß et al., 1994), M23/2 (Bleil et al., 1994), M23/3 (Wefer et al., 1994), M34/2 (Schulz et al., 1996), M34/4 (Fischer et al., 1996), RV Sonne cruise SO-84 (Devey et al., 1993), and RV Victor Hensen cruises VH/JOPS II-6 and VH/JOPS II-8 (Pätzold et al., 1996). The cores are ideally situated between 767 m and 4588 m water depth throughout the South Atlantic to monitor the inter-ocean exchange of intermediate and deep water (see Fig. 3 and Appendix 1 for sample locations). The shallowest cores are presently covered by AAIW and UCDW, whereas the mid-depth cores lie within UNADW and LNADW and the deepest cores within AABW. The investigated area extends from 6°N to 37°S and from 46°W to 15°E, which comprises most of the South Atlantic Ocean (Fig. 3). Pteropod-rich sediments are restricted mostly to shallow parts of the ocean. Therefore, aragonite oozes and muds are preferably found at elevated topographic structures such as continental slopes, ridges, and rises.

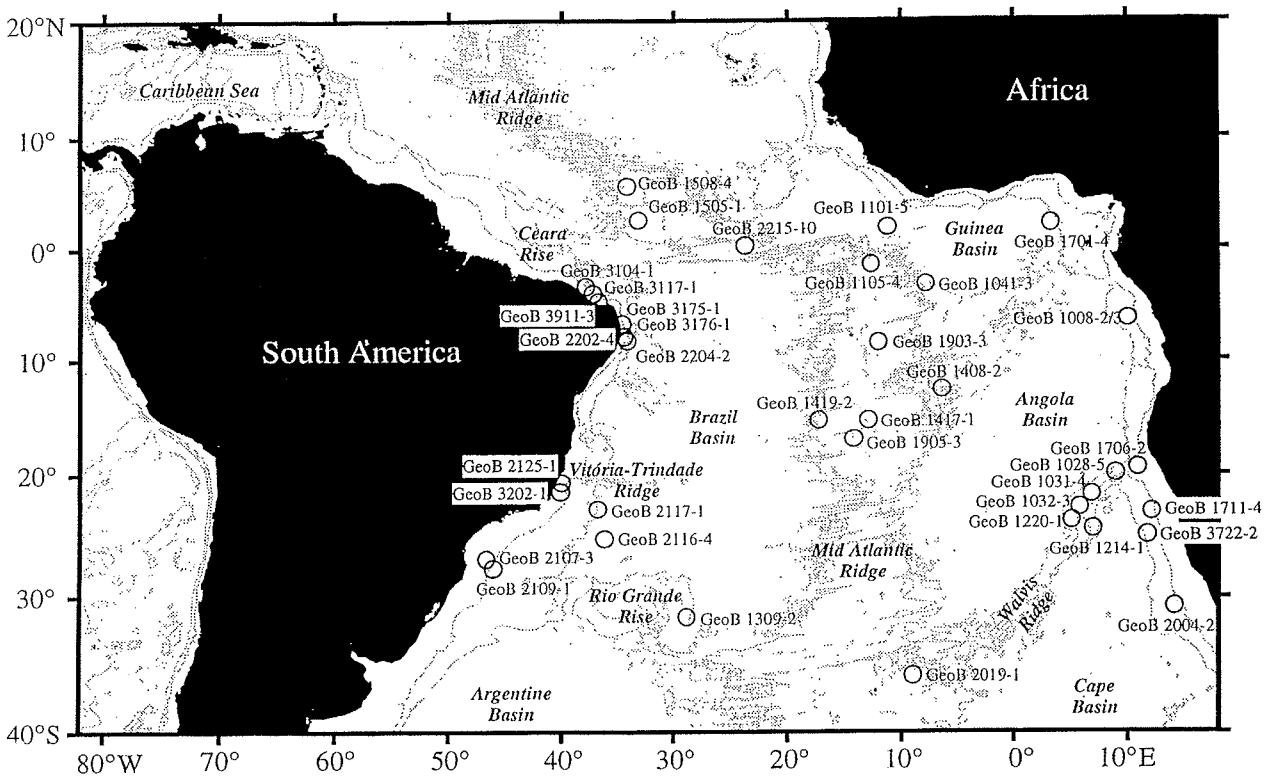

Fig. 3: Map of core locations (see Appendix 1 for details). Cores were predominantly recovered from submarine ridges, rises, and continental slopes.

2.2. Stratigraphy

Most of the studied samples represent a LGM age (23-19 cal-ka-BP). Only a few samples slightly older or younger than the LGM were analyzed as supplementary samples. The chronostratigraphy of 37 out of 38 cores is based on accelerator mass spectrometry (AMS) ^{14}C datings on planktic foraminifera coarser than 150 µm (Arz et al., 1999; Niebler et al., subm.). The dates were corrected for a reservoir age of 400 yrs and converted to calendar ages (cal-ka-BP) (see Bard, 1988; Bard et al., 1993; Hughen, 1998). Only an initial age model exists for the remaining core GeoB 2107-3 (Bleil et al., 1994) and is based on biostratigraphy.

2.3. Limacina *Dissolution Index (LDX)*

Limacina inflata (d'Orbigny, 1836) is one of the most common warm-water cosmopolitan pteropods and is widely distributed in the tropical and subtropical regions of all oceans (Bé and Gilmer, 1977). The reader is referred to Gerhardt and Henrich (in press) for a detailed

description about its present distribution in the oceans and its shell structure. The sample preparation was carried out by carefully wet sieving the bulk sediment to separate the fine (< 63 µm) and the coarse fraction (> 63 µm). After drying the coarse fraction, at least 10 adult tests per sample of *L. inflata* (about 1 mm in size) were picked and classified after six preservation stages which are briefly described below (according to Gerhardt et al., 2000). The resulting LDX is a mean value of all examined tests per sample (see Appendix 1 for respective test numbers). At least one sample per core representing a LGM age was investigated. Depending on the respective sedimentation rates, up to 14 LGM samples (GeoB 3104-1) were available (see Appendix 1). If more than one LGM sample was investigated, all determined LDX values were averaged. LDX failure is indicated if less than 10 tests of *L. inflata* were found in a sample. A variety of reasons may lead to LDX failure, such as low supply of tests into the sediment (either due to changes in the carbonate production within the surface waters or due to increased dilution by terrigenous material) or by enhanced aragonite dissolution at the sediment-water interface due to the decomposition of organic matter. In addition, if the investigated tests in a sample did not show a Gaussian distribution of preservation stages, they were excluded from this study as they were assumed to be influenced by lateral transport or bioturbation. Thus, all samples used in this study are believed to be unaffected by redeposition.

Stage 0: Transparent shells
This stage indicates best preservation. Only the shells of living pteropods and originally preserved pteropod assemblages in sediments show this mode of preservation.
Stage 1: Milky and cloudy shells, lustrous shell surface
This stage is reached when either slight shell corrosion has taken place or the organic parts of the shell have become cloudy through oxidation (Haddad and Droxler, 1996).
Stage 2: Opaque-white shells, lustrous shell surface
In this stage, pteropod shells are opaque and white (not just milky) which means they have truly experienced initial dissolution on their surface.
Stage 3: Opaque-white shells, partly lustreless shell surface
In this stage, parts of the surface layer have disappeared by dissolution. Consequently, the shell surface seems to be lustreless in those areas where the helical aragonite layer is exposed.
Stage 4: Opaque-white shells, totally lustreless shell surface
This stage is reached when the surface layer has been entirely removed by corrosion.
Stage 5: Opaque-white, totally lustreless and perforated shells
This stage is characterized by additional shell damage of any kind, neglecting the absence of the aperture tooth which is often broken off mechanically during sample preparation.

3. Results and discussion

LGM aragonite preservation patterns for the western and eastern South Atlantic Ocean are illustrated in Fig. 4 (the results are plotted against the LGM water mass distribution model of Bickert, 1992). Glacial (Fig. 4) to interglacial (Fig. 1) comparison of the LDX records reveals three important results: (1) aragonite preservation in intermediate depths is much better during the LGM than it is today; (2) just as in modern times, LDX failure is mainly found in the eastern South Atlantic; and (3) overall LDX failure due to bottom-water undersaturation, indicating the position of the ACD, is found at much shallower water depths during the LGM. Figure 5 shows a comparison of the LDX records for the modern and the LGM situation in the western South Atlantic.

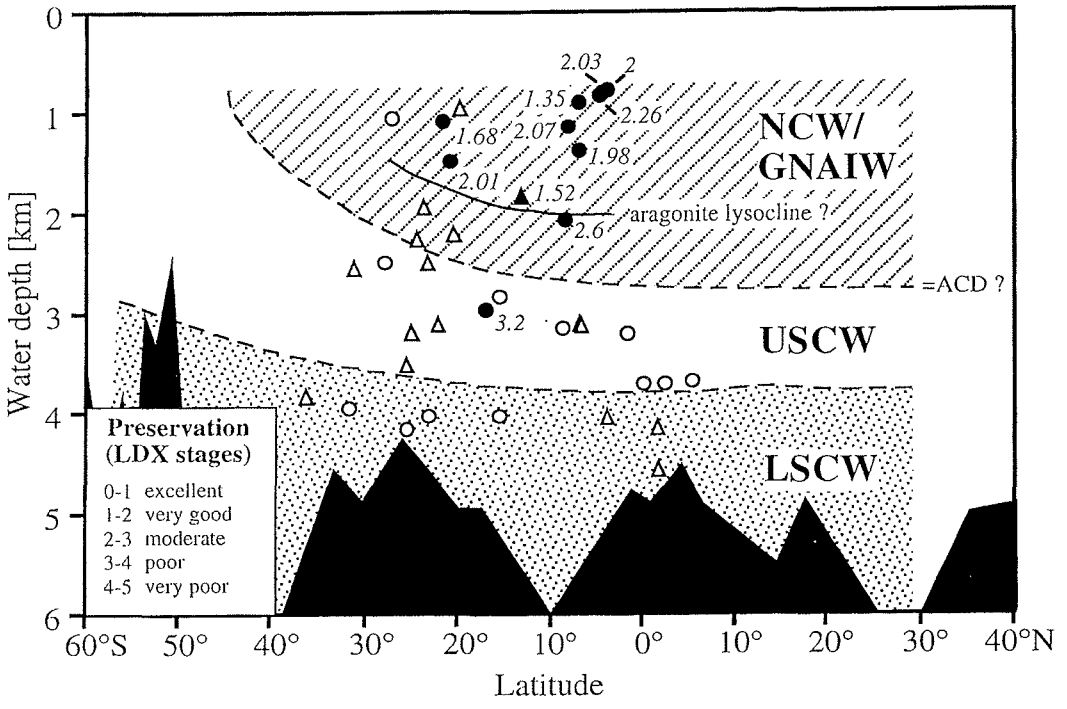

Fig. 4: LGM-LDX values in the western (circles) and in eastern (triangles) South Atlantic, with the 10°W meridian marking the border between the western and eastern basins. Filled circles and triangles mark samples on which LDX values were attained, whereas open circles and triangles indicate LDX failure. The results are plotted against the LGM water mass distribution model of Bickert (1992). Very good and moderate preservation is only found within the NCW at depths shallower than 2000 m, which most probably marks the aragonite lysocline of that time. Below, preservation worsens rapidly. The NCW/SCW-boundary indicates the Aragonite Compensation Depth (ACD).

It should be noted that we made two assumptions here to avoid confusion: firstly, we refer to the modern water depth of the cores from which the surface sediment samples were derived (Gerhardt and Henrich, in press), and assume that the glacial depths of the cores were ≈120 m shallower than today (Fairbanks, 1989). Secondly, we assume that the difference between the location of the gravity cores (LGM samples) and the related multicorer cores (surface sediments) is neglectible.

3.1 Intermediate water distribution

Limacina inflata displays very good (LDX: 1.35 to 1.98) to incipient moderate (LDX: 2.00 to 2.26) preservation at intermediate water depths above 2000 m during the LGM, indicating the presence of a water mass which is equally corrosive to modern UNADW (Fig. 4). We suggest that this intermediate water mass was non- to only slightly aragonite-corrosive, since LDX values ≥ 2 indicate initial aragonite dissolution (Gerhardt and Henrich, in press). It should be noted that the transition between very good and moderate aragonite preservation (i.e. LDX = 2) is considered to indicate the position of the aragonite lysocline in the modern ocean (see Fig. 1 and Gerhardt and Henrich, in press). However, we do not believe that this LDX value, as an indicator of the lysocline, can be applied on the LGM data, since it does not account for long-term diagenetic trends which may be superimposed on the initial bottom water signal. Gerhardt et al. (2000) observed a diagenetic trend in late Quaternary sediment cores from the western South Atlantic. They found that aragonite contents as well as preservation of *L. inflata* decreased, whereas the fragmentation of *L. inflata* increased significantly with increasing core depth. Therefore, we suggest that the LDX value which is indicative for the position of the aragonite lysocline should be higher during the LGM than today and should increase with core depth. If the diagenetic superposition could be evaluated for each core, then correction to the primary LDX data could reveal the respective LDX value indicative for the lysocline depth.

The findings agree well with the $\delta^{13}C$ and Cd/Ca data of Oppo and Horowitz (2000), who suggest that the glacial counterpart of NADW (i.e. GNAIW) extended at least as far south as 28°S at an intermediate water depth level. We suggest that the aragonite saturation state at the sediment-water interface within GNAIW was similar to that within modern UNADW conditions. However, LGM samples of two cores within the GNAIW display LDX failure (see Fig. 4). They were recovered at 1048 m (GeoB 2107-3) and 980 m (GeoB 1706-2) water depth in the western and eastern Atlantic Ocean, respectively. This LDX failure is most probably due to dilution with terrigenous material or supralysocline aragonite dissolution induced by the decomposition of organic matter within or on the sediment rather than by an

intrusion of aragonite-corrosive AAIW/UCDW into these regions. Comparison between LGM LDX values and surficial LDX values from the same sample locations of the western South Atlantic (Fig. 5) reveal that at intermediate water depths (767-1503 m), aragonite preservation is predominantly worse today than during the LGM. This is related to variations in the extent of glacial to interglacial intrusion of aragonite-corrosive AAIW and UCDW into the intermediate water level. Today, AAIW and UCDW can be clearly distinguished from the water masses above (SACW) and below (NADW) by their lower $[CO_3^{2-}]$, indicated by an S-shaped curve trend. Likewise, the LDX curve shows an S-shape, with good preservation within SACW and UNADW and bad preservation within AAIW/UCDW and below NADW (Gerhardt and Henrich, in press). It appears that in contrast to the modern situation, the LDX increases regularly with water depth during the LGM.

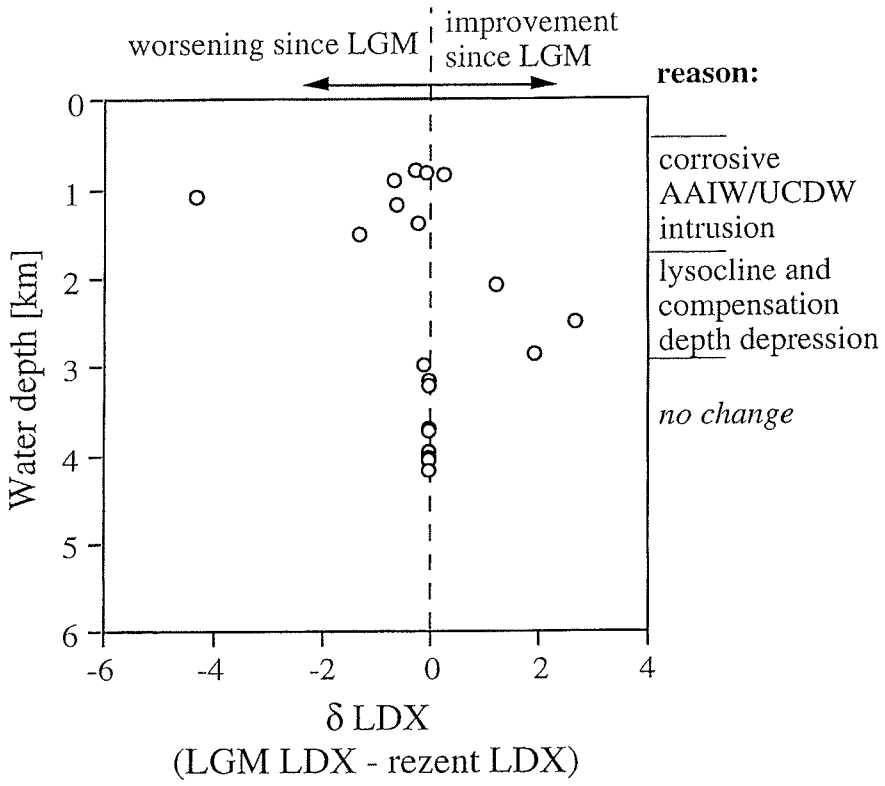

Fig. 5: Preservation changes of *L. inflata* in the western South Atlantic since the LGM. Between 767 m and 1503 m water depth, preservation is worse today due to aragonite-corrosive AAIW/UCDW intrusion since the LGM, whereas improved preservation is determined between 2072 m and 2845 m due to an aragonite lysocline and compensation depth depression since that time. Below 2845 m, almost no changes occur. Surface sample LDX values are taken from Gerhardt and Henrich (in press).

Although all data indicate that GNAIW was situated at the intermediate depth level of the western South Atlantic during the LGM, it remains questionable whether or not we can trace

the glacial distribution of AAIW and UCDW. We suggest three possible scenarios: (1) glacial reduction of AAIW and UCDW; (2) elimination of AAIW and UCDW; or (3) change in the relative positions of NADW, AAIW, and UCDW, with or without mixture of AAIW/UCDW with SCW (Fig. 6). The LDX data (see Fig. 4) support the idea of the glacial reduction of AAIW and UCDW and their replacement by GNAIW as far south as 20°S (Fig. 6b). Nevertheless, if AAIW and UCDW were reduced but not eliminated during the LGM, they should be traced with the LDX or other indices within the LGM sediments along the Argentine Continental Margin south of 20°S. Complete elimination of AAIW and UCDW (Fig. 6c) should also be imprinted in the sediment along the Argentine Continental Margin. More data from the southwestern South Atlantic are therefore needed to resolve the question of whether AAIW and UCDW were eliminated or only reduced. If not a reduction, but an inversion of water masses characterized the glacial South Atlantic (Fig. 6d), then significant changes in density of each water mass must have occurred. Curry and Lohmann (1982) suggested that even minor changes in density could lead to significant changes in the relative position of UCDW and NADW. As a result of the inversion, aragonite-corrosive AAIW and UCDW could have deepened. Moreover, they might have been situated below the NCW/SCW boundary (with or without mixing with SCW). If so, it is questionable if AAIW and UCDW could be traced at all by using the LDX, since AAIW and UCDW might be indistinguishable from equally corrosive SCW. In the modern South Atlantic Ocean, both UCDW and LCDW have similar CO_3^{2-} concentrations (see Fig. 1), but have different saturation states as the solubility of aragonite increases with pressure and hence with water depth. The present mid-depth position of corrosive AAIW/UCDW allows clear distinction from less-corrosive UNADW and surface water. If the AAIW and UCDW were positioned "too deep" for the LDX during the LGM, other proxies based on $\delta^{13}C$ or Cd/Ca of benthic foraminifera, or on calcite preservation, might be more useful.

Oppo and Horowitz (2000) suggest another scenario for the western South Atlantic, based on the analysis of intermediate depth sediment cores from the Rio Grande Rise region. To examine the significance of intermediate water mixing and aging, they modified their primary benthic $\delta^{13}C$ and Cd_{water} data to account for a 0.3‰ lower glacial mean ocean $\delta^{13}C$ (Duplessy et al., 1988), a 2‰ higher average organic matter $\delta^{13}C$ (Lynch-Stieglitz et al., 1995, 1996), a 4% increase in total inorganic carbon, and no change in the oceanic inventory of Cd during the LGM (Boyle, 1988, 1992; Rosenthal et al., 1995). On this basis, they suggest that a mixture of Circumpolar Deep Water (CDW) and GNAIW could have influenced the upper South Atlantic. Regardless of whether or not these corrections were applied to the $\delta^{13}C$ data, Oppo and Horowitz (2000) suggested that GNAIW strongly influenced the intermediate depth (≈1500 m) South Atlantic at least as far south as 28°S. The water above and below may have been composed entirely of aged GNAIW or may have

consisted of as much as two-thirds CDW. Interestingly, the low LGM $\delta^{13}C$ value at a 1268 m deep site implies the absence of a high $\delta^{13}C$ source like modern AAIW.

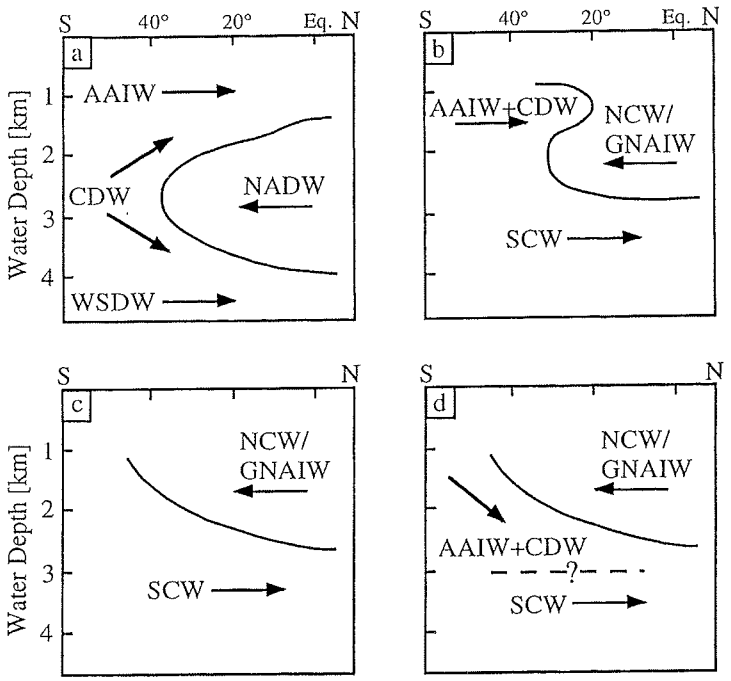

Fig. 6a-d: Speculations on the LGM water mass distribution in the western South Atlantic Ocean based on the results of this study. (a) Modern water mass distribution, (b) reduction of AAIW and CDW with a maximum northern distribution at 20°S, (c) elimination of AAIW and CDW, (d) change in the relative position of NCW, AAIW, and CDW, with or without mixture of AAIW/CDW with SCW. The NCW/SCW-boundary is drawn according to previous studies (e.g. Curry and Lohmann, 1982; Bickert, 1992).

3.2 West/east contrast

Just as in modern times, there is a striking contrast in the aragonite preservation state between the western and eastern Atlantic Ocean during the LGM. Along the western continental margin as well as on the Mid-Atlantic Ridge, predominantly good agreement between the LDX and the respective bottom-water saturation is observed (see Fig. 1), whereas LDX failure is common along the eastern continental margin (Gerhardt and Henrich, in press). The absence of pteropod tests in surface sediments of any depth along the southwestern African continental margin was also observed by Berger (1978). To a minor extent, this LDX failure is due to a considerably reduced occurrence of *L. inflata* in upwelling regions (Bé and Gilmer, 1977; Fig. 1) and thus a lack of supply into the sediment and to dilution by terrigenous material delivered by large rivers such as the Congo River. On the other hand, it is known that a large supply of organic matter into the sediment (which is a

typical feature of high productivity upwelling areas) and its subsequent decomposition releases additional CO_2 into the bottom-water, thereby driving aragonite dissolution. In situ electrode measurements of porewater O_2, pH, and $CO_{2(aq)}$ demonstrated that calcite dissolution driven by metabolic CO_2 produced within the sediments forms a significant part of the diagenesis of sedimentary calcite even in supralysoclinal waters (e.g. Hales and Emerson, 1996, 1997). In some areas, "metabolic dissolution" may account for 65-80% of the total dissolution (Hales and Emerson, 1996). We suggest that if the ratio of organic to inorganic carbon (="rain ratio") in the sediment is considerably enhanced, aragonite dissolution occurs rapidly. This may alter or even deface the first-order bottom-water signal. In addition, LDX failure due to metabolic dissolution is also observed in the vicinity of the mouths of large rivers, as observed in surface sediments nearby the Rio de la Plata and the Amazon River (Gerhardt and Henrich, in press). There, surface water productivity is enhanced due to the supply of nutrients.

3.3 Aragonite lysocline and compensation depth

In the deeper regions of the glacial South Atlantic, aragonite preservation worsened rapidly (Fig. 4), indicated by only moderate preservation (LDX: 2.60) within the lower GNAIW. Beneath GNAIW, LDX failure is common within the entire SCW except for one location with poor preservation (GeoB 1905-3, LDX: 3.20) at 2974 m water depth (see Fig. 4). In the deep eastern South Atlantic, overall LDX failure is observed (see section 3.2). Comparison between modern and glacial times (Fig. 5) reveals that between ≈2000 m and 3000 m, aragonite preservation is significantly better today than it was during the LGM. This is due to a glacial to interglacial depression of the aragonite lysocline and compensation depth in the South Atlantic. The δLDX (= LGM LDX - rezent LDX) value of 0 in Fig. 5 reveals that below 3000 m water depth, LDX failure is common in modern as well as in LGM times. The GNAIW/SCW boundary may be considered to represent the ACD of that time, hence the ACD was situated several hundred meters shallower during the LGM than today. It therefore appears that during the LGM, the equatorial aragonite lysocline was positioned ≈500 m shallower than today in ≈2000 m water depth, most probably rising parallel with the GNAIW/USCW boundary to the south (Fig. 4). The proposed uplift of the lower aragonite lysocline is consistent with the findings of Berger (1968) from the tropical North Atlantic, who also suggested that the glacial aragonite lysocline was 500 m shallower than today. However, this uplift is in contrast to the global situation, which suggests a global deepening of both the aragonite and calcite lysoclines during the LGM. Recently, Broecker et al. (1999) presented evidence for a major reduction in deep-sea CO_3^{2-} content of 11±2 μmol kg^{-1}

accompanied by an increase in atmospheric CO_2 content of ≈22 ppm (Indermühle et al., 1999) over the last 8000 yrs. Likewise, a reduced atmospheric CO_2 content during glacial times as proposed by many authors (e.g. Barnola et al., 1987) would have been accompanied by a corresponding rise in global oceanic $[CO_3^{2-}]$, as there is a roughly inverse relationship between $[CO_3^{2-}]$ and pCO_2 (Broecker et al., 1999). Such a rise in $[CO_3^{2-}]$, accompanied by low shallow-water $CaCO_3$ deposition rates during the LGM as proposed by Milliman (1974), would have caused a global deepening of both the aragonite and calcite lysoclines for compensation and hence would have increased the seafloor surface area upon which $CaCO_3$ preservation can occur. This difference between the globally and regionally induced aragonite dissolution signal assumes an asymmetry between the oceans and indeed, Howard and Prell (1994) determined a gradient in today's CO_3^{2-} content between the Atlantic and Pacific Oceans. At present, lysoclines in the Pacific are much shallower than in the Atlantic. Catubig et al. (1998) have found higher burial rates of $CaCO_3$ in the Pacific and North Atlantic, and lower burial rates in the tropical and South Atlantic, the Indian, and the Southern Ocean during the LGM. Howard and Prell (1994) suggested that today's Atlantic/Pacific CO_3^{2-} gradient also existed during the LGM, although it was smaller than today. That is, the lysoclines shoaled in the South Atlantic and Southern Ocean while they deepened in the Pacific.

It appears that aragonite preservation at the sediment-water interface primarily reflects the saturation state of the bottom water. Therefore, it should be possible to infer glacial to interglacial variations in deep and intermediate water mass circulation from aragonite preservation. Only in high productivity areas does an enhanced supply of organic matter into the sediment, and its subsequent degradation, lead to intensified dissolution (Emerson and Bender, 1981), which is the main reason for LDX failure in most eastern Atlantic Ocean sediments in modern as well as in LGM times (Gerhardt and Henrich, in press and this study). The LDX appears to provide useful information for the reconstruction of glacial/interglacial intermediate water variability. As already suggested by $\delta^{13}C$ and Cd/Ca data (Oppo and Horowitz, 2000), GNAIW occupied the glacial intermediate depth level of the western South Atlantic, but less is known about the distribution of AAIW and UCDW. In order to distinguish between differing scenarios for the glacial water mass distribution, more LDX data are required from the Argentine Basin. Perhaps a multi-proxy approach would help to improve our knowledge about glacial deep and intermediate water geometry.

5. Conclusions

Our results show that the *Limacina inflata* dissolution record (LDX) provides a very useful tool, with which to estimate the extent of aragonite dissolution that the sediment has undergone. Direct comparison of glacial-interglacial LDX values reveals significant changes in aragonite preservation and hence water mass distribution in the western South Atlantic since the LGM. Intermediate depth aragonite preservation was significantly better during the LGM than today, indicating that GNAIW extended at least as far south as 20°S in the western South Atlantic. An upper aragonite lysocline, as is found today at ≈750 m in the western South Atlantic (Gerhardt and Henrich, in press), was thus not developed during the LGM. The findings are in apparent agreement with $\delta^{13}C$ and Cd/Ca data, which suggest the presence of GNAIW at 28°S at intermediate water depths (Oppo and Horowitz, 2000). Less is known about the glacial distribution of AAIW and UCDW. They may have been reduced, completely eliminated, or may have changed their positions with or without mixing with SCW. South Atlantic $\delta^{13}C$ data suggest that a high $\delta^{13}C$ source such as modern AAIW was absent during the LGM and that the water above and below a central core of GNAIW at ≈1500 m may have consisted of as much as two-thirds CDW (Oppo and Horowitz, 2000). Preservation variations also indicate an upward expansion of the area upon which aragonite dissolution occurred during the LGM. The deep aragonite lysocline was located about 500 m shallower than today in the tropical Atlantic Ocean (i.e. at ≈2000 m water depth), rising slightly to the south parallel with the GNAIW/SCW-boundary, which itself is considered to mark the ACD of that time. No firm conclusion can be drawn about the distribution of AAIW and UCDW during the LGM. Perhaps, the answer to this question lies in the analysis of sediment material from the Argentine Continental Margin.

Acknowledgements

We thank the members of the research project SFB 261 ("The South Atlantic in the Late Quaternary: Reconstruction of Material Budget and Current Systems"), especially M. Frenz and H.W. Arz, for making most of the coarse fraction samples available for this study. We would also like to thank S. Rath and A. Volbers for discussions and comments on the manuscript and A. Vink for correcting the English. This research was funded by the Deutsche Forschungsgemeinschaft (Graduierten-Kolleg "Stoff-Flüsse in marinen Geosystemen"). This is SFB 261 contribution no. xxx.

All data presented in Appendix 1 are available electronically under http://www.pangaea.de/Projects/SFB261/SGerhardt_RHenrich_2000/

References

Arz, H.W., Pätzold, J., Wefer, G., 1999. The deglacial history of the western tropical Atlantic as inferred from high resolution stable isotope records off northeastern Brazil. Earth and Planetary Science Letters 167, 105-117.

Bard, E., 1988. Correction of accelerator mass spectrometry ^{14}C ages measured in planktonic foraminifera: paleoceanographic implications. Paleoceanography 3 (6), 635-645.

Bard, E., Arnold, M., Fairbanks, R.G., Hamelin, B., 1993. ^{230}Th-^{243}U and ^{14}C ages obtained by mass spectrometry on corals. Radiocarbon 35, 191-199.

Barnola, J.M., Raynaud, D., Korotkevitch, Y.S., Lorius, C., 1987. Vostok ice core: a 160,000-year record of atmospheric CO_2. Nature 329, 408-414.

Bé, A.W.H., Gilmer, R.W., 1977. A zoographic and taxonomic review of euthecosomatous pteropoda. In: Ramsay, A.T.S. (Ed.), Oceanic Micropalaeontology, volume 1. Academic Press, London, pp. 733-808.

Berger, W.H., 1968. Planktonic foraminifera selective solution and paleoclimatic interpretation. Deep-Sea Research 15, 31-43.

Berger, W.H., 1975. Deep-sea carbonates: dissolution profiles from foraminiferal preservation. In: Sliter, W.H., Bé, A.W.H., Berger, W.H. (Eds.), Dissolution of Deep-Sea Carbonate, Cushman Foundation, Special Publication 13, 82-86.

Berger, W.H., 1978. Deep-sea carbonate: pteropod distribution and the Aragonite Compensation Depth. Deep-Sea Research I 25, 447-452.

Bickert, T., 1992. Rekonstruktion der spätquartären Bodenwasserzirkulation im östlichen Südatlantik über stabile Isotope benthischer Foraminiferen. Berichte Fachbereich Geowissenschaften, Universität Bremen 27, 1-205.

Bickert, T., Wefer, G., 1996. Late Quaternary deep water circulation in the South Atlantic: Reconstruction from carbonate dissolution and benthic stable isotopes. In: Wefer, G., Berger, W.H., Siedler, G., Webb, D. (Eds.), The South Atlantic: Present and Past Circulation. Springer-Verlag, Berlin, Heidelberg, pp. 599-620.

Bleil, U., cruise participants, 1994. Report and preliminary results of METEOR-Cruise M23/2, Rio de Janeiro-Récife, 27.2.-19.3.1993. Berichte Fachbereich Geowissenschaften, Universität Bremen 43, pp. 1-133.

Boyle, E.A., 1988. Cadmium: chemical tracer of deepwater paleoceanography. Paleoceanography 3, 471-490.

Boyle, E.A., 1992. Cadmium and $\delta^{13}C$ paleochemical ocean distributions during the stage 2 glacial maximum. Annual Review of Earth and Planetary Sciences 20, 245-287.

Boyle, E.A., 1994. A comparison of carbon isotopes and cadmium in the modern and glacial maximum ocean: can we account for the discrepancies? In: Zahn, R., Pedersen, T.F., Kaminski, M.A., Labeyrie, L. (Eds.), Carbon Cycling in the Glacial Ocean: Constraints on the Ocean's Role in Global Change, NATO ASI Serie C 117, pp. 105-144.

Boyle, E.A., Keigwin, L.D., 1982. Deep circulation of the North Atlantic over the last 200,000 years: geochemical evidence. Science 218, 784-787.

Boyle, E.A., Keigwin, L.D., 1987. North Atlantic thermohaline circulation during the past 20,000 years linked to high-latitude surface temperature. Nature 330, 35-40.

Broecker, W.S., Clark, E., McCorkle, D.C., Peng, T.-H., Hajdas, I., Bonani, G., 1999. Evidence for a reduction in the carbonate ion content of the deep sea during the course of the Holocene. Paleoceanography 14 (6), 744-752.

Catubig, N.R., Archer, D.E., Francois, R., deMenocal, P.; Howard, W., Yu, E.-F., 1998. Global deep-sea burial rate of calcium carbonate during the last glacial maximum. Paleoceanography 13 (3), 298-310.

Curry, W.B., 1996. Late Quaternary deep circulation in the western equatorial Atlantic. In: Wefer, G., Berger, W.H., Siedler, G., Webb, D. (Eds.), The South Atlantic: Present and Past Circulation. Springer-Verlag, Berlin, Heidelberg, pp. 577-598.

Curry, W.B., Duplessy, J.C., Labeyrie, L.D., Shackleton, N.J., 1988. Changes in the distribution of $\delta^{13}C$ of deep water $\sum CO_2$ between the last glaciation and the Holocene. Paleoceanography 5, 487-506.

Curry, W.B., Lohmann, G.P., 1982. Carbon isotopic changes in benthic foraminifera from the western South Atlantic: reconstruction of glacial abyssal circulation patterns. Quaternary Research 18, 218-235.

Curry, W.B., Lohmann, G.P., 1983. Reduced advection into Atlantic Ocean deep eastern basins during last glaciation maximum. Nature 306, 577-580.

deMenocal, P.B., Oppo, D.W., Fairbanks, R.G., Prell, W.L., 1992. Pleistocene $\delta^{13}C$ variability of North Atlantic intermediate water. Paleoceanography 7 (2), 229-250.

Devey, C.W., cruise participants, 1993. Cruise report SO-84: The St Helena hotspot, Las Palmas-Cape Town, 2.1.-20.2.1993. Reports, Geologisch-Paläontologisches Institut der Universität Kiel 64, pp. 1-103.

Diester-Haass, 1977. Radiolarian/planktonic foraminiferal ratios in a coastal upwelling region. Journal of Foraminiferal Research 7 (1), 26-33.

Droxler, A.W., Morse, J.W., Glaser, K.S., Haddad, G.A., Baker, P.A., 1991. Surface sediment carbonate mineralgoy and water column chemistry: Nicaragua Rise versus the Bahamas. Marine Geology 100, 277-289.

Duplessy, J.C., Shackleton, N.J., Fairbanks, R.G., Labeyrie, L., Oppo, D., Kallel, N., 1988. Deepwater source variations during the last climatic cycle and their impact on the global deepwater circulation. Paleoceanography 3 (3), 343-360.

Emerson, S., Bender, M., 1981. Carbon fluxes at the sediment-water interface of the deep-sea: calcium carbonate preservation. Journal of Marine Research 39, 139-162.

Fairbanks, R.G., 1989. A 17,000 year glacio-eustatic sea level record: influence of glacial melting rates on the Younger Dryas and deep-ocean circulation. Nature 342, 637-642.

Fischer, G., cruise participants, 1996. Report and preliminary results of METEOR-Cruise M34/4, Récife-Bridgetown, 19.3.-15.4.1996. Berichte Fachbereich Geowissenschaften, Universität Bremen 80, pp. 1-105.

Gerhardt, S., Groth, H., Rühlemann, C., Henrich, R., 2000. Aragonite preservation in late Quaternary sediment cores on the Brazilian Continental Slope: implications for intermediate water circulation. International Journal of Earth Sciences 88 (4), 607-618.

Gerhardt, S., Henrich, R., 2001. Shell preservation of *Limacina inflata* (Pteropoda) in surface sediments from the Central and South Atlantic Ocean: a new proxy to determine the aragonite saturation state of water masses. Deep-Sea Research I, in press.

Haddad, G.A., Droxler, A.W., 1996. Metastable $CaCO_3$ dissolution at intermediate water depths of the Caribbean and western North Atlantic: implications for intermediate water circulation during the past 200,000 years. Paleoceanography 11 (6), 701-716.

Hales, B., Emerson, S., 1996. Calcite dissolution in sedimetns of the Ontong-Java Plateau: In situ measurements of pore water O_2 and pH. Global Biogeochemical Cycles 10 (3), 527-541.

Hales, B., Emerson, S., 1997. Calcite dissolution in sediments of the Ceara Rise: In situ measurements of porewater O_2, pH, and $CO_{2(aq)}$. Geochimica et Cosmochimica Acta 61 (3), 501-514.

Howard, W.R., Prell, W.L., 1994. Late Quaternary $CaCO_3$ production and preservation in the Southern Ocean: implications for oceanic and atmospheric carbon cycling. Paleoceanography 9 (3), 453-482.

Hughen, K.A., Overpeck, J.T., Lehman, S.J., Kashgarian, M., Southon, J., Peterson, L.C., Alley, R., Sigman, D M., 1998. Deglacial changes in ocean circulation from an extend radiocarbon calibration. Nature 391, 65-68.

Indermühle, A., Stocker, T.F., Joos, F., Fischer, H., Smith, H.J., Wahlen, M., Deck, B., Mastroianni, D., Tschumi, J., Blunier, T., Meyer, R., Stauffer, B., 1999. Holocene carbon cycle based on a high-resolution CO_2 ice record from Taylor Dome, Antarctica. Nature 398, 121-126.

Kaese, R.H., Zenk, W., 1987. Reconstructed Mediterranean salt lens trajectories. Journal of Physical Oceanography 17, 158-163.

Lynch-Stieglitz, J., Fairbanks, R.G., Charles, C.D., 1994. Glacial-interglacial history of Antarctic Intermediate Water: relative strengths of Antarctic versus Indian Ocean sources. Paleoceanography 9, 1-29.

Lynch-Stieglitz, J., Stocker, T.F., Broecker, W.S., Broecker, R.G., 1995. The influence of air-sea exchange on the isotopic composition of oceanic carbon: observation and modeling. Global Biogeochemical Cycles 9, 653-665.

Martin, P.A., Lea, D.W., 1998. Comparison of water mass changes in the deep tropical Atlantic derived from Cd/Ca and carbon isotope records: implications for changing Ba composition of deep Atlantic water masses. Paleoceanography 13 (6), 572-585.

Millero, F.J., 1996. Chemical oceanography. CRC Press, Boca Raton, pp. 1-469.

Milliman, J.D., 1974. Marine carbonates. Springer-Verlag, New York, pp. 1-375.

Morse, J.W., Mucci, A., Millero, F.J., 1980. The solubility of calcite and aragonite in seawater at various salinities, temperatures and 1 atmosphere total pressure. Geochimica et Cosmochimica Acta 44, 85-94.

Niebler, H.-S., Mulitza, S., Donner, B., Arz, H., Pätzold, J., Wefer, G., 2000. Sea-Surface-Temperatures in the Equatorial and South Atlantic Ocean during the Last Glacial Maximum (23-19 ka). Submitted to Paleoceanography.

Oppo, D.W., Fairbanks, R.G., 1987. Variability in the deep and intermediate water circulation of the Atlantic Ocean during the past 25,000 years: Northern Hemisphere modulation of the Southern Ocean. Earth and Planetary Science Letters 86, 1-15.

Oppo, D.W., Fairbanks, R.G., 1990. Atlantic Ocean thermohaline circulation of the last 150,000 years: relationship of climate and atmospheric CO_2 Paleoceanography 5, 227-288.

Oppo, D.W., Horowitz, M., 2000. Glacial deep water geometry: South Atlantic benthic foraminiferal Cd/Ca and $\delta^{13}C$ evidence. Paleoceanography 15 (2), 147-160.

Pätzold, J., cruise participants, 1993. Bericht und erste Ergebnisse über die METEOR-Fahrt M15/2, Rio de Janeiro-Vitória, 18.1.-7.2.1991. Berichte Fachbereich Geowissenschaften, Universität Bremen 17, pp. 1-46.

Pätzold, J., cruise participants, 1996. Report and preliminary results of VICTOR HENSEN cruise JOPS II, Leg 6, Fortaleza-Récife, 10.3.-26.3.1995 and Leg 8, Vitoria-Vitoria, 10.4.-23.4.1995. Berichte Fachbereich Geowissenschaften, Universität Bremen 76, pp. 1-87.

Peterson, L.C., Prell, W.L., 1985. Carbonate dissolution in recent sediments of the eastern equatorial Indian Ocean: preservation patterns and carbonate loss above the lysocline. Marine Geology 64, 259-290.

Raymo, M.E., Oppo, D.W., Curry, W., 1997. The mid-Pleistocene climate transition: a deep sea carbon isotopic perspective. Paleoceanography 12 (4), 546-559.

Raymo, M.E., Ruddiman, W.F., Shackleton, N.J, Oppo, D.W., 1990. Evolution of Atlantic-Pacific $\delta^{13}C$ gradients over the last 2.5 m.y. Earth and Planetary Science Letters 97, 353-368.

Reid, J.L., 1989. On the total geostrophic circulation of the South Atlantic Ocean: flow patterns, tracers, and transports. Program of Oceanography 23 (3), 149-244.

Reid, J.L. 1996. On the circulation of the South Atlantic Ocean. In: Wefer, G., Berger, W.H., Siedler, G., Webb, D. (Eds.), The South Atlantic: Present and Past Circulation, Springer-Verlag, Berlin, Heidelberg, pp. 13-44.

Rosenthal, Y., Boyle, A., Labeyrie, L., 1997. Last glacial maximum paleochemistry and deepwater circulation in the Southern Ocean: evidence from foraminiferal cadmium. Paleoceanography 12 (6), 787-796.

Rosenthal, Y., Lam, P., Boyle, E.A., Thomson, J., 1995. Authegenic cadmium enrichments in suboxic sediments: precipitation and postdepositional mobility. Earth and Planetary Science Letters 132, 99-111.

Sarnthein, M., Winn, K., Jung, S.J.A., Duplessy, J.-C., Labeyrie, L., Erlenkeuser, H., Ganssen, G., 1994. Changes in east Atlantic deepwater circulation over the last 30,000 years: eight time slice reconstructions. Paleoceanography 9 (2), 209-267.

Schulz, H.D., cruise participants, 1991. Bericht und erste Ergebnisse über die METEOR-Fahrt M16/2, Récife-Belem, 28.4.-20.5.1991. Berichte Fachbereich Geowissenschaften, Universität Bremen 19, pp. 1-149.

Schulz, H.D., cruise participants, 1992. Bericht und erste Ergebnisse der METEOR-Fahrt M20/2, Abidjan-Dakar, 27.12.1991-3.2.1992. Berichte Fachbereich Geowissenschaften, Universität Bremen 25, pp. 1-173.

Schulz, H.D., cruise participants, 1996. Report and preliminary results of METEOR-Cruise M34/2, Walvis Bay-Walvis Bay, 29.1.-18.2.1996. Berichte Fachbereich Geowissenschaften, Universität Bremen 78, pp. 1-133.

Siedler, G., Müller, T.J., Onken, R., Arhan, M., Mercier, H., King, B.A., Saunders, P.M., 1996. The Zonal WOCE Sections in the South Atlantic. In: Wefer, G., Berger, W.H., Siedler, G., Webb, D. (Eds.), The South Atlantic: Present and Past Circulation, Springer-Verlag, Berlin, Heidelberg, pp. 83-104.

Spieß, V., cruise participants, 1994. Report and preliminary results of METEOR-Cruise M23/1, Kapstadt-Rio de Janeiro, 4.-25.2.1993. Berichte Fachbereich Geowissenschaften, Universität Bremen 42, pp. 1-139.

Talley, L.D., 1996. Antarctic Intermediate Water in the South Atlantic. In: Wefer, G., Berger, W.H., Siedler, G., Webb, D. (Eds.), The South Atlantic: Present and Past Circulation, Springer-Verlag, Berlin, Heidelberg, pp. 219-238.

Venz, K.A., Hodell, D.A., Stanton, C., Warnke, D.A., 1999. A 1.0 Myr record of Glacial North Atlantic Intermediate Water variability from ODP site 982 in the northeast Atlantic. Paleoceanography 14 (1), 42-52.

Volbers, A.N.A., Henrich, R., 2000. Late Quaternary variations in calcium carbonate preservation of deep-sea sediments in the northern Cape Basin: results from a multiproxy approach. Submitted to Marine Geology.

Wefer, G., cruise participants, 1988. Bericht über die METEOR-Fahrt M6/6, Libreville-Las Palmas, 18.2.-23.3.1988. Berichte Fachbereich Geowissenschaften, Universität Bremen 3, pp. 1-97.

Wefer, G., cruise participants, 1989. Bericht über die METEOR-Fahrt M9/4, Dakar-Santa Cruz, 19.2.-16.3.1989. Berichte Fachbereich Geowissenschaften, Universität Bremen 7, pp. 1-103.

Wefer, G., cruise participants, 1990. Bericht über die METEOR-Fahrt M12/1, Kapstadt-Funchal, 13.3.-14.4.1990. Berichte Fachbereich Geowissenschaften, Universität Bremen 11, pp. 1-66.

Wefer, G., cruise participants, 1991. Bericht und erste Ergebnisse über die METEOR-Fahrt M16/1, Point Noire-Récife, 27.3.-25.4.1991. Berichte Fachbereich Geowissenschaften, Universität Bremen 18, pp. 1-120.

Wefer, G., cruise participants, 1994. Report and preliminary results of METEOR-Cruise M23/3, Récife-Las Palmas, 21.3.-12.4.1993. Berichte Fachbereich Geowissenschaften, Universität Bremen 44, pp. 1-71.

3. Aragonite preservation in late Quaternary sediment cores on the Brazilian Continental Slope: implications for intermediate water circulation

Sabine Gerhardt, Harald Groth, Carsten Rühlemann, and Rüdiger Henrich

Dept. of Geosciences, University of Bremen, P.O. Box 33 04 40, D-28334 Bremen, Germany

Abstract

We present late Quaternary records of aragonite preservation determined for sediment cores recovered on the Brazilian Continental Slope (1790-2585 m water depth) where North Atlantic Deep Water (NADW) dominates at present. We have used various indirect dissolution proxies (carbonate content, aragonite/calcite contents, and sand percentages) as well as gastropodal abundances and fragmentation of *Limacina inflata* to determine the state of aragonite preservation. In addition, microscopic investigations of the dissolution susceptibility of three *Limacina* species yielded the *Limacina* Dissolution Index which correlates well with most of the other proxies. Excellent preservation of aragonite was found in the Holocene section, whereas aragonite dissolution gradually increases downcore. This general pattern is attributed to an overall increase in aragonite corrosiveness of pore waters. Overprinted on this early diagenetic trend are high-frequency fluctuations of aragonite preservation, which may be related to climatically induced variations of intermediate water masses.

Keywords: Pteropods, Aragonite preservation, South Atlantic, Brazilian Continental Slope, North Atlantic Deep Water, Antarctic Intermediate Water

1. Introduction

A major purpose of palaeoceanography is to learn as much as possible about water mass properties, their extent and circulation modes in the present, and about shifts in the past. Understanding changes in temporal and spatial carbonate preservation is of great importance for the reconstruction of water masses. During the last glacial period, Antarctic Bottom Water (AABW) production may have been enhanced (Duplessy et al. 1996), whereas the North

Atlantic Deep Water (NADW) flow was reduced (Sarnthein et al. 1994). Thus, the NADW-AABW boundary in the South Atlantic moved upwards through the water column, as recorded in the $^{13}C/^{12}C$ ratio in shells of benthic foraminifera and in lower sand fraction and carbonate values (Berger and Wefer 1996). Moreover, it has been demonstrated that during glacial periods when the production of Lower North Atlantic Deep Water (LNADW) was considerably reduced, the intermediate water circulation was enhanced and Upper North Atlantic Deep Water (UNADW) was found to be much more extensive (Boyle and Keigwin 1987; Curry et al. 1988; Duplessy et al. 1988; Oppo et al. 1995; Venz et al. 1999).

Past work on carbonate dissolution has dealt almost exclusively with calcite dissolution or the reconstruction of deep water masses (e.g. Berger 1973; Crowley 1983a, 1983b; Bickert and Wefer 1996; Bickert et al. 1997). Much less is known about aragonite preservation and its imprint on glacial/interglacial variations of intermediate water masses. Since aragonite is more soluble than calcite, it dissolves at much shallower depths. Hence, the Aragonite Compensation Depth (ACD) generally lies above the Calcite Compensation Depth (CCD). Aragonite dissolution was firstly used to define the ACD in the oceans by fixing the water depth at which pteropod shells no longer occur in seafloor sediments (e.g. Chen 1964; Berger 1977, 1978; Berner 1977). In the past, aragonite production and dissolution as part of the global carbon cycle has been neglected because of the relative lack of aragonite in deep-sea sediments due to dissolution. This has led to a serious underestimation of the amount of $CaCO_3$ in the oceans. Berner and Honjo (1981) calculated the present worldwide aragonite flux to be at least 12% of the total $CaCO_3$ flux. However, subsequent studies of continental slope and shelf environments have moved the focus from the deep sea to shallower water depths (e.g. Almogi-Labin 1982; Droxler et al. 1983, 1988, 1990; Almogi-Labin et al. 1986, 1991, 1998; Haddad and Droxler 1996). Droxler et al. (1983) observed late Quaternary aragonite cycles in sediments near the Bahamas Bank that result from variations in metastable $CaCO_3$ preservation with high interglacial aragonite content (good preservation) and low glacial aragonite content (poor preservation). These findings correspond to calcite preservation cycles in deep Atlantic Ocean sediments (e.g. Gardner 1975; Crowley 1983a, 1983b; Howard and Prell 1994). In order to reveal more detailed information about carbonate dissolution in sediments, preservation variations recorded in the shell structure of planktonic foraminifera, pteropods and associated fossils have been studied by several authors (e.g. Bé et al. 1975; Hecht et al. 1975; Almogi-Labin et al. 1986; Henrich and Wefer 1986; Henrich 1989).

In this study we apply a multiparameter approach to differentiate the state of aragonite preservation in four sediment cores from three locations on the Brazilian Continental Slope (Fig. 1; Table 1).

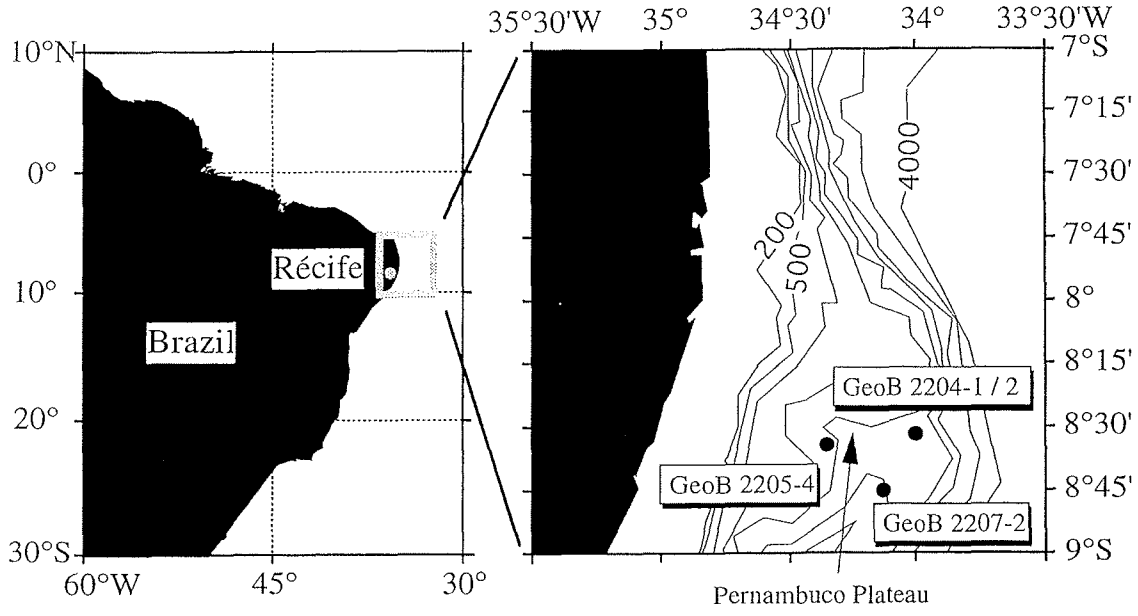

Fig. 1: Location map for the sediment cores used in this study. The cores were recovered from the Pernambuco Plateau, on the continental slope offshore Récife between 1790 to 2585 m water depth.

Table 1: Core locations.

Core GeoB	Latitude/ longitude	Water depth (m)	Core length (cm)
2205-4	08°34'S/ 34°21'W	1790	45
2204-1	08°32'S/	2080	43
2204-2	34°01'W	2072	897
2207-2	08°44'S/ 34°08'W	2585	34

1.1 Oceanography

As shown in Fig. 2, the studied area is covered by the warm North Brazil Current at the surface. Below the surface water mass, aragonite-corrosive Antarctic Intermediate Water (AAIW) and the upper arm of Circumpolar Water (UCPW) flow northward. UCPW has similar properties to the AAIW and loses its identity on its way north near 10°S. Beneath these, the broad core of southward flowing North Atlantic Deep Water (NADW), in which the investigated cores are positioned, is found. The lowermost water masses are the northward flowing Lower Circumpolar Water (LCPW) and the strongly carbonate-corrosive, northward flowing Antarctic Bottom Water (AABW; after Reid 1989, 1994, 1996).This complex water mass configuration is attended by a correspondingly complex pattern of carbonate saturation.

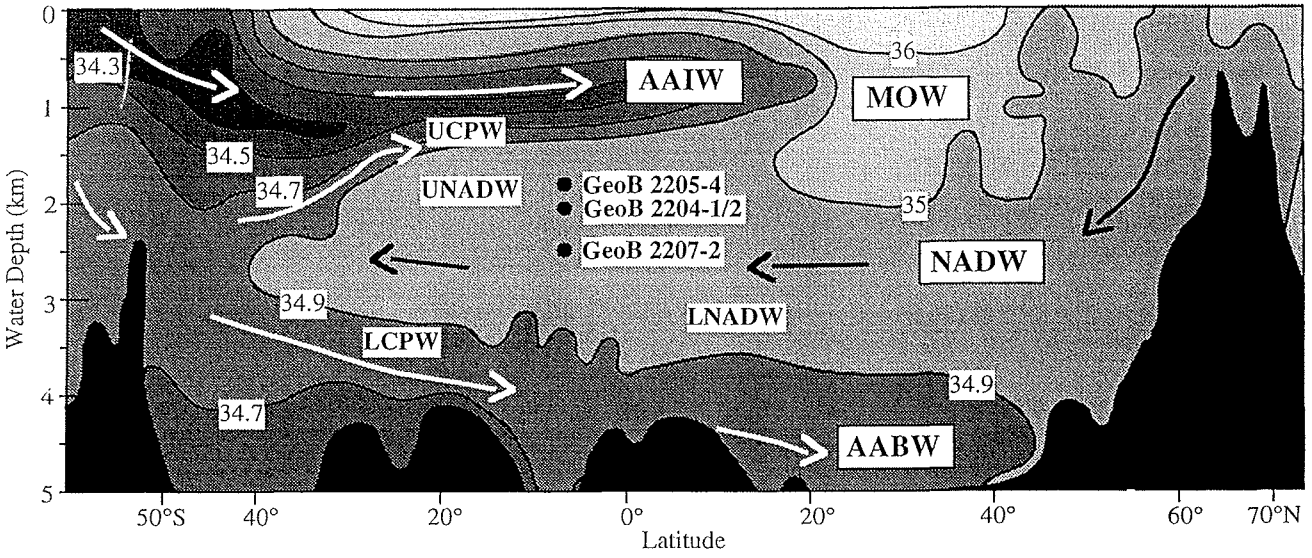

Fig. 2: Schematic north-south cross-section of modern salinity distribution (in ‰) in the western Atlantic (GEOSECS data, modified after Bainbridge 1981, and Haddad and Droxler 1996). White arrows mark the northward-flowing water masses Antarctic Bottom Water (AABW), Lower Circumpolar Water (LCPW), Upper Circumpolar Water (UCPW) and Antarctic Intermediate Water (AAIW). Black arrows indicate the southward-flowing North Atlantic Deep Water (NADW) with its differentiation in Lower North Atlantic Deep Water (LNADW) and Upper North Atlantic Deep Water (UNADW). Mediterranean Overflow Water (MOW) enters the Caribbean and probably has no importance for the studied region.

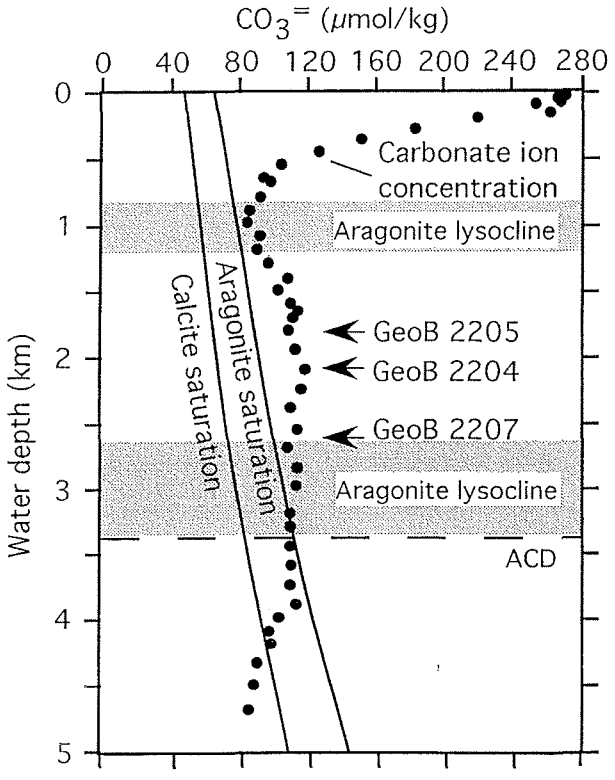

Fig. 3: Plot of carbonate ion concentration versus water depth in the western South Atlantic Ocean measured at GEOSECS-Station 39 (7°57'N, 43°51'W; Bainbridge 1981; modified after Broecker and Peng 1982). Also shown are the aragonite and calcite saturation horizons, aragonite lysoclines, Aragonite Compensation Depth (ACD), and core locations.

Figure 3 illustrates that two aragonite lysoclines are developed in the studied region. The upper lysocline can be recognized in approximately 800-1200 m water depth which corresponds well to aragonite-corrosive AAIW presence, whereas the lower lysocline is found beneath approximately 2600 m water depth which is due to increasing pressure and decreasing temperature with water depth (modified after Bainbridge 1981 and Broecker and Peng 1982).

2. Materials and methods

One gravity core (GeoB 2204-2) and three multicorer cores (GeoB 2204-1, GeoB 2205-4, GeoB 2207-2) from the Brazilian Continental Slope were selected for this study (see Fig. 1; see Table 1 for core locations and water depths). They were taken during Meteor cruise M23/3 (Wefer et al. 1994). The investigated cores were recovered from the gently sloping Pernambuco Plateau on the continental slope offshore Récife from 1790 to 2585 m water depths. By visual core description no disturbances and intercalation of turbidites or debris flows were detected.

2.1 Stratigraphy

In core GeoB 2204-2, oxygen isotope measurements were made for samples taken at intervals of 5 cm. Supplementary samples were taken from GeoB 2204-1. The data have been published by Rühlemann (1996) and slightly differing by Dürkoop et al. (1997); however, we have used the data of Rühlemann (1996). No oxygen isotope data exists for GeoB 2205-4 and GeoB 2207-2; thus, all records are expressed vs core depth.

2.2 Determination of bulk carbonate, calcite, aragonite, and sand contents

For determining the carbonate content, GeoB 2204-2 was sampled in 5-cm intervals over a depth range representing the last 230 ka. All three multicorer cores were sampled in 3-cm intervals. The carbonate content (weight percent) of each sample was calculated based on total carbon (TC) and total organic carbon (TOC) contents measured using a LECO-CS 300 element analyzer. The calculation was made according to the equation $CaCO_3\%=8.33*(TC\%-TOC\%)$. To achieve high-resolution data in GeoB 2204-2, the data was combined with previous measurements (Rühlemann 1996).

X-ray diffraction analysis (XRD) was used to determine calcite and aragonite percentages. In GeoB 2204-2 samples were taken at 5-cm intervals in the upper 150 cm and thereafter at 10-cm intervals down to 350 cm. GeoB 2204-1 and GeoB 2207-2 were sampled and measured in 3-cm intervals. The sediment samples were ground to obtain a grain size <63 µm. The diffractometer settings used are shown in Table 2. Quantitative analysis was made by determining aragonite peak heights and calcite peak areas for each sample and subsequent comparisons with the respective calibration curves (after Klug and Alexander 1954; Cullity 1956; Milliman 1974).

Table 2: Diffractometer settings.

Equipment	X-ray diffractometer Siemens D-500
Technique	Powder diffraction
X-ray tube	Cu, 40 kV, 30 mA
Radiation	Cu kα 1= 1.540562 Å kα 2= 1.544390 Å
Measuring range	2θ = 20-50°
Measuring steps	2θ = 0.02°
Measuring time per step	4.8 s

To obtain more information about carbonate preservation, the sand content (weight percent of >63-µm fraction) was determined (in GeoB 2204-2 every 5 cm and in all three multicorer cores every 3 cm). The sand record of GeoB 2204-2 was previously determined and published (Rühlemann 1996). As a first approximation, in previous studies high sand contents were considered to indicate good shell preservation, whereas low percentages were attributed to shell fragmentation due to increased dissolution (Johnson et al. 1977; Berger et al. 1982; Wu and Berger 1991).

2.3 Species determination

To determine gastropodal and foraminiferal abundances, particle counts were carried out by light microscope (in ≈10-cm intervals in GeoB 2204-2 for the past 140 ka and in 3-cm intervals in the multicorer cores). Each sample was carefully wet sieved to separate the fine fraction (<63 µm) and the coarse fraction (>63 µm). After freeze drying, the coarse fraction was sieved with a Sonic Sifter into subsamples and the 250- to 1000-µm fraction was subsequently divided with a microsplitter until an adequate number of particles remained for

counting (≈700-3400 particles in GeoB 2204-2 and ≈200-400 in the multicorer cores). Planktonic foraminifera and gastropods are the principal biogenic components in the coarse fraction. Each particle was counted as whole (intact), damaged (at least 50% of the shell existing) or as a fragment. The counted particle number was strongly dependent on the availability of whole and damaged gastropod shells. In most of the samples further subdivision of the >1000-µm fraction was not necessary, since only a few particles were found in this fraction (≈0-2000). Pteropods were identified on species level after Van Der Spoel (1967) and Bé and Gilmer (1977). Non-identifiable fragments of foraminiferas and gastropods are recorded together with rarely found tests of other organisms (e.g. benthic foraminifera, radiolarians, echinoids, brachiopods, other molluscs, bryozoens, ostracods) in the assemblage curves (box 1 of Fig. 5a-c, box 5 of Fig. 6, "others").

2.4 Aragonite dissolution proxies

We have chosen *L. inflata* for a fragmentation index since this species is very common. Moreover, though *L. inflata* breaks into many fragments it has one typical fragment which is always identifiable. The last whorl of *L. inflata* is swollen with an aperture tooth on the outer border, which is supported mostly by a strong rib (Van Der Spoel 1967). This swollen shell part is often the only remaining or the only identifiable part after the shell has broken up. However, determining the ratio of whole plus damaged shells to fragments of *L. inflata* yields a very reliable proxy for the state of aragonite preservation. In the following, the fragmentation index of *L. inflata* will be abbreviated by LFX (*Limacina* Fragmentation Index). This proxy is strongly dependent on sample preparation, since intense sieving results in artificial fragmentation. The proxy was used only when at least ten *L. inflata* particles (i.e. intact, damaged, or fragments) were available.

The Limacinidae, with the exception of *L. inflata,* possess a crossed-lamellar shell microstructure beneath a smooth surface layer, which underlies the periostracum. The innermost aragonite layer is prismatically structured (Bé and Gilmer 1977). In contrast, *L. inflata* has a central layer which has a helical structure (Richter 1976). The reader is referred to Rhoads and Lutz (1980) and Carter (1990) for more detailed information about general skeletal growth and biomineralization. Shell sizes and thicknesses vary within the Limacinidae and even within the species. *Limacina inflata* is sinistrally coiled in one level with shell diameters up to 1.5 mm, whereas *L. bulimoides* and *L. lesueuri* have shell heights up to 2 and 0.8 mm and shell widths up to 1.4 and 1.3 mm, respectively (Van Der Spoel 1972). Moreover, shell thicknesses vary within individual shells and with developmental

stage. Thus, variations of shell thicknesses and sizes of the Limacinidae picked in the surface sample of GeoB 2204-1 were measured under the SEM.

More reliable proxies are based on microscopic determinations of changes in the shell ultrastructure of various *Limacina* species, e.g. *L. inflata*, *L. bulimoides*, and *L. lesueuri*. A basic feature is the increasing roughening of pteropod shell surfaces with increasing dissolution (e.g. Byrne et al. 1984, Almogi-Labin et al. 1986; Acker and Byrne 1989; Haddad and Droxler 1996). Shells of the three species were picked and examined by light microscopy with a minimum of ten tests, but often 40 and more were available. In addition, we decided to use only adult shells for the LDX (≈900-1200 µm in size). The resultant dissolution index is the *Limacina* Dissolution Index (LDX) and comprises the arithmetical mean calculated by the observed preservation stages (box 4 of Fig. 5, box 8 of Fig. 6, box 4 of Fig. 7).

Six preservation stages were determined in three steps: Firstly, a general impression of shell transparency (transparent, milky, opaque); secondly, shell surface lustre (whether lustrous or lustreless); thirdly, any shell damage. It should be noted that only the central shell of *L. inflata* was examined. The previously mentioned swollen aperture tooth region was neglected in all steps, since its presence is strongly dependent on sample preparation. According to the progressive structural breakdown the following six preservation stages were distinguished (0=best preservation, 5=strongest dissolussion).

Stage 0: Transparent shells

Stage 0 indicates highest preservation. Only shells of living pteropods and originally preserved pteropod assemblages in the sediment show this mode of preservation.

Stage 1: Milky and cloudy shells, lustrous shell surface

Stage 1 is reached when either slight shell corrosion has taken place or according to Haddad and Droxler (1996) the organic membrane within the shell has become cloudy through oxidation.

Stage 2: Opaque-white shells, lustrous shell surface

In stage 2 pteropod shells are opaque and white, not just milky, which means they have truly experienced dissolution of the shell surface (Haddad and Droxler 1996).

Stage 3: Opaque-white shells, partly lustreless shell surface

In stage 3, extensive surface roughening has taken place. Consequently, the shell surface seems to be lustreless in those areas where the crossed-lamellar or helical aragonite layer is exposed.

Stage 4: Opaque-white shells, totally lustreless shell surface

Stage 4 is reached when the surface layer has been entirely removed by corrosion.

Stage 5: Opaque-white, totally lustreless and perforated shells

Stage 5 is characterized by additional shell damage of any kind, neglecting again the absence of the aperture tooth of *L. inflata*.

3. Results

Our study reveals three important results: (a) varying aragonite preservation during the past 430 ka; (b) a long-term diagenetic trend; and (c) differences in the susceptibility to dissolution of the three Limacinidae species.

Excellent aragonite preservation can only be found during the Holocene (e.g. box 4 of Fig. 5, box 8 of Fig. 6). Moreover, from oxygen isotope stages 2 to 1 a general increase in preservation is observed. Comparison of GeoB 2204-1 and GeoB 2207-2 (Fig. 4b,c) record this trend in all the carbonate proxies, i.e. an increase in the bulk carbonate content (box 1 of Fig. 4), as well as in the bulk aragonite content (box 2 of Fig. 4). Compared with this, a less well-defined increase in the bulk calcite content can be observed (box 2 of Fig. 4) which can be seen in particular in the aragonite/calcite ratio (box 3 of Fig. 4). In addition, the sand contents of all three multicorer sections display the same feature, i.e. an overall increase, although variations do occur (box 4 of Fig. 4). Figure 5 illustrates a different trend with respect to the assemblages proxies, the LFX, and the LDX. Although an increase in bulk aragonite and sand content can be observed, the abundances of whole and damaged gastropod (box 1 of Fig. 5) and Limacinidae shells (box 2 of Fig. 5) decrease during the past 10 ka. The fragmentation of *L. inflata* (box 3 of Fig. 5) decreases from isotope stages 2 to 1, but remains constantly low with the exception of a slight increase during the past ≈7 ka, which can be particularly observed in the uppermost multicorer section. Finally, the LDX records (box 4 of Fig. 5) are mostly consistent with the carbonate and aragonite records, which indicates that all carbonate proxies are influenced by aragonite dissolution.

Regarding the past 430 ka (Figs. 6, 7), aragonite preservation displays strong fluctuations which are not necessarily associated with glacial/interglacial variations, although increased aragonite dissolution is observed during most glacial periods (particularly during oxygen isotope stages 2, 4, 8, 10, and 12), even though worse preservation does occur during specific interglacial intervals as well (e.g. stages 3, 5, 7.1, and 11). This pattern is particularly clearly displayed in the LFX and LDX records (boxes 7 and 8 of Fig. 6, boxes 3 and 4 of Fig. 7).

Moreover, a few aragonite dissolution events are most noticeably reflected in several records, for instance during isotope stage 4 when the aragonite content (boxes 2 and 3 of Fig. 6), as well as the gastropodal and Limacinidae abundances (boxes 5 and 6 of Fig. 6) decrease, the fragmentation of *L. inflata* increases (box 7 of Fig. 6) and no preservation of adults of this species is found (box 8 of Fig. 6). Similar consistencies can be observed around Terminations I, II, and IV, additionally associated with low concentrations of bulk carbonate and sand (boxes 1 and 4 of Fig. 6, boxes 1 and 2 of Fig. 7).

In addition to the short-term variations in aragonite preservation during the past 430 ka, several parameters in the core GeoB 2204-2 display a long-term trend of worse aragonite preservation with increasing core depth (e.g. boxes 3, 7, and 8 of Fig. 6), which is interpreted as a diagenetic feature. However, this diagenetic overprinting has not extinguished the original signals, but it results in a general decrease of aragonite values (box 3 of Fig. 6), as well as an increase in fragmentation (box 7 of Fig. 6), and an increase in dissolution (box 8 of Fig. 6) with core depth.

Concerning dissolution features, *L. inflata*, *L. bulimoides*, and *L. lesueuri* distinctly show different degrees of susceptibility to dissolution. *Limacina inflata* shells are much more easily dissolved than those of *L. bulimoides* and *L. lesueuri*. The SEM examinations reveal average shell thicknesses (last whorl of adult shells) of 9.4 µm for *L. bulimoides* (average shell height 1205 µm), 8.7 µm for *L. lesueuri* (average shell size 1074 µm), and 11.2 µm for *L. inflata* (average shell size 1035 µm), suggesting that *L. inflata* possesses a smaller, but thicker shell than *L. bulimoides* and *L. lesueuri*.

4. Discussion

Principally, aragonite dissolution may begin to affect shells during settling through the water column, or later at the sediment-seawater interface and after burial. Dissolution can be caused by undersaturated water masses and by corrosive pore waters, established under various diagenetic regimes and stages of burial. In addition, the extent of dissolution is strongly dependent on many factors, e.g. on shell size and thickness, on shell sinking speed, on bacterial activity, on exposure time of particles at the sediment surface (and hence on sedimentation rates), on bottom current velocity, and on any sediment disturbances.

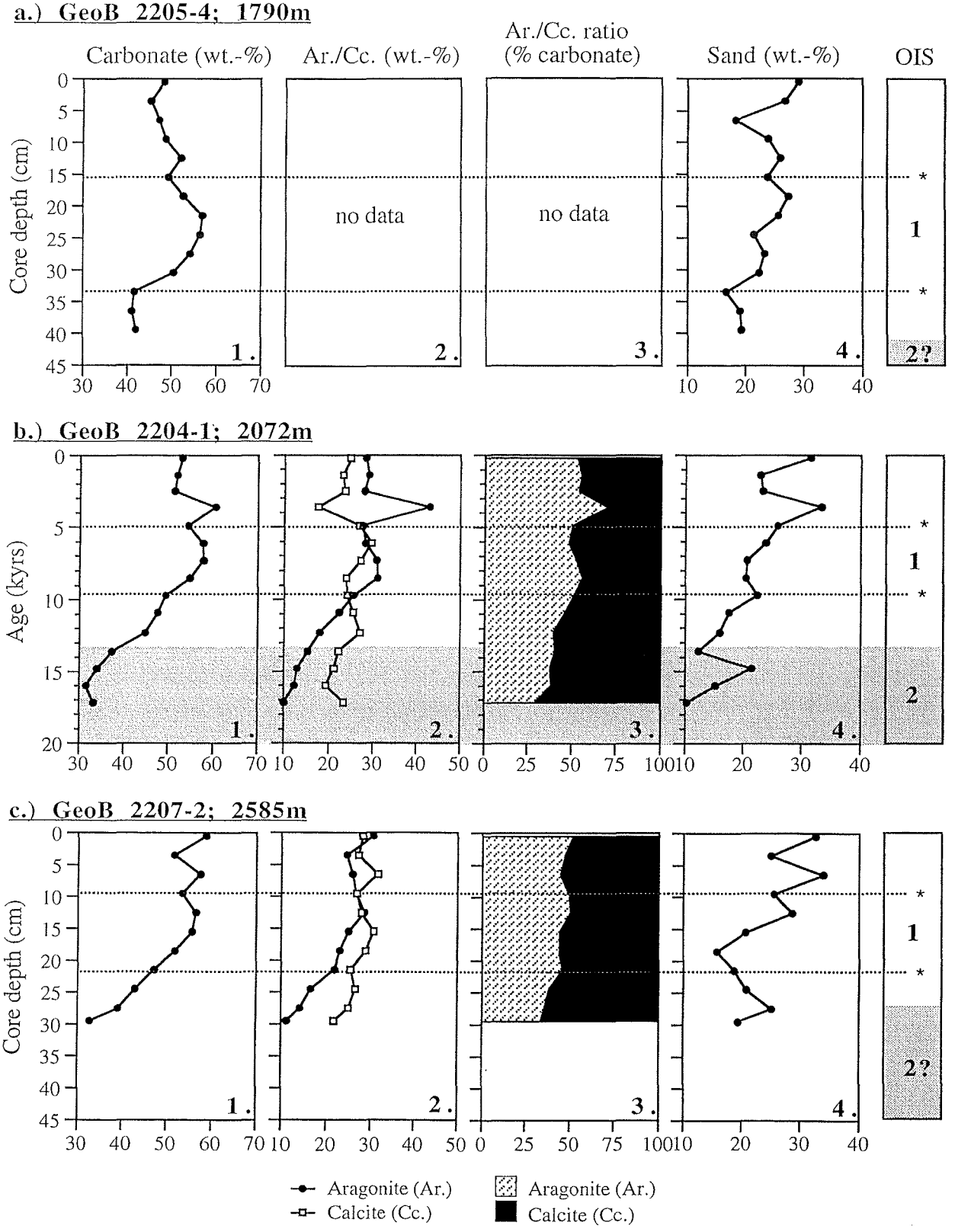

Fig. 4a-c: Aragonite preservation indices for the last ≈17 ka as recorded in the three multicorer cores; OIS = Oxygen Isotope Stages; asteristik indicates significant peaks (≈5 and 9-10 ka) that can be used for core correlation. Shaded areas mark glacial time intervals.

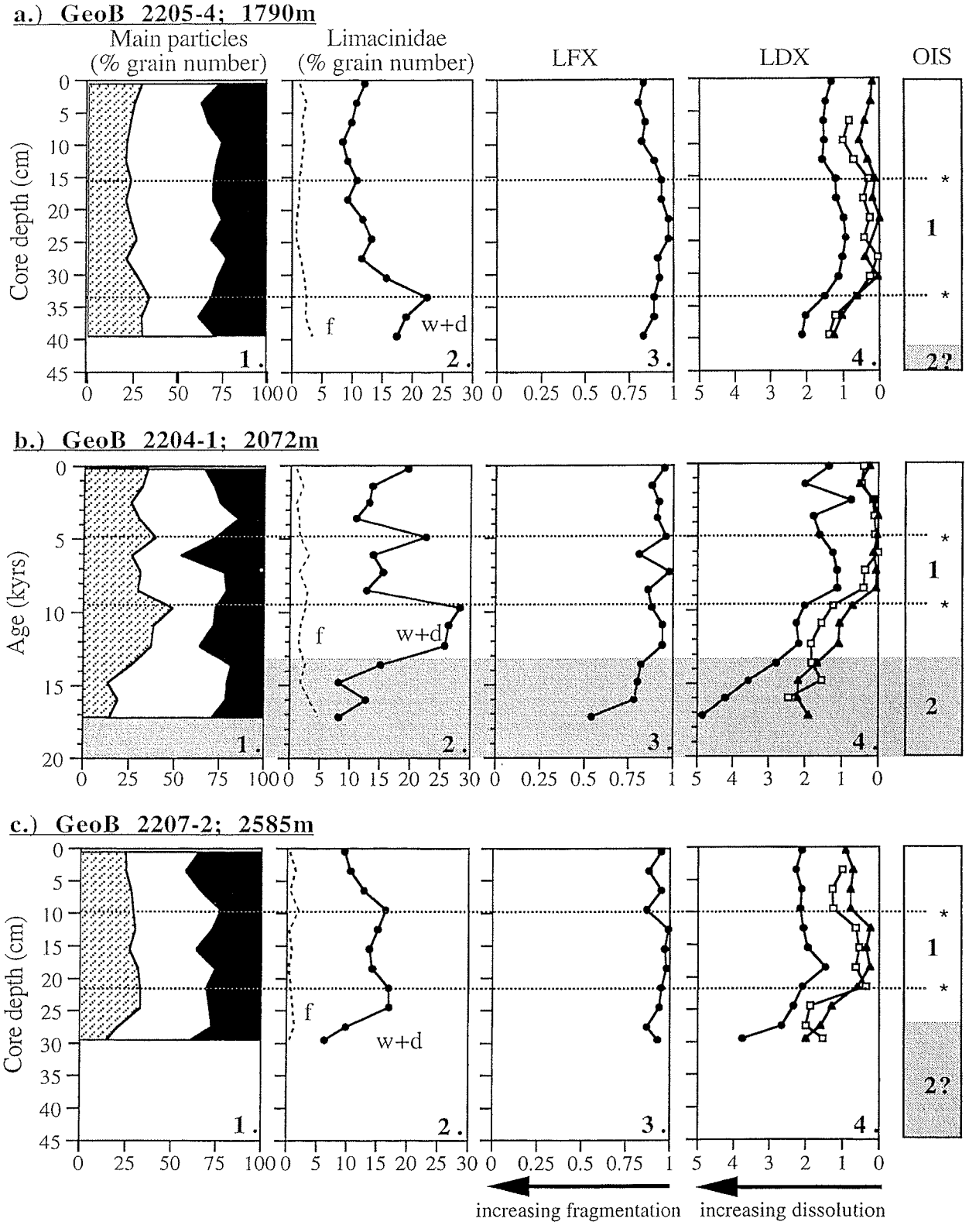
a.) GeoB 2205-4; 1790m
Main particles (% grain number)
Limacinidae (% grain number)
LFX
LDX
OIS
Core depth (cm)
f
w+d
1.
2.
3.
4.
1
2?
b.) GeoB 2204-1; 2072m
Age (kyrs)
1
2
c.) GeoB 2207-2; 2585m
Core depth (cm)
1
2?
increasing fragmentation
increasing dissolution
Gastropods (w+d)
Planktonic Foraminiferas (w+d)
Others (w+d+f)
f fragments
w+d whole+damaged
L. inflata
L. bulimoides
L. lesueuri

GeoB 2204-2; 2072m

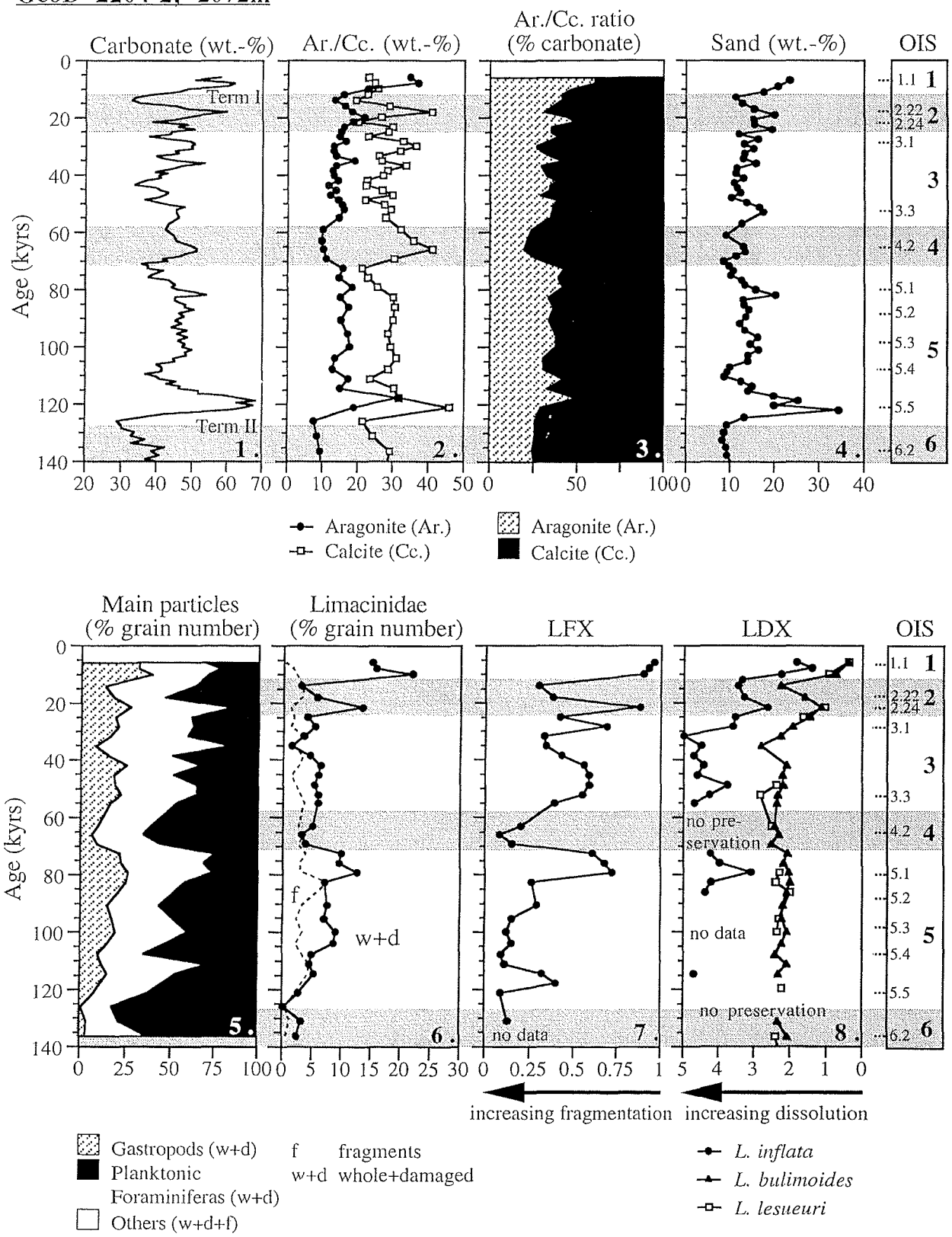

Fig. 5a-c: More multicorer results. 1 Main particles in the >250-µm fraction. The grains are whole (w) and damaged (d) planktonic foraminifera, and gastropods. Others consists mainly of gastropod fragments (f) and other organisms like benthic foraminifera. 2 Limacinidae in the >250-µm fraction. 3 Fragmentation Index of *L. inflata* (LFX) in the 250- to 1000-µm fraction (ratio of whole+damaged shells to fragments, at least ten particles). 4 Dissolution Index (LDX) of *L. inflata* (dots), *L. bulimoides* (triangles), *L. lesueuri* (squares). Shells are 900-1200 µm in size. Every dot represents the arithmetical mean of at least 40 shells for *L. inflata* (except the oldest sample in GeoB 2204-1) and at least ten shells for *L. bulimoides* and *L. lesueuri*; OIS = Oxygen Isotope Stages. Asteristik indicates significant peaks (≈5 and 9-10 ka) that can be used for core correlation. Shaded areas mark glacial time intervals.

Fig. 6: Aragonite preservation indices for the last 140 ka as recorded in the gravity core GeoB 2204-2 as a function of time. Carbonate data partly and sand data completely from Rühlemann (1996); OIS = Oxygen Isotope Stages. Shaded areas mark glacial time intervals.

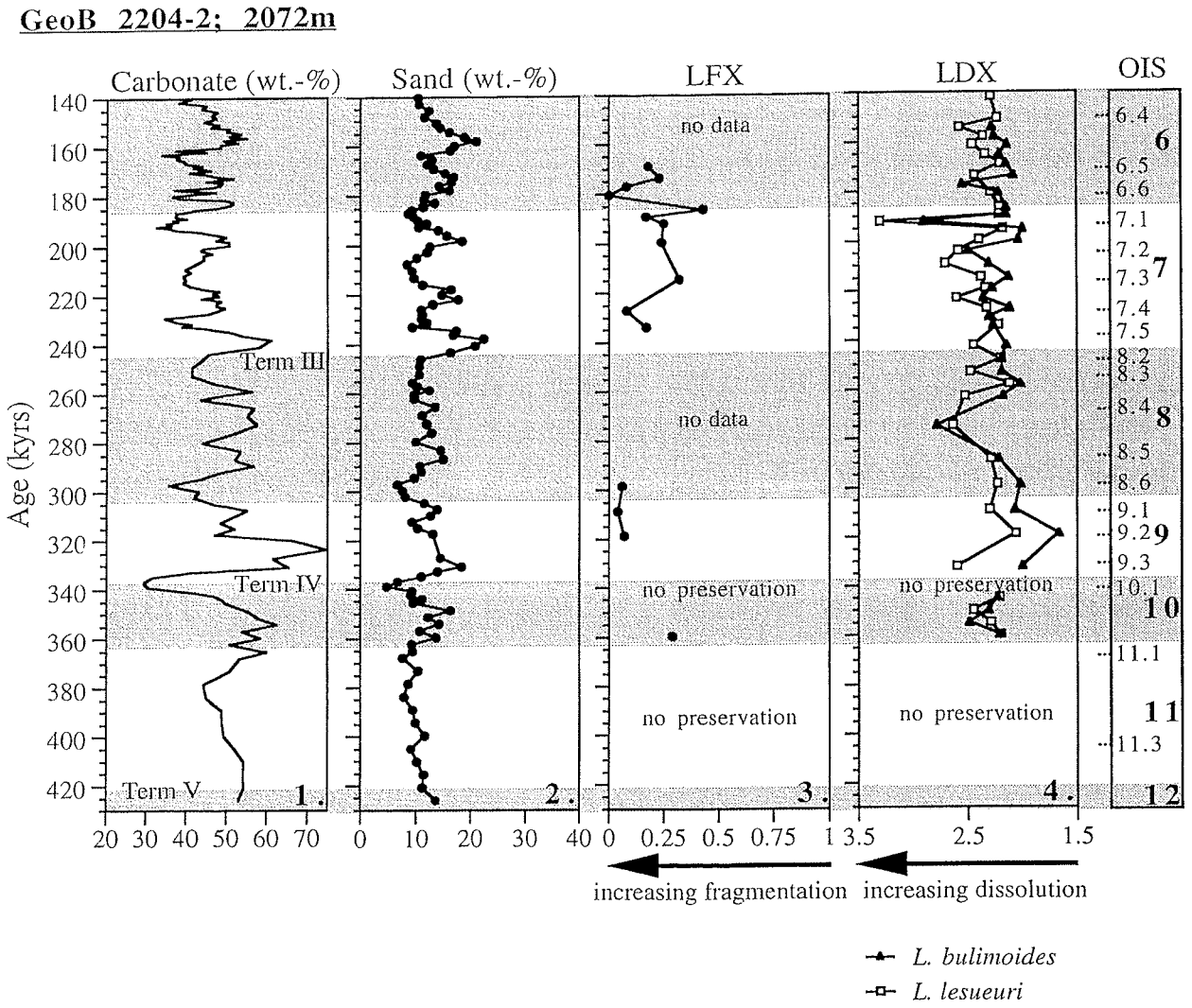

Fig. 7: As Fig. 6, results for the time span between 430-140 ka. Carbonate data partly and sand data completely from Rühlemann (1996); OIS = Oxygen Isotope Stages. Shaded areas mark glacial time intervals.

At first, we have to consider whether shells mainly dissolve during settling, or on the sea floor, or after burial. Settling velocities of *L. inflata* and *L. bulimoides* in the North Pacific were determined by Byrne et al. (1984) in the laboratory. According to this study, juveniles of *L. inflata* (≈300 µm in size) settle slowly with a velocity of 1 cm/s and adults of *L. bulimoides* (≈3 mm in height) settle rapidly with 2.5 cm/s. Considering that adults of *L. inflata* can possess much greater shell lengths up to 1.5 mm, we suppose that adults of *L. inflata*, *L. bulimoides* and *L. lesueuri* traverse 2000 m of the water column in approximately 1 day to reach the sea floor. We do not agree with the conclusion of Byrne et al. (1984) that dissolution occurs mainly during settling, since we have found many transparent and milky shells of *L. inflata* in South Atlantic surface sediments below 2300 m water depth (unpublished data). Adelseck and Berger (1975) studied net tow and box core samples from 3000 m depth in the eastern tropical Pacific Ocean and demonstrated that larger foraminifera and pteropods experience little solution during settling. They assumed that solution occurs mainly at the sediment-seawater interface. Herman and Rosenberg (1969) anticipated that, due to their relatively large size, pteropod postmortem settling velocities are much greater than those of other pelagic organisms. Consequently, we suppose that initial dissolution occurs mainly at the sediment-seawater interface. After burial, additional dissolution may occur depending on the aragonite corrosiveness of pore water environments. The investigated preservation records of core 2204-2 (e.g. boxes 3, 7, and 8 of Fig. 6) are good examples of such a diagenetic trend, which has considerably induced aragonite dissolution despite low TOC contents (0.17 wt.% on average; Rühlemann 1996) and a low potential of bacterial CO_2 supply after passing through the zone of oxidation at the surface.

We now consider possible factors that define the extent of aragonite dissolution at the sediment-seawater interface. Differences in the dissolution susceptibility of the Limacinidae (e.g. box 8 of Fig. 6) led us to determine the importance of shell size and thickness variations between the species. The SEM examination of the three Limacinidae species indicate that *L. inflata* possesses the thickest shell, although it appears to be the most soluble and fragile. The stronger solubility of *L. inflata* in comparison to *Limacina trochiformis* (a very thin-walled pteropod species) has been mentioned by Almogi-Labin et al. (1986). Consequently, we conclude that thicker shells are not necessarily better preserved, although the reasons are not fully understood. Furthermore, aragonite dissolution may be induced by the microbial degradation of organic matter within the sediment and the shell. Even in supralysoclinal waters, particles undergo a significant carbonate dissolution induced by bacterial activity, whereby the CO_3^{2-} concentration in the bottom water and the pore water is reduced (e.g. Archer and Maier-Reimer 1994; Martin and Sayles 1996). GeoB 2204-2 yields generally low amounts of TOC (0.17 wt.% on average; Rühlemann 1996), which are typical for oligotrophic oceanic regions. Consequently, degradation of organic matter cannot have caused such

apparent preservation variations. A further crucial element for the extent of dissolution is the time for which particles are exposed to dissolving conditions at the sediment-seawater interface. Therefore, suddenly increasing sedimentation rates may lead to faster shell burial and hence shorter exposure time to corrosive bottom waters and thus enhanced aragonite preservation (Berger 1977). Despite that, sedimentation rate in GeoB 2204-2 is 2.3 cm/ka on average with only minor changes during the past 430 ka (Rühlemann 1996) and disturbances by turbidites or similar features were not observed. Thus, we suspect that variations in the sedimentation rate did not result in such preservation variations as investigated in core GeoB 2204-2. According to Berger (1977), increasing the speed of bottom currents could affect carbonate preservation as well. Rhein et al. (1996) determined present deep-water velocities in the western equatorial Atlantic, but the connection between velocity and carbonate dissolution has not been studied thus far.

We suppose that the aforementioned elements play a minor role in the investigated area, and tnat bottom water corrosiveness causes initial aragonite dissolution. This is particularly interesting with regard to water mass reconstructions, because preservation variations may be attributed to shifting corrosive (e.g. AAIW/UCPW) and less corrosive (NADW) water masses. To obtain an idea about possible variations in intermediate water mass configuration during time, our results were compared with previous studies from the Atlantic. For instance, Venz et al. (1999) recently reconstructed major changes in the intermediate water structure of the North Atlantic for the past 1.0 m.a, which are attributed to spatial and seasonal variations in sea ice cover in the Nordic Seas. Evidence from Caribbean records indicates variations in the flow of AAIW and other corrosive southern-source water masses into the Caribbean during the past 200 ka, attended by a direct link to NADW production (Haddad and Droxler 1996). Evidence from $\delta^{13}C$ measurements from the western South Atlantic implies that the present water mass configuration (Fig. 2) could have been inverted in glacials with respect to northern and southern component water masses (Bickert 1992). This may have resulted in enhanced bottom water corrosiveness in the investigated area during glacials; however, it is evident that intermediate water mass structure in the South Atlantic is much more complex than previously supposed.

5. Conclusions

The following conclusions were reached as a result of this study:

1. Alternating modes of preservation of pteropod shells occur in Brazilian Continental Slope sediments during the past 430 ka due to varying preservation conditions at the sediment-water interface.

2. In order to study aragonite preservation we determined preservation modes on three *Limacina* species (*L. inflata, L. bulimoides, L. lesueuri*) as supplements to common proxies. *Limacina inflata* is more easily dissolved than the two other *Limacina* species, though average shell thickness is greater.
3. Excellent preservation is only found during the Holocene section. All older sediments are influenced by corrosion. Bad preservation is mainly found in glacials and most noticeably around Terminations I, II, and IV, but a long-term aragonite dissolution trend can be observed as well, which is diagenetically induced.
4. We interpret the aragonite preservation variations as caused by shifting water masses. Good preservation indicates the presence of NADW and poor preservation is correlatable to corrosive AAIW/UCPW influence.

All data sets used in this study are available as computer files from the corresponding author upon request or via Internet:
http://www.pangaea.de/Projects/SFB261/SGerhardt_et_al_2000/

Acknowledgements

We thank B. Karwath, S. Rath, Prof. Dr. C. Devey, and two anonymous reviewers for valuable comments on the manuscript. We also thank Prof. Dr. O. Brockamp, Dr. M. Zuther and A. Schlegel for the XRD analyses. Thanks are also due to R. Henning and I. Shokati for sample preparation. This research was funded by the Deutsche Forschungsgemeinschaft (Graduierten-Kolleg "Stoff-Flüsse in marinen Geosystemen"). This is contribution no. 291 of the SFB 261 (Bremen University).

References

Acker JG, Byrne RH (1989) The influence of surface state and saturation state on the dissolution kinetics of biogenetic aragonite in seawater. Am J of Sci 289: 1098-1116

Adelseck CG, Berger WH (1975) On the dissolution of planktonic foraminifera and associated microfossils during settling and on the sea floor. In: Sliter WV, Bé AWH, Berger WH (eds) Dissolution of Deep-Sea Carbonates. Cushman Found Foram Res Spec Publ Ithaka, NY 13, pp 70-81

Almogi-Labin A (1982) Stratigraphic and paleoceanographic significance of late Quaternary pteropods from deep-sea cores in the Gulf of Aqaba (Elat) and northernmost Red Sea. Mar Micropal 7: 53-72

Almogi-Labin A, Hemleben Ch, Meischner D (1998) Carbonate preservation and climatic changes in the Central Red Sea during the last 380 kyr as recorded by pteropods. Mar Micropal 33: 87-107

Almogi-Labin A, Hemleben Ch, Meischner D, Erlenkeuser H (1991) Paleoenvironmental events during the last 13,000 years in the Central Red Sea as recorded by pteropoda. Paleoceanography 6: 83-98

Almogi-Labin A, Luz B, Duplessy J-C (1986) Quaternary Paleo- Oceanography, pteropod preservation and s table-isotope record of the Red Sea. Paleogeo, Paleocli, Paleoecol 57: 195-211

Archer DE, Maier-Reimer E (1994) Effect of deep-sea sedimentary calcite preservation on atmospheric CO_2 concentration. Nature 367: 260-264

Bainbridge AE (1981) GEOSECS Atlantic Expedition, Hydrographic Data, 1972-1973. National Science Foundation, Superintendent of Documents, US Government Printing Office, Washington DC, pp 1-121

Bé AWH, Gilmer RW (1977) A Zoographic and taxonomic review of euthecosomatous pteropoda. In: Ramsay ATS (ed) Oceanic Micropalaeontology. Academic Press, London 1, pp 733-808

Bé AWH, Morse JW, Harrison SM (1975) Progressive dissolution and ultrastructural breakdown in planktonic foraminifera. In: Sliter WV, Bé AWH, Berger WH (eds) Dissolution of Deep-Sea Carbonates. Cushman Found Foram Res Spec Publ Ithaka, NY 13, pp 27-55

Berger WH (1973) Deep-sea carbonates: Pleistocene dissolution cycles. J Foram Res 3(4): 187-195

Berger WH (1977) Deep-sea carbonate and the deglaciation preservation spike in pteropods and foraminifera. Nature 269: 301-304

Berger WH (1978) Deep-sea carbonate: Pteropod distribution and the Aragonite Compensation Depth. Deep Sea Res 25: 447-452

Berger WH, Bonneau MC, Parker FL (1982) Foraminifera on the deep-sea floor: lysocline and dissolution rate. Oceanologica Acta 5: 249-258

Berger WH, Wefer G (1996) Central themes of South Atlantic circulation. In: Wefer G, Berger WH, Siedler G, Webb D (eds) The South Atlantic: Present and Past Circulation, Springer-Verlag, Berlin, Heidelberg, pp 3-11

Berner RA (1977) Sedimentation and dissolution of pteropods in the ocean. In: Anderson NR, Malahoff A (eds) The Fate of Fossil Fuel CO_2 in the Oceans. Plenum Press, New York, NY, pp 243-260

Berner RA, Honjo S (1981) Pelagic sedimentation of aragonite: its geochemical significance. Science 211: 940-942

Bickert T (1992) Rekonstruktion der spätquartären Bodenwasserzirkulation im östlichen Südatlantik über stabile Isotope benthischer Foraminiferen. Berichte, Fachbereich Geowissenschaften, Universität Bremen 27, pp 1-205

Bickert T, Cordes R, Wefer G (1997) Late Pliocene to Mid-Pleistocene (2.6-1.0 M.Y.) carbonate dissolution in the western equatorial Atlantic: Results of Leg 154, Ceara Rise. In: Shackleton NJ, Curry WB, Richter C, Bralower TJ (eds) Proc of the ODP, Sci Results 154, pp 229-237

Bickert T, Wefer G (1996) Late Quaternary deep water circulation in the South Atlantic: Reconstruction from carbonate dissolution and benthic stable isotopes. In: Wefer G, Berger WH, Siedler G, Webb D (eds) The South Atlantic: Present and Past Circulation, Springer-Verlag, Berlin, Heidelberg, pp 599-620

Boyle EA, Keigwin LD (1987) North Atlantic thermohaline circulation during the past 20,000 years linked to high-latitude surface temperature. Nature 30: 35-40

Broecker WS, Peng TH (1982) Tracers in the Sea. Eldigio Press, New York, NY, pp 1-689

Byrne RH, Acker JG, Betzer PR, Feely RA, Cates MH (1984) Water column dissolution of aragonite in the Pacific Ocean. Nature 312: 321-326

Carter JG (1990) Skeletal biomineralization: patterns, processes and evolutionary trends, volume 1. Van Nostrand Reinhold, New York, pp 1-832

Chen C (1964) Pteropod ooze from Bermuda Pedestal. Science 144: 60-62

Crowley TC (1983a) Calcium carbonate preservation patterns in the central North Atlantic during the last 150,000 years. Mar Geol 51: 1-14

Crowley TC (1983b) Depth-dependent carbonate dissolution changes in the eastern North Atlantic during the last 170,000 years. Mar Geol 54: 25-31

Cullity BD (1956) Elements of x-ray diffraction. Addison-Wesley Publ Co, Inc, Reading, Massachusetts; Menlo Park, California; London; Amsterdam; Don Mills, Ontario; Sydney, pp 1-555

Curry WB, Duplessy JC, Labeyrie LD, Shackleton NJ (1988) Changes in the distribution of $\delta^{13}C$ of deep water ΣCO_2 between the last glaciation and the Holocene. Paleoceanography 5: 487-506

Droxler AW, Haddad GA, Mucciarone DA, Cullen JL (1990) Pliocene- Pleistocene aragonite cyclic variations in Holes 714A and 716B (The Maledives) compared with Hole 633A (The Bahamas): records of climate-induced $CaCO_3$ preservation at intermediate water depths. Proc Ocean Drill Program Sci Results 115: 539-577

Droxler AW, Morse JW, Kornicker WA (1988) Controls on carbonate mineral accumulation in Bahamian Basins and adjacent Atlantic Ocean sediments. J Sediment Petrol 58: 120-130

Droxler AW, Schlager W, Whallon CC (1983) Quaternary aragonite cycles and oxygen-isotope record in Bahamian carbonate ooze. Geology 11: 235-239

Dürkoop A, Hale W, Mulitza S, Pätzold J, Wefer G (1997) Late Quaternary variations of sea surface salinity and temperature in the western tropical Atlantic: Evidence from $\delta^{18}O$ of *Globigerinoides sacculifer*. Paleoceanography 12(6): 764-772

Duplessy JC, Labeyrie L, Paterne M, Hovine S, Fichefet T, Duprat J, Labracherie M (1996) High latitude deep water sources during the Last Glacial Maximum and the intensity of the global oceanic circulation. In: Wefer G, Berger WH, Siedler G, Webb D (eds) The South Atlantic: Present and Past Circulation, Springer-Verlag, Berlin, Heidelberg, pp 445-460

Duplessy JC, Shackleton NJ, Fairbanks RG, Labeyrie LD, Oppo D, Kallel N (1988) Deepwater source variations during the last climatic cycle and their impact on the global deepwater circulation. Paleoceanography 3: 343-360

Gardner JV (1975) Late Pleistocene carbonate dissolution cacles in the eastern equatorial Atlantic. In: Sliter WV, Bé AWH, Berger WH (eds) Dissolution of Deep-Sea Carbonates. Cushman Found Foram Res Spec Publ Ithaka, NY 13, pp 129-141

Haddad GA, Droxler AW (1996) Metastable $CaCO_3$ dissolution at intermediate water depths of the Caribbean and western North Atlantic: Implications for intermediate water circulation during the past 200,000 years. Paleoceanography 11(6): 701-716

Hecht AD, Eslinger EV, Garmon LB (1975) Experimental Studies on the dissolution of planctonic foraminifera. In: Sliter WV, Bé AWH, Berger WH (eds) Dissolution of Deep-Sea Carbonates. Cushman Found Foram Res Spec Publ Ithaka, NY 13, pp 56-69

Henrich R (1989) Glacial/interglacial cycles in the Norwegian Sea: Sedimentology, paleoceanography, and evolution of late Pliocene to Quaternary northern hemisphere climate. In: Eldholm O, Thiede J, Taylor E (eds) Proc ODP, Sci Results. College Station, TX 104, pp 189-232

Henrich R, Wefer G (1986) Dissolution of biogenic carbonates: Effects of skeletal structure. Mar Geol 71: 341-362

Herman Y, Rosenberg PE (1969) Pteropods as bathymetric indicators. Mar Geol 7: 169-173

Howard WR, Prell WL (1994) Late Quaternary $CaCO_3$ production and preservation in the Southern Ocean: implications for oceanic and atmospheric carbon cycling. Paleoceanography 9(3): 453-482

Johnson TC, Hamilton EL, Berger WH (1977) Physical properties of calcareous ooze: Control by dissolution at depth. Mar Geol 24: 259-277

Klug HP, Alexander LE (1954) X-ray diffraction procedures for polycrystalline and amorphous materials. John Wiley & Sons, New York, London, Sydney, Toronto, pp 1-966

Martin WR, Sayles FL (1996) $CaCO_3$ dissolution in sediments of the Ceara Rise, western equatorial Atlantic. Geochim Cosmochim Acta 60: 243-263

Milliman JD (1974) Marine Carbonates. Springer-Verlag, New York, pp 1-363

Oppo DW, Raymo ME, Lohmann GP, Mix AC, Wright JD, Prell WL (1995) A $\delta^{13}C$ record of Upper North Atlantic Deep Water during the past 2.6 million years. Paleoceanography 10(3): 373-394

Reid JL (1989) On the total geostrophic circulation of the South Atlantic Ocean: Flow patterns, tracers, and transports. Prog Oceanog 23(3): 149-244

Reid JL (1994) On the total geostrophic circulation of the North Atlantic Ocean: Flow patterns, tracers, and transports. Prog Oceanog 33(1): 1-92

Reid JL (1996) On the circulation of the South Atlantic Ocean. In: Wefer G, Berger WH, Siedler G, Webb D (eds) The South Atlantic: Present and Past Circulation, Springer-Verlag, Berlin, Heidelberg, pp 13-44

Rhein M, Schott F, Fischer J, Send U, Stramma L (1996) The deep water regime in the Equatorial Atlantic. In: Wefer G, Berger WH, Siedler G, Webb D (eds) The South Atlantic: Present and Past Circulation, Springer-Verlag, Berlin, Heidelberg, pp 262-271

Rhoads DC, Lutz RA (1980) Skeletal growth of aquatic organisms: biological records of environmental change. Plenum Press, New York, London, pp 1-750

Richter G (1976) Zur Frage der Verwandtschaftsbeziehungen von Limacinidae und Cavolinidae (Pteropoda: Thecosomata). Arch Moll 107(1/3): 137-144

Rühlemann C (1996) Akkumulation von Carbonat und organischem Kohlenstoff im tropischen Atlantik: Spätquartäre Produktivitäts-Variationen und ihre Steuerungsmechanismen. Berichte, Fachbereich Geowissenschaften, Universität Bremen 84, pp 1-139

Sarnthein M, Winn K, Jung SJA, Duplessy JC, Labeyrie LD, Erlenkeuser H, Ganssen G (1994) Changes in East Atlantic deepwater circulation over the last 30,000 years: Eight time slice reconstructions. Paleoceanography 9: 209-267

Van Der Spoel S (1967) Euthecosomata, a group with remarkable development stages.(Gastropoda, Pteropoda). Ph.D. thesis, Univ. Amsterdam, J. Noorduijn en Zoon, Gorinchem, pp 1-375

Van Der Spoel S (1972) Pteropoda Thecosomata. Conseil international pour l'exploration de la mer: 1-12

Venz KA, Hodell DA, Stanton C, Warnke DA (1999) A 1.0 Myr record of Glacial North Atlantic Intermediate Water variability from ODP site 982 in the northeast Atlantic. Paleoceanography 14(1): 42-52

Wefer G, Beese D, Berger WH, Buschhoff H, Cepek M, Diekamp V, Fischer G, Holmes E, Kemle von Mücke S, Kerntopf B, Lange C, Mulitza S, Otto S, Plugge R, Ratmeyer V, Rühlemann C, Schmidt W, Schwarze M, Wallmann K and Zabel M (1994) Report and preliminary results of *Meteor*-cruise M 23/3, Recife - Las Palmas, 21.3.-12.4.93. Berichte, Fachbereich Geowissenschaften, Universität Bremen 44, pp 1-71

Wu G, Berger WH (1991) Pleistocene $\delta^{18}O$ record from Ontong Java Plateau: effects of winnowing and dissolution. Mar Geol 96: 193-209

4. Millennial-scale changes of surface- and deep-water flow in the western tropical Atlantic linked to Northern Hemisphere high-latitude climate during the Holocene

Helge W. Arz, Sabine Gerhardt, Jürgen Pätzold, and Ulla Röhl

Fachbereich Geowissenschaften, Universität Bremen, Klagenfurter Str., 28359 Bremen

Abstract

There is increasing evidence that the preceding Holocene climate was as unstable as the last glacial period, although variations occurred at much lower amplitudes. However, low-latitude climate records that confirm this variability are sparse. Here we present a radiocarbon dated Holocene marine record from the tropical western Atlantic. Aragonite dissolution derived from the degree of preservation of the pteropod *Limacina inflata* records changes in the corrosiveness of the bottom water at the core site due to changing influence of northern versus southern water masses. The $\delta^{18}O$ difference between the shallow-living planktonic foraminifera *Globigerinoides sacculifer* and the deep-living *Globorotalia tumida* is used as proxy for changes in the vertical stratification of the surface water, hence the trade wind strength at this latitude. We compared our data to high-latitude records of the North Atlantic region. A good agreement is found between the aragonite dissolution and the strength in the Iceland-Scotland Overflow Water, which contributes significantly to the North Atlantic Deep Water. This suggests that large-scale variations in the Atlantic thermohaline circulation occurred throughout the Holocene. Concurrently, the comparison of our $\Delta\delta^{18}O$ with the GISP2 glaciochemical records points to global Holocene atmospheric reorganizations seen both in the tropics and high northern latitudes.

Keywords: Holocene, tropical Atlantic, oceanography, stable oxygen isotopes, carbonate preservation, thermohaline circulation

Introduction

The global significance of millennial-scale climate shifts during the last glacial is widely accepted. In addition to the rather irregular Dansgaard-Oeschger/Bond cyclicity and associated Heinrich events, a more pervasive 1-2 k.y. cycle has been recently reported from

North Atlantic ice-rafted detritus records (Bond et al., 1999). Various high-resolution paleoclimatic investigations on ice cores (e.g., the GISP2 in Greenland, O'Brien et al., 1995) and marine sediment cores (e.g., the North Atlantic, Bond et al., 1997) indicate a continuation, although much less pronounced, of this variability throughout the Holocene. The quasiperiodic components of these climatic records vary between several hundreds to thousands of years, giving rise to a broad variety of possible forcing mechanisms such as astronomically induced variations (~900 yr, Loutre et al., 1992), internally forced oscillations of the ocean-atmosphere system (~1.5 k.y., Bond et al., 1999), and changes in solar activity (~2.5 k.y., Stuiver and Reimer, 1993).

The glacial North Atlantic ice-rafted detritus events were accompanied by significant changes in the intensity of thermohaline circulation (e.g., Curry and Oppo, 1997; Vidal et al., 1997; Keigwin and Boyle, 1999) that probably acted, in addition to atmospherical forcing (e.g., Curry and Oppo, 1997; Arz et al., 1998), as global climatic amplifiers. Consequently, this gives rise to the major question to what extent the Atlantic or even global thermohaline circulation was affected by such quasiperiodic events during the Holocene. General circulation model simulations show that variations in the thermohaline circulation strongly affect deep and intermediate water-mass configuration, also at subtropical and tropical latitudes (Manabe and Stouffer, 1997). Previous studies in this region demonstrated that glacial millennial-scale changes are documented in the deep-water as well as surface-water configuration (Curry and Oppo, 1997; Arz et al., 1998, 1999b). The aim of our study is therefore to trace and examine such Holocene variations in the western tropical Atlantic, where climate-relevant processes such as the interhemispheric heat exchange and the regulation of the atmospheric water vapor content take place.

Study area

Surface hydrology in the southwestern tropical Atlantic is dominated by seasonally varying southeast trade winds, the annual movement of the Intertropical Convergence Zone, and the north-northwestward-flowing boundary current, the North Brazil Current (NBC). Altogether, these influences result in a seasonally deepening mixed layer from 60 m in austral summer to 100 m in winter (Hastenrath and Merle, 1987). At depths of ~700-1500 m, oxygen-enriched and low-salinity Antarctic Intermediate Water (AAIW) and Upper Circumpolar Deep Water (UCDW) flow northward. At the core depth the sediment surface is within the southward-flowing upper branch of the North Atlantic Deep Water (UNADW) (Fig. 1).

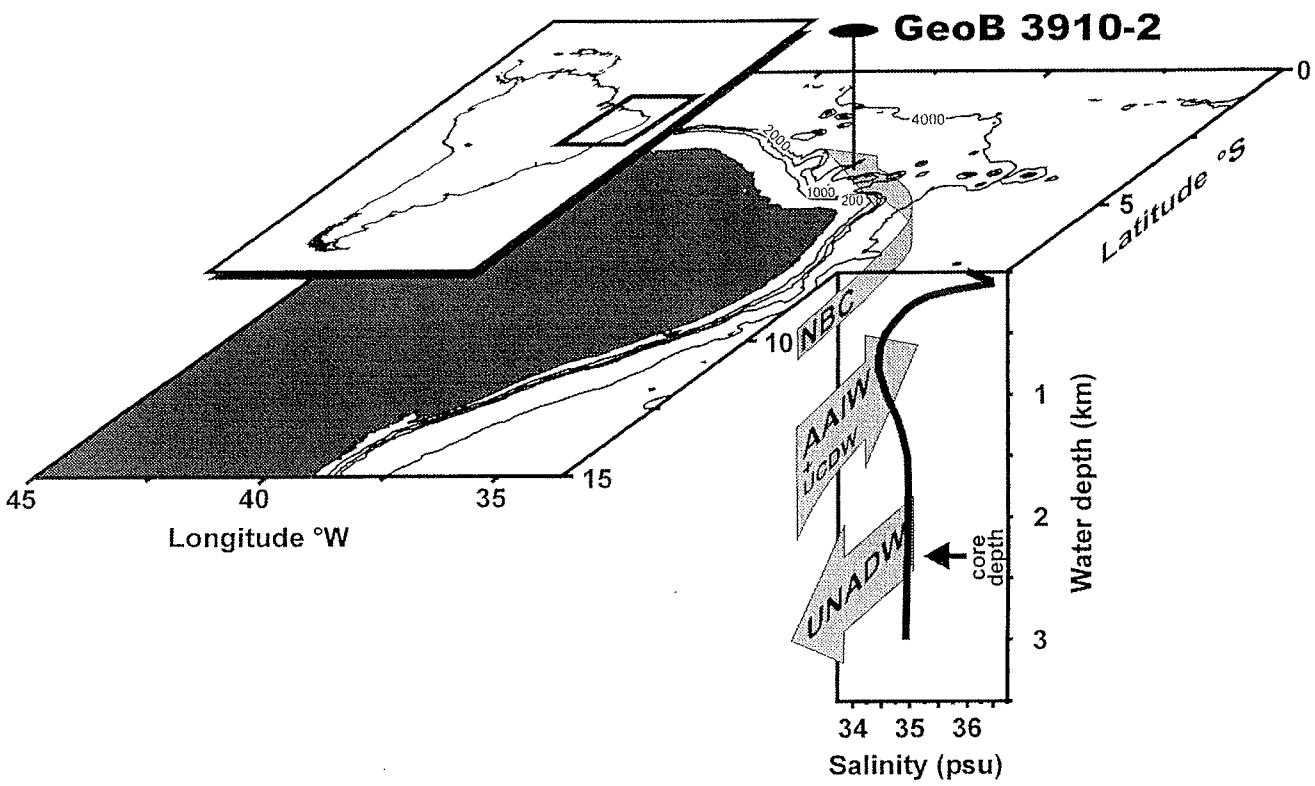

Fig. 1: Location of sediment core GeoB 3910-2 and circulation patterns in the western South Atlantic. NBC, North-Brazil Current; AAIW, Antarctic Intermediate Water; UCPDW, Upper Circumpolar Deep Water; UNADW, Upper North Atlantic Deep Water. Salinity is schematically plotted versus water depth.

Material and methods

We investigated the Holocene section of the sediment core GeoB 3910-2, recovered from the continental slope off northeastern Brazil at lat 4°14.7'S, long 36°20.7'W from a water depth of 2362 m (Fig. 1). Monospecific carbonate samples (*Globigerinoides sacculifer*) were dated at the Leibniz Labor in Kiel, Germany. Five dated samples cover the Holocene and indicate undisturbed, continuous sedimentation with rates of 4 to 10 cm/k.y. (Fig. 2, a and b). Ages are reservoir corrected and are reported in calibrated calendar years. With 0.5 cm sampling intervals for all measurements a time resolution of <100 yrs was achieved.

Bulk sediment chemistry was determined by means of nondestructive, profiling X-ray fluorescence (XRF). Ca intensities reported in this study are closely related to the carbonate content. Holocene slope sediments in the western equatorial Atlantic contain as much as 80 wt% carbonate, and aragonite constitutes approximately half of it (Gerhardt et al., 2000). Using the degree of preservation of the aragonitic shells of *Limacina inflata*, an abundant

euthecosomatous pteropod, we estimated the degree of aragonite dissolution, the *L. inflata* dissolution index (LDX), as described by Gerhardt et al. (2000). High LDX values document an increased dissolution of aragonite.

The stable oxygen isotope composition was determined on the tests of the surface-dwelling planktonic foraminifera *G. sacculifer* (350-400 µm) and the thermocline-dwelling *Globorotalia tumida* (700-800 µm). Homogenized samples of 50 specimens of *G. sacculifer* and 10 specimens of *G. tumida* were processed with an automatic carbonate preparation system attached to a Finnigan MAT 251 mass spectrometer. Analytical precision is better than ±0.07‰. Sea-surface temperatures were estimated from foraminiferal assemblages with the Imbrie and Kipp transfer function method.

Results and discussion

Holocene variations in aragonite preservation

The records of Ca intensity and the LDX are clearly dominated by a long-term trend. LDX values decrease from 2.3 at the beginning of the Holocene to 0.7, i.e., preservation improves during the late Holocene (Fig. 2g) and the aragonite content increases by ~20% relative to bulk carbonate (Gerhardt et al. 2000; Gerhardt and Henrich, in press). Ca intensities are almost doubling at the same time (Fig. 2f). The long-term trend in the Ca intensities mainly reflects the dilution of the biogenic carbonate by continental terrigenous sediments (Arz et al., 1999a). The improved preservation of aragonite probably reflects the increased postglacial influence of NADW at the expense of the more corrosive AAIW and UCDW at this water depth. However, a diagenetically induced decrease in aragonit content down core must also be taken into account (Gerhardt et al., 2000). The short-term changes in Ca intensities are inversely related to the LDX variations. By removing the long-term trends, the Holocene short-term variability in both records is amplified (Fig. 3, b and c).

Both parameters suggest that aragonite preservation varied significantly during the Holocene and is most probably associated with a changing corrosiveness of the bottom water. Several processes, however, such as early dissolution during settling, exposure time at the sediment surface, dissolution related to bottom current velocity, and pore-water dissolution can bias the actual proxy for the aragonite saturation state of the bottom water masses (Gerhardt et al. 2000; Gerhardt and Henrich, in press). Major effects can be ruled out at least for the settling time, which is short for *L. inflata* (1-2 days), as well as for the exposure time at the sediment surface, which is also relatively short due to the high sedimentation rates at this site. The effect of pore-water dissolution driven by organic degradation strongly affects

carbonate preservation. But as the content of organic matter is very low in these sediments (0.2-0.6 wt%; Arz et al., 1999a) and one would expect that short-term variations in the LDX are rather flattened out by this effect, we assume that it plays only a minor role.

At present, the sediment surface at the core site is situated above the deep aragonite lysocline (a shallower one is located at ~1000 m due to the highly corrosive core of the AAIW; Gerhardt et al., 2000, and references therein) within the upper branch of the southward flowing NADW. If NADW weakens, one would expect a slightly increased influence of more corrosive water masses of southern origin. The reorganization of water masses at intermediate and deep water levels in the tropical Atlantic is commonly attributed to changes in the Atlantic thermohaline circulation. Many of these changes originate in the high latitudes of the North Atlantic, where the process of deep-water formation acts as one of the drive wheels for the thermohaline conveyor belt. Using the sortable silt mean size as a near-bottom paleocurrent proxy, Bianchi and McCave (1999) reported Holocene oscillations in the strengths of the ISOW-a water mass contributing significantly to the present thermohaline circulation-thus suggesting short-term changes in the thermohaline circulation during the Holocene. In Figure 3 (a-c) the Ca intensities and the LDX of core GeoB 3910-2 are compared with the silt mean size of core NEAP-15K (Bianchi and McCave, 1999). Within the limits of the stratigraphical accuracy of both records, the tentative correlation implies that periods of enhanced ISOW flow parallel the intervals of increased aragonite preservation, and vice versa. Cross spectra between the records (Fig. 4a) indicate high spectral density and cross coherency at periods of around 1540, 730, and 510 yr. The periods have been reported also from other paleoclimatologic studies in the North Atlantic region (e.g., Bond et al., 1997) and may be the expression of internally forced oscillations of the ocean-atmosphere system. Although these findings do not allow any quantitative statement concerning the reorganization of water masses at tropical latitudes and secondary processes influencing aragonite preservation cannot be ruled out, the results suggest that quasiperiodic variations in the thermohaline circulation could have contributed to the overall Holocene climate instability.

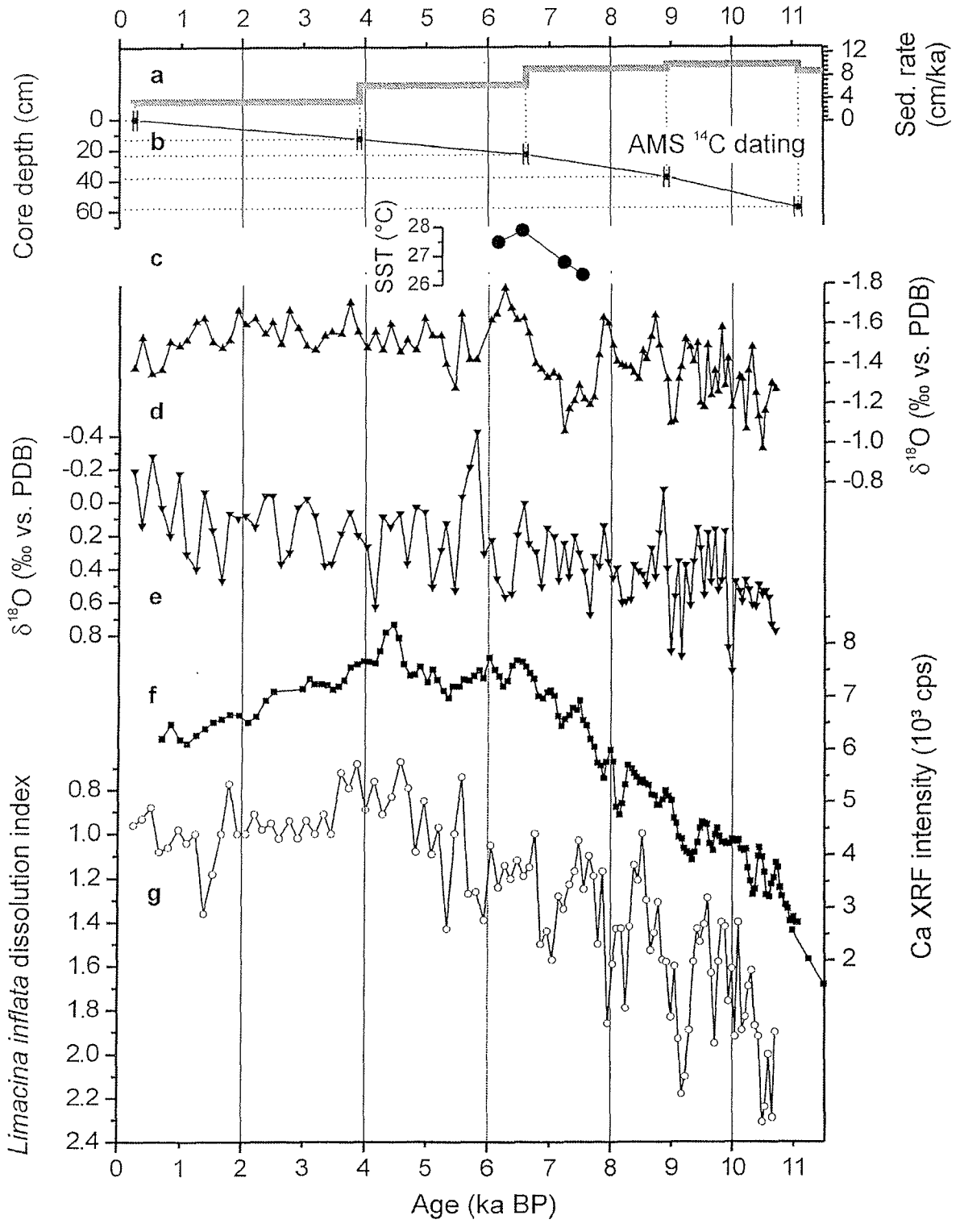

Fig. 2: Results obtained on Holocene section of sediment core GeoB 3910-2. (a) sedimentation rates, (b) age-depth relation based on calibrated ^{14}C accelerator mass spectrometry data, (c) annual sea-surface temperature estimates from foraminiferal assemblages between 6 and 8 k.y. B.P., (d) δ^{18}O record of *G. sacculifer*, (e) δ^{18}O record of *G. tumida*, (f) Ca intensities measured by X-ray fluorescence (XRF), and (g) *L. inflata* Dissolution Index (LDX; Gerhardt et al. 2000). PDB is Peedee belemnite.

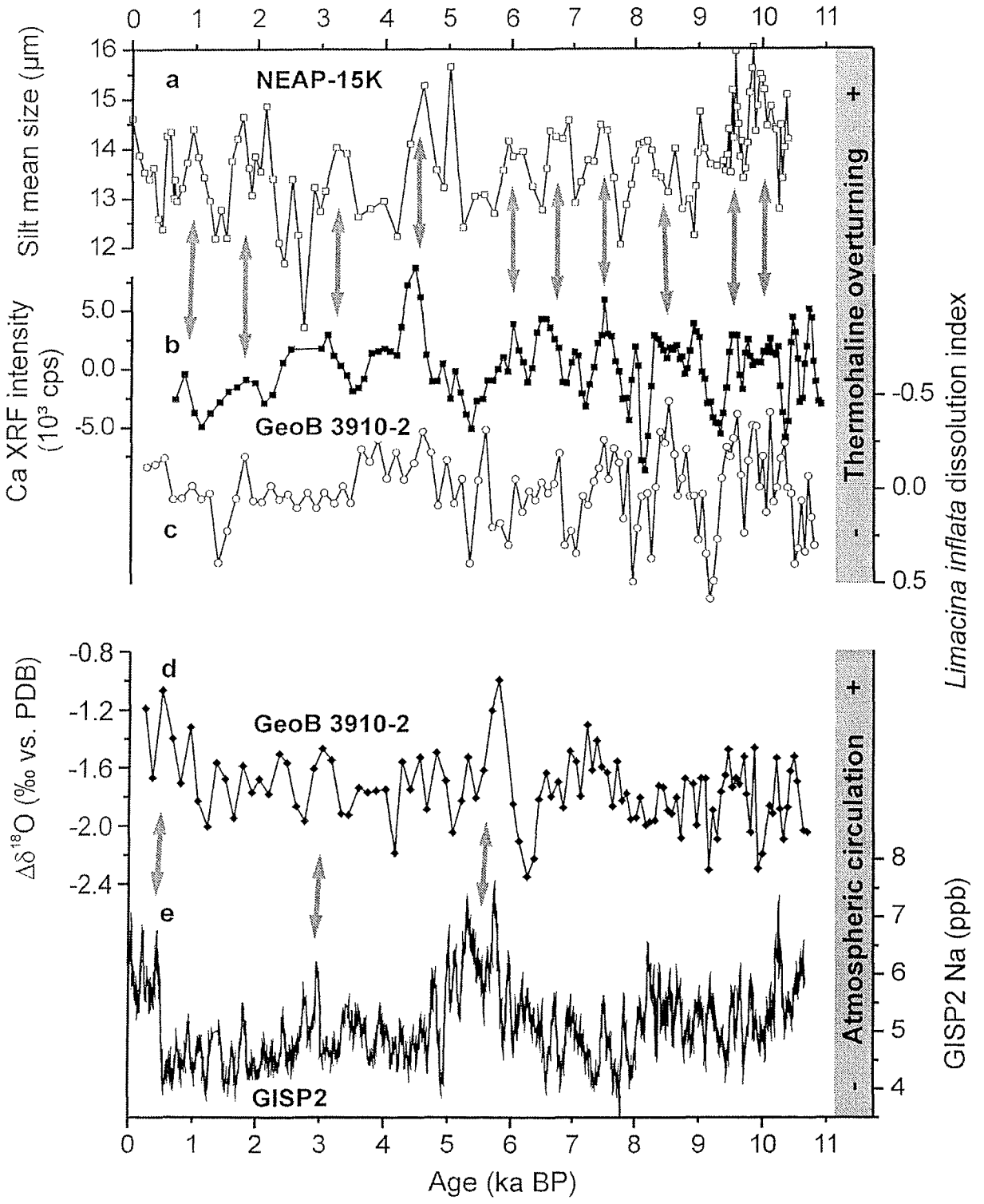

Fig. 3: Comparison (b) Ca-intensities and (c) the *Limacina inflata* Dissolution Index (LDX) with (a) silt mean size of core NEAP-15K (Bianchi and McCave, 1999), and (d) $\Delta\delta^{18}O$ *G. sacculifer – G. tumida* with (e) Na-ion concentration of the GISP2 ice core (Mayewski et al., 1997; O'Brien et al., 1995). Trends in Ca-intensities and LDX were removed by subtracting 30 point moving average from original data. Arrows indicate tentative correlation of periods where thermohaline circulation is enhanced. PDB is Peedee belemnite, XRF is X-ray fluorescence.

Surface-water stratification and atmospheric circulation

Both the isotope records of *G. sacculifer* and *G. tumida* show short-term excursions of as much as 0.7‰, all of which were verified by replicate measurements (Fig. 2, d and e). Exemplary, faunal SST determinations for the interval 6.2-7.2 k.y. B.P., where the $\delta^{18}O$ *G. sacculifer* record shows a prominent shift of 0.7‰, indicate that SST changes of as much as 1.5 °C (Fig. 2c) occurred during the Holocene.

The isotopic difference between the shallow-dwelling *G. sacculifer* and the deep-dwelling *G. tumida* ($\Delta\delta^{18}O$, Fig. 3d) is used in this study as a proxy for the thermal stratification of the surface water (e.g., Rühlemann et al., 2001), which is closely related to atmospheric circulation patterns over the tropical Atlantic (Hastenrath and Merle, 1987). Low $\Delta\delta^{18}O$ values indicate low vertical gradients, hence a deep vertical mixing that is related to an increased zonality of the trade winds and vice versa. A modern gradient of ~-1.6‰ can be assessed for the western tropical Atlantic (Rühlemann et al., 2001).

That millennial-scale climatic variations are documented in various marine and continental environments implies that changes in the atmospheric circulation significantly contributed to the regional and global expression of such variations. Holocene glaciochemical time series from the GISP2 ice core (Fig. 3e) suggest that the northern polar vortex intensified and expanded episodically at ~2.6 k.y. intervals throughout the Holocene, and that this was related to generally colder climates on both hemispheres (O'Brien et al., 1995). In addition to these major episodes, a series of secondary quasiperiodic variations (between 1.5 and 0.5 k.y.) determine the variability in the GISP2 record (Fig. 4b). In Figure 3 (d and e) we compare the $\Delta\delta^{18}O$ record of GeoB 3910-2, which we assume to be indicative for changes in the mixed layer depth and therefore also in trade wind intensity at equatorial latitudes, with the GISP2 record of Na-ion concentration (O'Brien et al., 1995; Mayewski et al., 1997). Although only some of the major episodes (around 600, 3000, and 5600 yr B.P.) can be directly paralleled, high spectral density and cross coherency between the two records is found at periods of ~1440, ~930, ~650, and ~490 yr (Fig. 4b). An equatorward displacement of the westerlies associated with an expanded polar vortex during the periods of increased sea salt and dust accumulation over Greenland could have resulted in an episodically enhanced trade wind circulation at tropical latitudes.

Variations in the trade wind intensity as well as changes in the thermohaline circulation determine the surface circulation in the western tropical Atlantic, i.e., the intensity of the NBC. Variations in the NBC could have therefore contributed to changes in the heat and salt flux into the North Atlantic, thus acting as an amplifying mechanism for the Holocene climate variation by substantially affecting the deep-water-generating processes at high latitudes.

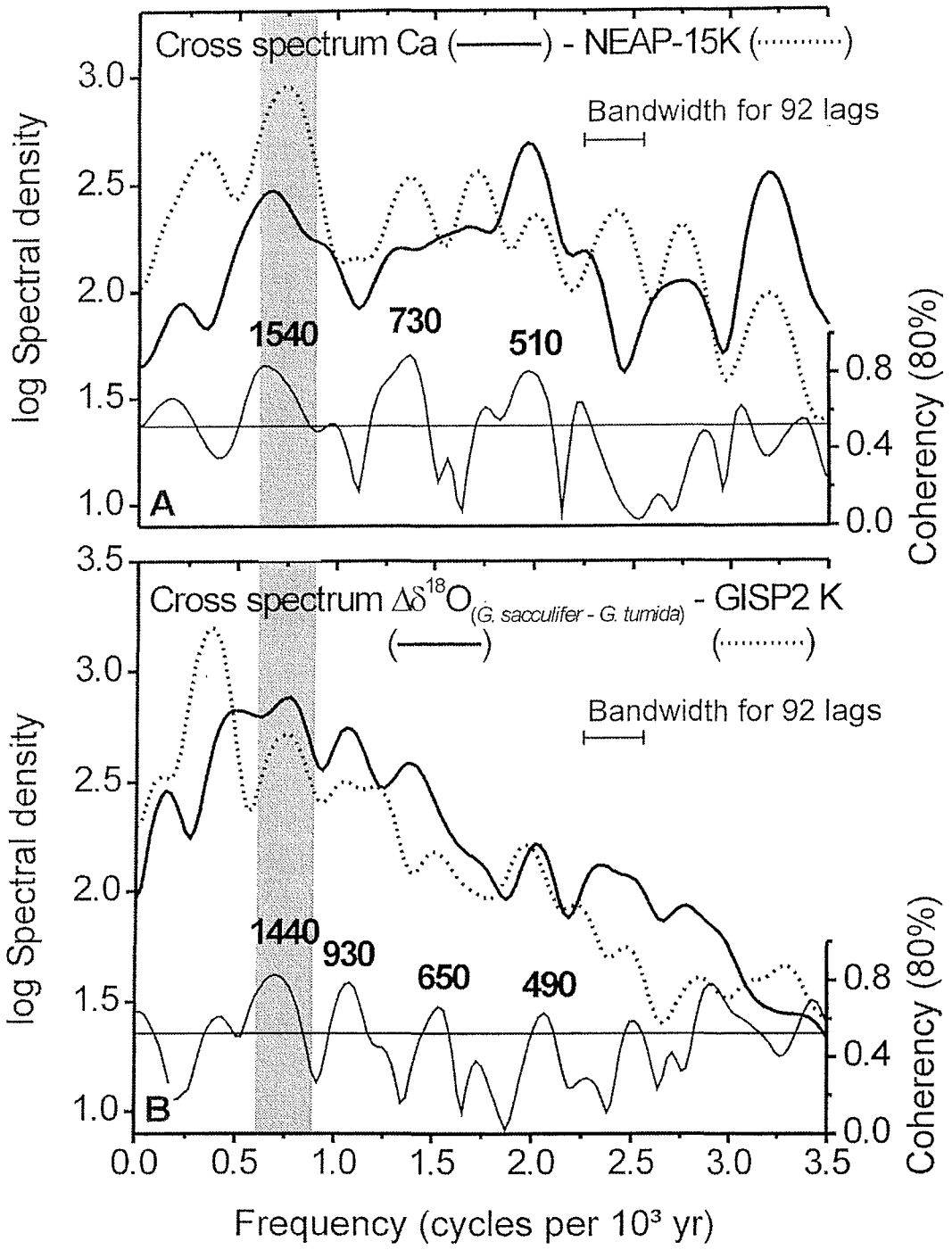

Fig. 4: Results of Blackman-Tukey cross-spectral analysis (a) between detrended Ca intensities, GeoB 3910-2, and silt mean size of core NEAP-15K (Bianchi and McCave, 1999), and (b) between $\Delta\delta^{18}O$, GeoB 3910-2, and Na-ion-concentration of the GISP2 ice core (O'Brien et al., 1995; Mayewski et al., 1997). Each upper panel shows high-resolution variance spectra of the time series; each lower panel shows coherency at 80% confidence level. Coherent periods are labeled.

Summary and conclusions

We presented a Holocene record of aragonite preservation (Ca intensity/LDX) at intermediate water depth in the western tropical Atlantic, which we interpret as a proxy record for the bottom-water corrosiveness at the core site, thus being indicative of changes in the Atlantic thermohaline circulation during the Holocene. In addition, we used the $\Delta\delta^{18}O$ in this study as a proxy for past surface-water stratification, reflecting changes in the tropical atmospheric circulation, i.e., changes in the zonality of the southwest trade winds. Comparisons with high-latitude records suggest that forcing mechanisms such as solar forcing, astronomically induced forcing, and internal oscillations of the climate system trigger the observed climatic changes, but also that the various mechanisms can hardly be distinguished from each other. An ~1.5 k.y. periodicity can be observed in all the records that points to some dominance of the internally forced global-scale oscillations of the ocean-atmosphere system. The variety of possible forcing mechanisms and the rather complex atmosphere-ocean interaction, however, result in a broad band of quasiperiodic oscillations at the millennial and centennial scale.

Acknowledgements

We thank M. Segl, and B. Meyer-Schack for isotope measurements and Stefan Niebler for processing the foraminiferal assemblage data. The work was funded by the Deutsche Forschungsgemeinschaft (Sonderforschungsbereich 261 at Bremen University, Contribution No. 319).

References

Arz, H.W., Pätzold, J., and Wefer, G., 1998, Correlated millennial-scale changes in surface hydrography and terrigenous sediment yield inferred from last-glacial marine deposits off Northeastern Brazil: Quaternary Research, v. 50, p. 157-166.

Arz, H., Pätzold, J., and Wefer, G., 1999a, Climatic changes during the last deglaciation recorded in sediment cores from the Northeast Brazilian Continental Margin: Geo-Marine Letters, v. 19, p. 209-218.

Arz, H.W., Pätzold, J., and Wefer, G., 1999b, The deglacial history of the western Tropical Atlantic as inferred from high resolution stable isotope records off northeastern Brazil: Earth and Planetary Science Letters, v. 167, p. 105-117.

Bianchi, G., and McCave, N., 1999, Holocene periodicity in North Atlantic climate and deep-ocean from south of Iceland: Nature, v. 397, p. 515-517.

Bond, G., Broecker, W., Johnsen, S., McManus, J., Labeyrie, L., Jouzel, J., and Bonani, G., 1993, Correlations between climate records from North Atlantic sediments and Greenland ice: Nature, v. 365, p. 143-147.

Bond, G., Showers, W., Cheseby, M., Lotti, R., Almasi, P., DeMenocal, P., Priore, P., Cullen, H., Hadjas, I., and Bonani, G., 1997, A pervasive millennial-scale cycle in North Atlantic Holocene and Glacial climates: Science, v. 278, p. 1257-1266.

Bond, G., Showers, W., Elliot, M., Evans, M., Lotti, R., Hadjas, I., Bonani, G., and Johnson, S., 1999, The North Atlantic's 1-2 kyr climate rhythm: relation to Heinrich events, Dansgaard/Oeschger Cycles and the Little Ice Age, *in* Clark, P.U., Webb, R.S., and Keigwin, L.D., eds., Mechanisms of global climate change at millennial time scales, Volume 112: Geophysical Monograph: Washington, American Geophysical Union, p. 23-34.

Curry, W.B., and Oppo, D.W., 1997, Synchronous, high-frequency oscillations in tropical sea surface temperatures and North Atlantic Deep Water production during the last glacial cycle: Paleoceanography, v. 12, p. 1-14.

Gerhardt, S., Groth, H., Rühlemann, C., and Henrich, R., 2000, Aragonite preservation in late Quaternary sediment cores on the Brazilian Continental Slope: implications for intermediate water circulation: International Journal of Earth Sciences, v. 88, p. 607-618.

Gerhardt, S., Henrich, R., 2001, Shell preservation of *Limacina inflata* (Pteropoda) in surface sediments from the Central and South Atlantic Ocean: a new proxy to determine the aragonite saturation state of water masses: Deep-Sea Research I, in press.

Hastenrath, S., and Merle, J., 1987, Annual cycle of subsurface thermal structure in the Tropical Atlantic Ocean: Journal of Physical Oceanography, v. 17, p. 1518-1538.

Keigwin, L.D., and Boyle, E.A., 1999, Surface and deep ocean variability in the northern Sargasso Sea during marine isotope Stage 3: Paleoceanography, v. 14, p. 164-170.

Loutre, M.F., Berger, A., Bretagnon, P., and Blanc, P.-L., 1992, Astronomical frequencies for climate research at the decadal to century time scale: Climate Dynamics, v. 7, p. 181-194.

Manabe, S., and Stouffer, R.J., 1997, Coupled ocean-atmosphere model response to freshwater input: Comparison to Younger Dryas event: Paleoceanography, v. 12, p. 321-336.

Mayewski, P.A., Meeker, L.D., Morrison, M.C., Twickler, M.S., Whitlow, S.I., Ferland, K.K., Meese, D.A., Legrand, M.R., and Steffensen, J.P., 1993, Greenland ice core "Signal" characteristics; an expand view of climate change: Journal of Geophysical Research, v. 98, p. 12,839-12,847.

Mayewski, P.A., Meeker, L.D., Twickler, M.S., Whitlow, S.I., Yang, Q., Lyons, W.B., and Prentice, M., 1997, Major features and forcing of high-latitude northern hemisphere atmospheric circulation using a 110,000-year-long glaciochemical series: Journal of Geophysical Research, v. 102, p. 26345-26366.

O'Brien, S.R., Mayewski, P.A., Meeker, L.D., Meese, D.A., Twickler, M.S., and Whitlow, S.I., 1995, Complexity of Holocene climate as reconstructed from a Greenland ice core: Science, v. 270, p. 1962-1964.

Rühlemann, C., Diekmann, B., Mulitza, S., and Frank, M., 2001, Late Quaternary changes of western equatorial Atlantic surface circulation and Amazon lowland climate recorded in Ceará Rise deep sea sediments: Paleoceanography, in press.

Sarkar, A., Ramesh, R., Somayajulu, B.L.K., Agnihotri, R., Jull, A.J.T., and Burr, G.S., 2000, High resolution Holocene monsoon record from the eastern Arabian Sea: Earth and Planetary Science Letters, v. 177, p. 131-345.

Stuiver, M., and Reimer, P.J., 1993, Extended ^{14}C database and revised CALIB 3.0 ^{14}C age calibration program: Radiocarbon, v. 35, p. 215-230.

Vidal, L., Labeyrie, L., Cortijo, E., Arnold, M., Duplessy, J.C., Michel, E., Becqué, S., and van Weering, T.C.E., 1997, Evidence for changes in the North Atlantic Deep Water linked to melt water surges during the Heinrich events: Earth and Planetary Science Letters, v. 146, p. 13-27.

Part III *Summary*

1. Results

The interaction between ocean and atmosphere plays a key role in climate change. Understanding changes in intermediate and deep water circulation through time will greatly improve our knowledge about ocean history and can contribute significantly to models predicting future climate change. During the course of this thesis, two new methods were developed in order to determine spatial and temporal variations in aragonite preservation of late Quaternary sediments. The *Limacina* Dissolution Index (LDX) was determined by using a binocular microscope and applied on three members of the genus *Limacina* (L. inflata, which turned out to be most reliable, *L. bulimoides,* and *L. lesueuri*). The LDX was tested in surface sediments from the South and Central Atlantic and from the Caribbean, and it was applied to the LGM and to the late Quaternary section of several sediment cores.

Calibration of the LDX in surface sediments demonstrated that differences in pteropod shell preservation reflect the saturation state of the overlying water mass with respect to aragonite (part II-1). However, regional differences were observed. In the western Atlantic Ocean, including the Mid-Atlantic Ridge, the LDX predominantly displays good correlation with the presence of aragonite-corrosive AAIW/UCDW and non-corrosive UNADW. In contrast, the LDX fails in most cases in the eastern Atlantic Ocean, even in intermediate and shallow water depths, which is due to extensive supralysoclinal aragonite dissolution. Within the Caribbean Sea, the LDX reveals a more complex aragonite dissolution pattern due to local differences in circulation and carbonate production. Where AAIW/UCDW influence is the greatest (SE Caribbean), aragonite preservation is poor, whereas preservation is better where the UNADW influence is greatest (NE Caribbean). Near the Pedro Bank, aragonite preservation may be improved due to the additional input of bank-derived aragonitic material, which locally depresses the aragonite saturation depth (Droxler et al., 1991). It was observed that both the LDX values and $\%CaCO_3$ versus water depth display S-shaped curve trends due to variations in the aragonite-corrosiveness. The S-shape becomes narrower from the South Atlantic to the NE Caribbean due to both northward aging of AAIW/UCDW and mixing with overlying saline surface waters and underlying UNADW. Moreover, our results suggest that two aragonite lysoclines are developed under modern conditions, i.e. an upper lysocline within AAIW/UCDW (≈750 m) and a lower lysocline within LNADW (≈2500 m). Comparison of regional aragonite contents and LDX values reveals a close connection, which might be considered as a reliable estimation for the aragonite loss that sediments have undergone.

The applicability of the LDX as a water mass indicator was tested in LGM sediments (23-19 cal-ka-BP) (part II-2). The LDX indicates very good to moderate aragonite preservation in mid-depth western South Atlantic sediments, indicating the presence of non- to slightly aragonite-corrosive GNAIW as far south as 20°S. This is consistent with recent findings of Oppo and Horowitz (2000), who determined benthic foraminiferal Cd/Ca and $\delta^{13}C$ and suggested that GNAIW extended at least as far south as 28°S in the western South Atlantic. The equatorial aragonite lysocline was most likely positioned ≈500 m shallower than today at ≈2000 m water depth, rising parallel to the NCW/USCW boundary to the south. The NCW/SCW boundary most probably coincided with the Aragonite Compensation Depth (ACD) during the LGM. In contrast to the S-shaped curve trend in modern times, it appears that aragonite dissolution during the LGM increased more regularly with water depth. However, if GNAIW was positioned at intermediate depths, the glacial distribution of AAIW and UCDW remains uncertain. Three different intermediate circulation modes are considered: (1) glacial reduction of AAIW and UCDW; (2) elimination of AAIW and UCDW; or (3) change in the relative position of NADW, AAIW, and UCDW with or without mixing with SCW.

Significant variations in aragonite preservation are also observed in the late Quaternary section of four sediment cores covering the last 430 ka (part II-3). Here, the LDX is applied on three species (i.e. *L. inflata*, *L. bulimoides*, and *L. lesueuri*). The LDX records and several other indices revealed three major results: (1) varying aragonite preservation during the past 430 ka; (2) a long-term diagenetic trend; and (3) differences in the susceptibility to dissolution of the three Limacinidae species. Aragonite preservation fluctuated strongly during the studied time interval, with excellent preservation occurring only during the Holocene. The variations are not necessarily associated with glacial/interglacial periods, although increased aragonite dissolution is observed during most glacial periods (particularly during oxygen isotope stages 2, 4, 8, 10, and 12). In addition to the short-term variations in aragonite preservation during the past 430 ka, several parameters in core GeoB 2204-2 display a long-term trend of worse aragonite preservation with increasing core depth, which is interpreted as a diagenetic feature.

The Holocene section of a high-resolution sediment core (GeoB 3910-2) from the western tropical Atlantic (part II-4) shows that variations in the strength of the Atlantic thermohaline circulation and changes in surface water stratification and atmospheric circulation can be inferred. The Ca intensity and LDX records are clearly dominated by long-term as well as short-term trends. The long-term increase in Ca intensity during the Holocene may be attributed to a decrease in dilution of the marine biogenic carbonate by continental terrigenous sediment input, which is strongly controlled by the postglacial sea level rise. Long-term improving aragonite preservation during the Holocene points to increased

influence of NADW at the expense of the more corrosive AAIW and UCDW. Short-term variations in the order of several hundreds to thousands of years are probably due to changing aragonite-corrosiveness of the bottom water, which is connected to changes in the strength of the ISOW. That is, periods of enhanced flow of Iceland-Scotland Overflow Water (ISOW) parallel the intervals of increased aragonite preservation and vice versa. Both of the isotope records of *G. sacculifer* and *G. tumida* show short-term excursions of up to 0.7‰, and the isotopic difference between these species displays changes in the thermal stratification of the surface water and therefore also in trade wind intensity at equatorial latitudes. Especially a ≈1500-year periodicity can be observed in all the records, which probably reflects the internally-forced, global-scale oscillations of the ocean-atmosphere system.

2. Conclusions

Pteropods have proven to be useful organisms for paleoceanograpic studies. However, their use in paleoecologic/paleoenvironmental reconstructions is still rather questionable as pteropods are highly fragile, producing many unidentifiable fragments. The LDX appears to be indicative for the bottom-water saturation state with respect to aragonite and is thus useful for the reconstruction of water masses, especially at intermediate water depths. The LDX can be applied on members of the genus *Limacina*, including *L. inflata*, *L. bulimoides*, and *L. lesueuri*, although differences in their susceptibility to dissolution are observed. The LDX appears to be reliable in the Central and western South Atlantic, including the Mid-Atlantic-Ridge, and within the Caribbean Sea, whereas it mainly fails in the eastern South Atlantic. LDX failure may be caused by changes in carbonate production in the surface waters, leading to a decrease in the supply of tests. Other reasons for LDX failure may be dilution by terrigenous particles or enhanced amounts of organic matter in the sediment, causing "supralysoclinal dissolution". The downcore use of the LDX is limited because of the fragility of pteropodal tests. The connection between LDX values and bulk aragonite contents might be used to evaluate the aragonite loss that a sediment has undergone.

LGM South Atlantic LDX data are in agreement with Cd/Ca and $\delta^{13}C$ data (Oppo and Horowitz, 2000) in suggesting that different water masses occupied the intermediate depth western South Atlantic and Caribbean during much of the late Quaternary. Observed glacial to interglacial differences may be related to variations in the relative strength of northern versus southern water masses. The glacial intermediate depth Caribbean and western South Atlantic were dominated by non- or slightly aragonite-corrosive GNAIW, whereas AAIW and UCDW occupied the intermediate depth during interglacial periods. These water mass

variations have influenced Caribbean and western South Atlantic carbon chemistry substantially.

3. Future outlook

Current knowledge of the LGM water mass configuration in the South Atlantic should be improved by extending the pteropod investigations on ^{14}C dated sediment cores along the Argentine Continental Margin. In addition, the LDX data should be compared with benthic foraminiferal $\delta^{13}C$ and Cd/Ca data, determined at the same sample depths. The spatial investigations should be extended to include other regions, for instance the tropical and subtropical regions of the Indian or Pacific Oceans and on other time slices, such as the OIS transition from 2 to 1 or OIS 5.5. Evaluation of the aragonite loss should be improved by carrying out dissolution experiments on *L. inflata* to reveal the degree of aragonite loss for each preservation stage. Since the three pteropod species used in this thesis inhabit the circumglobal warm-water region, it would be interesting to apply the LDX on other Limacinidae species, such as *Limacina helicina*, which is an arctic/antarctic species, and *Limacina retroversa*, which inhabits the subarctic/subantarctic regions. Moreover, the LDX should be modified and applied on abundant species of the family Cavoliniidae, such as *Styliola subula*, *Creseis acicula*, and *Cavolinia inflexa*. Since aragonite preservation proxies are limited by the water depth, it would be interesting to compare the LDX with calcite preservation proxies, such as the *Globigerina bulloides* dissolution index (BDX'; Volbers and Henrich, subm.), in order to obtain a complete depth profile of calcium carbonate preservation patterns.

4. Data

All data sets used in this study are available as computer files from the corresponding authors upon request or via Internet under the following sites:

Part II-1, 2: http://www.pangaea.de/Projects/SFB261/SGerhardt_RHenrich_2000/

Part II-3: http://www.pangaea.de/Projects/SFB261/SGerhardt_et_al_2000/

5. References

Droxler, A.W., Morse, J.W., Glaser, K.S., Haddad, G.A., Baker, P.A., 1991. Surface sediment carbonate mineralogy and water column chemistry: Nicaragua Rise versus the Bahamas. Marine Geology 100, 277-289.

Oppo, D.W., Horowitz, M., 2000. Glacial deep water geometry: South Atlantic benthic foraminiferal Cd/Ca and $\delta^{13}C$ evidence. Paleoceanography 15 (2), 147-160.

Volbers, A.N.A., Henrich, R., 2000. Present water mass calcium carbonate corrosiveness in the eastern South Atlantic inferred from ultrastructural breakdown of *Globigerina bulloides* in surface sediments. Submitted to Earth and Planetary Science Letters.

Danksagung

An erster Stelle möchte ich mich bei Herrn Prof. Dr. Rüdiger Henrich für die Vergabe der Arbeit und deren Betreuung bedanken. Außerdem danke ich Herrn Prof. Dr. Helmut Willems für die freundliche Übernahme das Zweitgutachtens.

Allen Kolleginnen und Kollegen der Arbeitsgruppe "Sedimentologie/Paläozeanographie" möchte ich für fachliche Diskussionen, Probenaustausch und Kaffeekränzchen danken. Ich danke insbesondere Helga Heilmann und Renate Henning für die Probenbearbeitung, für die Hilfe in den diversen Laboren und für viele unterhaltsame Gespräche. Dr. Claudia Sprengel danke ich für das Korrekturlesen der Arbeit und dafür, daß die Wochenenden in der Uni in unser beider Endphase nicht ganz so langweilig waren.

Den Arbeitsgruppen Mineralogie (Prof. Dr. Olaf Brockamp und Dr. Michael Zuther) und Kristallographie (Prof. Dr. Reinhard Fischer, Dr. Michael Wendschuh-Josties, Dr. Christoph Vogt) möchte ich für die freundliche Unterstützung bei der Röntgendiffraktometrie danken. Den Kolleginnen und Kollegen aus dem Sonderforschungsbereich 261 "Der Südatlantik im Spätquartär" danke ich für die Zusammenarbeit. Außerdem bedanke ich mich ganz herzlich bei Prof. Dr. Colin Devey und Dr. Annemiek Vink für die Englischkorrektur der Arbeit.

Mein besonderer Dank geht an meine Kolleginnen und Freundinnen Dr. Britta Karwath, Stefanie Rath, Miriam Rudolph und Andrea Volbers. Danke für alles!

Schließlich danke ich meinen Eltern für die jahrelange Unterstützung, die es mir ermöglichte, meine Arbeit ohne Geldsorgen zu beenden. Justus danke ich für die regelmäßigen Spieletage und -wochen, die mir eine willkommene Ablenkung waren ("ich gewinne jederzeit gegen dich in Tekken, sogar mit Kuma!").

Die Finanzierung dieser Arbeit erfolgte durch die Deutsche Forschungsgemeinschaft im Rahmen des Graduiertenkollegs "Stoff-Flüsse in marinen Geosystemen".

Publications of this series:

No. 1 **Wefer, G., E. Suess and cruise participants**
Bericht über die POLARSTERN-Fahrt ANT IV/2, Rio de Janeiro - Punta Arenas, 6.11. - 1.12.1985.
60 pages, Bremen, 1986.

No. 2 **Hoffmann, G.**
Holozänstratigraphie und Küstenlinienverlagerung an der andalusischen Mittelmeerküste.
173 pages, Bremen, 1988. (out of print)

No. 3 **Wefer, G. and cruise participants**
Bericht über die METEOR-Fahrt M 6/6, Libreville - Las Palmas, 18.2. - 23.3.1988.
97 pages, Bremen, 1988.

No. 4 **Wefer, G., G.F. Lutze, T.J. Müller, O. Pfannkuche, W. Schenke, G. Siedler, W. Zenk**
Kurzbericht über die METEOR-Expedition No. 6, Hamburg - Hamburg, 28.10.1987 - 19.5.1988.
29 pages, Bremen, 1988. (out of print)

No. 5 **Fischer, G.**
Stabile Kohlenstoff-Isotope in partikulärer organischer Substanz aus dem Südpolarmeer (Atlantischer Sektor). 161 pages, Bremen, 1989.

No. 6 **Berger, W.H. and G. Wefer**
Partikelfluß und Kohlenstoffkreislauf im Ozean.
Bericht und Kurzfassungen über den Workshop vom 3.-4. Juli 1989 in Bremen.
57 pages, Bremen, 1989.

No. 7 **Wefer, G. and cruise participants**
Bericht über die METEOR - Fahrt M 9/4, Dakar - Santa Cruz, 19.2. - 16.3.1989.
103 pages, Bremen, 1989.

No. 8 **Kölling, M.**
Modellierung geochemischer Prozesse im Sickerwasser und Grundwasser.
135 pages, Bremen, 1990.

No. 9 **Heinze, P.-M.**
Das Auftriebsgeschehen vor Peru im Spätquartär. 204 pages, Bremen, 1990. (out of print)

No. 10 **Willems, H., G. Wefer, M. Rinski, B. Donner, H.-J. Bellmann, L. Eißmann, A. Müller, B.W. Flemming, H.-C. Höfle, J. Merkt, H. Streif, G. Hertweck, H. Kuntze, J. Schwaar, W. Schäfer, M.-G. Schulz, F. Grube, B. Menke**
Beiträge zur Geologie und Paläontologie Norddeutschlands: Exkursionsführer.
202 pages, Bremen, 1990.

No. 11 **Wefer, G. and cruise participants**
Bericht über die METEOR-Fahrt M 12/1, Kapstadt - Funchal, 13.3.1990 - 14.4.1990.
66 pages, Bremen, 1990.

No. 12 **Dahmke, A., H.D. Schulz, A. Kölling, F. Kracht, A. Lücke**
Schwermetallspuren und geochemische Gleichgewichte zwischen Porenlösung und Sediment im Wesermündungsgebiet. BMFT-Projekt MFU 0562, Abschlußbericht. 121 pages, Bremen, 1991.

No. 13 **Rostek, F.**
Physikalische Strukturen von Tiefseesedimenten des Südatlantiks und ihre Erfassung in Echolotregistrierungen. 209 pages, Bremen, 1991.

No. 14 **Baumann, M.**
Die Ablagerung von Tschernobyl-Radiocäsium in der Norwegischen See und in der Nordsee.
133 pages, Bremen, 1991. (out of print)

No. 15 **Kölling, A.**
Frühdiagenetische Prozesse und Stoff-Flüsse in marinen und ästuarinen Sedimenten.
140 pages, Bremen, 1991.

No. 16 **SFB 261 (ed.)**
1. Kolloquium des Sonderforschungsbereichs 261 der Universität Bremen (14.Juni 1991):
Der Südatlantik im Spätquartär: Rekonstruktion von Stoffhaushalt und Stromsystemen.
Kurzfassungen der Vorträge und Poster. 66 pages, Bremen, 1991.

No. 17 **Pätzold, J. and cruise participants**
Bericht und erste Ergebnisse über die METEOR-Fahrt M 15/2, Rio de Janeiro - Vitoria,
18.1. - 7.2.1991. 46 pages, Bremen, 1993.

No. 18 **Wefer, G. and cruise participants**
Bericht und erste Ergebnisse über die METEOR-Fahrt M 16/1, Pointe Noire - Recife,
27.3. - 25.4.1991. 120 pages, Bremen, 1991.

No. 19 **Schulz, H.D. and cruise participants**
Bericht und erste Ergebnisse über die METEOR-Fahrt M 16/2, Recife - Belem, 28.4. - 20.5.1991.
149 pages, Bremen, 1991.